博士論文

Molecular mechanisms of cyanobacteriochrome signaling via c-di-GMP

（シアノバクテリオクロムが制御する c-di-GMP を介したシグナリングの分子機構）

榎本　元

Abstract

Acclimation to the light is important for almost all of life, and especially crucial for phototrophs such as cyanobacteria and plants. Cyanobacteriochrome photoreceptors have been identified as a new family of photoreceptors in cyanobacteria almost a decade ago. They show various optical properties covering entire visible spectrum and they are usually found in a large number in each cyanobacterial genome. However, how multiple and diverse cyanobacteriochromes work together in cyanobacteria was unknown. Some of cyanobacteriochromes carry output domains that are involved in regulation of a bacterial second messenger, c-di-GMP. C-di-GMP regulates a lifestyle transition, motility, cell cycle, and virulence in other bacteria, but its role in cyanobacteria remained elusive.

In this thesis, I use a thermophilic cyanobacterium *Thermosynechococcus* as a model organism to study the three cyanobacteriochromes that are directly involved in production and degradation of c-di-GMP. Firstly, I describe the optical properties of one of the cyanobacteriochromes, focusing mainly on the functions of conserved cysteine residues by chemical modification analyses (Chapter 1). Then, I demonstrate that three cyanobacteriochromes cooperatively regulate cell aggregation by c-di-GMP signaling (Chapter 2). Finally, I propose a two-step signaling system to induce the cell aggregation based on the detailed analyses of product feedback inhibition in the c-di-GMP production and c-di-GMP binding affinity of the target cellulose synthase (Chapter 3). This study will pave the way for elucidation of how cyanobacteriochromes orchestrate the c-di-GMP signaling for light-color acclimation responses in cyanobacteria.

Table of Contents

Abbreviations

A_{XXX}	absorbance at XXX nm
Ala	alanine residue
Arg	arginine residue
ATPase	adenosine triphosphatase
BLUF	sensors of blue-light using FAD domain
BV	biliverdin IXα
cAMP	cyclic adenosine monophosphate
CBB	Coomassie Brilliant Blue
CBCR	cyanobacteriochrome
CBS	cystathionine beta synthase domain
c-di-AMP	cyclic diadenylate monophosphate
c-di-GMP	bis(3′-5′)-cyclic dimeric guanosine monophosphate; cyclic dimeric GMP
chl	chlorophyll
CFP	cyan fluorescent protein
cGMP	cyclic guanosine monophosphate
Cys	cysteine residue
Da	Dalton
DGC	diguanylate cyclase
DTT	dithiothreitol
EAL	c-di-GMP phosphodiesterase domain named from the conserved sequence motif (Glu-Ala-Leu)
EDTA	ethylenediaminetetraacetic acid
eq	equivalent
FL	full length
FRET	fluorescence resonance energy transfer
GAF	cGMP phosphodiesterase/adenylyl cyclase/FhlA domain
GGDEF	diguanylate cyclase domain named from the conserved sequence motif (Gly-Gly-Asp-Glu-Phe)
HATP	histidine kinase-like ATPases domain
HD	metal dependent phosphohydrolases
HD-GYP	c-di-GMP phosphodiesterase domain that belongs to HD family and has the conserved sequence motif (Gly-Tyr-Pro)
HEPES	2-[4-(2-hydroxyethyl)-1-piperazinyl]ethanesulfonic acid
HK	dimerization and phosphoacceptor of histidine kinases

HPLC	high performance liquid chromatography
IAM	iodoacetamide
IPTG	isopropyl β-D-1-thiogalactopyranoside
LB	Luria-Bertani medium
LED	light emitting diode
LOV	light-oxygen-voltage-sensing domain
MA	methyl-accepting chemotaxis protein domain
NAD	nicotinamide adenine dinucleotide
OD_{XXX}	optical density at XXX nm
OX	overexpression
PAGE	polyacrylamide gel electrophoresis
PAS	Per/ARNT/Sim domain
Pb	blue light-absorbing form
PCB	phycocyanobilin
PCC	Pasteur culture collection
PCR	polymerase chain reaction
PDE	phosphodiesterase
Pg	green light-absorbing form
pGpG	5'-phosphoguanylyl-(3'-5')-guanosine
Phy	phytochrome
PHY	phytochrome-specific domain
(p)ppGpp	guanosine pentaphosphate and guanosine tetraphosphate
Pr	red light-absorbing form
Pt	teal light-absorbing form
PVB	phycoviolobilin
PØB	phytochromobilin
REC	receiver domain (cheY-homologous)
SD	standard deviation
SDS	sodium dodecyl sulfate
sp.	species (singular)
spp.	species (plural)
TEV	tobacco etch virus
TM	transmembrane
Tris	tris(hydroxymethyl)aminomethane
YFP	yellow fluorescent protein
βME	β-mercaptoethanol

General introduction

Light in Cyanobacteria

Cyanobacteria are photoautotrophic prokaryotes that carry out oxygenic photosynthesis and they occupy a wide range of ecological niches (Bryant & Frigaard, 2006). Light is an important environmental signal for almost all forms of life, and it is crucial for phototrophs because it brings energy necessary to support phototrophic growth. Cyanobacteria have a very large number of and photochemically diverse photosensory systems that respond to a broad range of the spectrum of light. For example, certain cyanobacteria sense far-red light and express far-red light–absorbing chlorophylls, namely chlorophyll *d* and *f*, to optimize photosynthesis (Gan *et al.*, 2014, Gan & Bryant, 2015, Chen *et al.*, 2012). Certain cyanobacteria have the ability to sense the ratio of green light to red light and to optimize their antenna pigment and protein compositions during the complementary chromatic acclimation (Kehoe & Gutu, 2006, Hirose *et al.*, 2013). The ability of cyanobacteria to move toward or away from the light (phototaxis) is also a light color-dependent process by sensing UV/blue- or green/red-light (Yoshihara & Ikeuchi, 2004, Savakis *et al.*, 2012, Song *et al.*, 2011b, Narikawa *et al.*, 2011, Ng *et al.*, 2003).

Photoreceptors: Cyanobacteriochromes

Light signals are perceived by diverse classes of photoreceptors such as LOV, BLUF, cryptochromes, xanthopsins, rhodopsins, and phytochromes, (Möglich *et al.*, 2010). Cyanobacteria contain photoreceptors, denoted cyanobacteriochromes (CBCRs) (Ikeuchi & Ishizuka, 2008, Rockwell & Lagarias, 2010), which are unique in their diversity and multiplicity (see below). The first CBCR gene was discovered by complementation assay of complementary chromatic acclimation mutant nearly twenty years ago

(Kehoe & Grossman, 1996). Almost a decade later, the first CBCR protein was characterized *in vitro* and confirmed as a member of a new group of photoreceptors by Ikeuchi's laboratory (Yoshihara *et al.*, 2004). CBCRs are distantly related to phytochromes, which are red and far-red light receptors that regulate a wide range of physiological responses not only in plants but also in bacteria and fungi (Auldridge & Forest, 2011, Karniol *et al.*, 2005, Rockwell *et al.*, 2006). Both photoreceptors covalently bind a linear tetrapyrrole (bilin) chromophore autocatalytically at the conserved Cys residue and cradle it mainly in their GAF (cGMP phosphodiesterase/adenylyl cyclase/FhlA) (Aravind & Ponting, 1997) domain (Anders & Essen, 2015, Wagner *et al.*, 2005, Essen *et al.*, 2008, Narikawa *et al.*, 2013). They reversibly convert between two photo-states (C15-*Z* and C15-*E*) according to their bilin chromophore *Z*/*E* isomerization of the C15=C16 double bond between the pyrrole rings C and D (**Fig. 0_1**) (Rockwell *et al.*, 2006, Song *et al.*, 2011a, Braslavsky *et al.*, 1997, Dasgupta *et al.*, 2009, Ishizuka *et al.*, 2007, Rockwell & Lagarias, 2010). The photoisomerization of the chromophore induces a series of chromophore–protein rearrangements, resulting in the switching of the biochemical output activity of the output domain (Burgie & Vierstra, 2014).

CBCRs and phytochromes, however, differ in some important features. The first difference is found in the protein domain compositions. The photosensory module of phytochromes consists of three domains, PAS-GAF-PHY (PAS, Per/ARNT/Sim (Ponting & Aravind, 1997); PHY, phytochrome-specific) or PAS-less two domains, GAF-PHY (Rockwell *et al.*, 2006). On the other hand, the photosensory module of CBCRs consists of only a GAF domain (Ikeuchi & Ishizuka, 2008). CBCR-GAF domains are multifunctional by itself *in vivo*: it acts as a bilin autolyase and a bilin photoisomerase. The domain compositions of full-length proteins of phytochromes are conserved, consisting of the N-terminal photosensory

module typically combined with a C-terminal histidine kinase (-like) domain, in some case with a few PAS domains and/or a receiver (REC) domain (Li *et al.*, 2015). On the other hand, the domain compositions of full-length CBCR proteins are astonishingly more diverse. Various domains such as PAS, non-CBCR-GAF, CBS (cystathionine beta synthase), and REC are often found not only at the N-terminus but also C-terminus of a CBCR-GAF domain in a single polypeptide, though their functions are yet to be identified (**Table 0_1**). The number of CBCR-GAF domains in a single polypeptide is also diverse, ranging from one to six, whereas there is a single photosensory module (PAS-GAF-PHY or GAF-PHY) in phytochromes. Finally, the putative signal output domain is diverse, including histidine kinase, MA (methyl-accepting chemotaxis protein domain), diguanylate cyclase (DGC), and phosphodiesterase (PDE). In some CBCRs, no putative signal output domain is found, suggesting that protein-protein interaction could be a signal output.

The second difference is in the optical properties. Phytochromes basically perceive the lights of red and far-red, although algal phytochromes were recently found to perceive orange, green, and even blue lights (Rockwell *et al.*, 2014a). Conversely, CBCRs sense a wide spectral range of light from the near UV to the far red. The diverse optical properties of CBCRs have drawn many researchers' attention, and recent studies are gradually uncovering the mechanisms of spectral tuning such as (1) bilin isomerization, (2) additional covalent ligation of a "second" conserved Cys to the chromophore, (3) change in protonation, and (4) incorporation of different chromophore species, and I briefly describe them below.

*(**1**) bilin isomerization*: Almost all of CBCRs utilize a red light-absorbing bilin, phycocyanobilin (PCB) as a chromophore (Rockwell & Lagarias, 2010). During assembly of the holoprotein of some of the [D/E]XCF type CBCRs (details given below), after PCB is covalently linked to the apoprotein, the

PCB is autocatalytically isomerized to an orange light-absorbing bilin, phycoviolobilin (PVB) by shifting the C4=C5 double bond to the C2-C3 position, resulting in the shorter conjugated system (**Fig. 0_2**) (Ishizuka *et al.*, 2011). PVB is suitable for absorbing shorter wavelength lights such as green light (Rockwell *et al.*, 2012a, Ishizuka *et al.*, 2007).

*(**2**) additional covalent ligation of a "second" conserved Cys to the chromophore*: The widely conserved Cys (the "canonical" or the "first" Cys) binds to $C3^1$ of ring A to anchor the chromophore stably (Narikawa *et al.*, 2013, Burgie *et al.*, 2013). Another Cys residue (the "second" Cys) is also able to bind to the chromophore at C10, disrupting the conjugated system. As a result, the second Cys-bound chromophore absorbs considerably shorter wavelength lights such as near-UV or blue light. To date three types of Cys residues serving as second Cys have been identified at different positions in CBCR-GAF domains (**Fig. 0_3**): [D/E]XCF type (Rockwell *et al.*, 2012a, Rockwell *et al.*, 2012b, Rockwell *et al.*, 2008), insert Cys type (Rockwell *et al.*, 2011), and AM1_1186 type (Narikawa *et al.*, 2014).

*(**3**) change in protonation*: The bilin chromophore of CBCRs is usually assumed to be protonated in both of the two light-absorbing forms (Velazquez Escobar *et al.*, 2013, Rockwell *et al.*, 2015b, Rockwell *et al.*, 2014b, Lim *et al.*, 2014). However, the chromatic acclimation sensor RcaE photoconverts between a deprotonated green light-absorbing form (Pg) in C15-*Z* and a protonated red light-absorbing form (Pr) in C15-*E* (Hirose *et al.*, 2013). Interestingly, the artificial modification of the pH in the medium could produce C15-*E* Pg and C15-*Z* Pr, suggesting that the protonation state rather than chromophore configuration is responsible for the determination of the wavelengths of absorbed light. Whether RcaE senses not only light but also intracellular pH remains elusive.

*(**4**) incorporation of different chromophore species*: Although almost all of CBCRs incorporate PCB as a chromophore, some CBCRs incorporate a

far-red light-absorbing bilin, biliverdin IXα (BV) (**Fig. 0_2**) (Narikawa *et al.*, 2015a, Narikawa *et al.*, 2015b). The BV is utilized for absorbing longer wavelength lights such as far-red light. Such BV-incorporating CBCRs were found in *Acaryochloris marina*, which contains mainly the far-red light absorbing chlorophyll *f* as photosynthetic pigments instead of prevailing chlorophyll *a* (Chen, 2014). The finding implies that far-red light sensing is important for far-red light utilizing cyanobacteria (Gan & Bryant, 2015, Narikawa *et al.*, 2015b). BV but not PCB is abundant in mammalian cells as a degradation product of heme and far-red light is absorbed poorly by mammalian tissue, underpinning that the far-red absorbing CBCRs by BV are promising for utilization in mammalian cell biology as an optogenetic tool or a fluorescent marker (Möglich & Moffat, 2010, Ryu *et al.*, 2014, Yu *et al.*, 2014).

These diverse optical properties of CBCRs seem to reflect the needs of cyanobacterial acclimation to fluctuating and various light conditions (**Table 0_1**).

c-di-GMP Second Messenger

When cells sense an environmental stimulus (i.e., the first messenger), they transduce the signal by synthesis/degradation of a small molecule (i.e., the second messenger), which then elicits physiological responses. Second messenger signaling can integrate many sensory inputs, amplify the signal, and regulate various responses, offering rapid and flexible acclimation. Non-DNA/RNA nucleotides such as cyclic nucleotides and (p)ppGpp are known to work as second messengers (Hauryliuk *et al.*, 2015, Agostoni & Montgomery, 2014, Kalia *et al.*, 2013). Bis(3′-5′)-cyclic dimeric guanosine monophosphate (c-di-GMP) was discovered as an allosteric activator of the cellulose synthase in *Komagataeibacter xylinus* (formerly called *Gluconacetobacter xylinus*) nearly thirty years ago (Ross et al., 1987).

Initially, it had been considered that c-di-GMP is a regulator specific for the cellulose synthase, but identification of genes that control cellular turnover of c-di-GMP (Tal *et al.*, 1998), and subsequent bioinformatics description of prevalence of domains that are found in those identified genes in many bacterial genomes (Galperin *et al.*, 2001), suggested that c-di-GMP has a general role as a bacterial second messenger (Jenal, 2004). Indeed, subsequent numerous studies revealed that c-di-GMP is universally found in bacteria, including cyanobacteria, and generally induces sessile multicellular lifestyles and cell cycle progression, and represses motility and virulence (Römling *et al.*, 2013, Hengge, 2009). GGDEF domains were found to synthesize c-di-GMP via its DGC activity by condensation of two GTP molecules (Ryjenkov *et al.*, 2005, Paul *et al.*, 2004). The EAL and HD-GYP domains were disclosed to degrade c-di-GMP via their PDE activities, by two-step hydrolysis via the linear intermediate 5'-phosphoguanylyl-(3'-5')-guanosine (pGpG) to two GMP molecules (**Fig. 0_4**) (Christen *et al.*, 2005, Ryan *et al.*, 2006, Schmidt *et al.*, 2005). A bioinformatic study predicted PilZ domains as a long-sought c-di-GMP receptor (Amikam & Galperin, 2006), and soon it was experimentally validated (Ryjenkov *et al.*, 2006, Benach *et al.*, 2007). Besides PilZ domains, c-di-GMP has a variety of target proteins and RNAs including RNA riboswitches (Sudarsan *et al.*, 2008, Lee *et al.*, 2010), many unrelated transcription factors (Hickman & Harwood, 2008, Krasteva *et al.*, 2010, Tao *et al.*, 2010), and enzymatically inactive GGDEF (Duerig *et al.*, 2009, Lee *et al.*, 2007), EAL (Navarro *et al.*, 2009, Newell *et al.*, 2009) or HD-GYP domains. Furthermore, even more novel c-di-GMP receptors are expected to be identified (Ryan *et al.*, 2012). Such great diversity of c-di-GMP receptors complicates the identification of c-di-GMP receptors based only on amino acid sequences. c-di-GMP appears to be a more prevalent bacterial second messenger than a more famous one, cyclic adenosine monophosphate (cAMP),

because GGDEF domain is found in more bacterial genomes than do adenylate cyclases (Galperin, 2005).

Although much has been explored in bacterial c-di-GMP signaling, the role of it in cyanobacteria is far less described and there are only a few reports. Mutation of the DGC gene *all2874* resulted in decreased heterocyst differentiation and reduced vegetative cell size under relatively high light condition in *Anabaena* sp. PCC 7120 (Neunuebel & Golden, 2008). In *Synechococcus elongatus* PCC 7942, a LOV-type blue light inducible PDE protein was characterized *in vitro* (Cao *et al.*, 2010), but its physiological function is unknown. The (CBCR-)GAF-GGDEF fragment of the phytochrome-CBCR fusion protein Cph2 has a blue light-induced DGC activity and is involved in inhibiting phototaxis toward blue light in *Synechocystis* sp. PCC 6803, although the full-length Cph2 protein has not been studied (Savakis *et al.*, 2012). Intracellular c-di-GMP levels are higher under blue light than under other qualities of light in *Synechocystis,* whereas c-di-GMP levels were relatively low under blue light condition in *Fremyella diplosiphon* (Agostoni *et al.*, 2013), in both of which the responsible DGC/PDEs are still unknown. Recently c-di-GMP is also implicated in biofilm formation and cellular buoyancy in *Synechocystis* (Agostoni *et al.*, 2016). A putative c-di-GMP receptor is neither identified nor predicted in these previous studies.

CBCR and c-di-GMP Proteins: Abundant Signaling Players

A common feature of CBCR-GAF and c-di-GMP synthesis/degradation domains (GGDEF/EAL/HD-GYP) is their large number encoded in bacterial genomes. CBCR-GAF domains are abundant compared with other types of photoreceptors, such as LOV or BLUF (Losi & Gärtner, 2012). For example, in *Synechocystis* sp. PCC 6803, there are seven CBCR genes, whereas there are two phytochromes and only one each for LOV and BLUF (Mandalari *et*

al., 2013). There are 29 genes in *Escherichia coli*, 41 genes in *Pseudomonas aeruginosa* PAO1, and 28 genes in *Synechocystis* sp. PCC 6803, which encode c-di-GMP synthesis/degradation domains (Römling *et al.*, 2013, Agostoni *et al.*, 2013), contrasting with a handful of cAMP synthesis/degradation domains (Simm *et al.*, 2004, McDonough & Rodriguez, 2012). Although canonical second messengers, such as c-di-GMP, are thought to be a diffusible intracellular pool of molecules, many of the c-di-GMP synthesis/degradation proteins have been shown to be specifically involved in a particular response pathway (Massie *et al.*, 2012). The highly specific c-di-GMP signaling systems are achieved by, for example, transcriptional regulation (Hengge, 2009), protein–protein interaction(s) (Tuckerman *et al.*, 2011), and variation in the binding affinity of c-di-GMP receptors for c-di-GMP (Römling *et al.*, 2013, Pultz *et al.*, 2012). Conversely, little is known about whether multiple CBCRs work specifically or redundantly in cyanobacteria.

Thermosynechococcus as a Model Cyanobacterium

To study the photobiochemical and signaling mechanisms of CBCRs and c-di-GMP, I have focused on those in the thermophilic cyanobacterium *Thermosynechococcus elongatus* strain BP-1 and its close-relative *Thermosynechococcus vulcanus* strain RKN. The genome sequences and natural transformation system are available in these species (Nakamura *et al.*, 2002, Iwai *et al.*, 2004). These thermophilic organisms are valuable for protein studies because thermostable proteins are desirable for protein crystallization (Shen, 2015) and more tolerant to amino-acid substitutions and even deletion mutagenesis (Raghunathan *et al.*, 2012).

Multiple CBCRs and c-di-GMP synthesis/degradation domain proteins are found in *Thermosynechococcus* spp., but the number of them is relatively small and therefore easier to explore the individual functions and the overall

integrated system. Of the five putative CBCRs identified according to their genomic sequences, four (PixJ, Tlr0924, Tlr0911, and Tlr1999) contain the [D/E]XCF-motif (**Fig. 0_3**), whereas the fifth (Tll0899) is homologous to CikA. *Thermosynechococcus elongatus* PixJ is one of the most intensely investigated CBCRs and the crystal structures of both of two photo-states (the blue light-absorbing form, Pb and the green light-absorbing form, Pg) are available (Ishizuka *et al.*, 2006, Burgie *et al.*, 2013, Narikawa *et al.*, 2013). *Thermosynechococcus* PixJ and CikA are homologs of the protein involved in the pathways involved in phototaxis and circadian rhythm in other cyanobacteria, respectively (Yoshihara & Ikeuchi, 2004, Narikawa *et al.*, 2008). A phytochrome homolog has not been found encoded in the genome. There are 10 c-di-GMP synthesis/degradation domain proteins, of which only SesA (Tlr0924), SesB (Tlr1999), and SesC (Tlr0911) contain a photosensory domain, that is, a CBCR-GAF domain.

The CBCR SesA shows a reversible photoconversion between Pb and Pg (Rockwell *et al.*, 2008). Previous study in my laboratory reported that SesA from *T. elongatus* has blue light-activated DGC activity, and disruption of *sesA* impaired cell aggregation of *T. vulcanus* (Enomoto *et al.*, 2014). The cellulose synthase *T. vulcanus* Tll0007, which has also been shown essential for cell aggregation (Kawano *et al.*, 2011), contains a putative c-di-GMP–binding PilZ domain (Amikam & Galperin, 2006, Morgan *et al.*, 2014) and may be the acceptor for SesA-produced c-di-GMP. The functions of SesB and SesC had not been characterized before, but the presence of a CBCR-GAF domain in these two proteins implied that they might also be involved in the light-regulated cell aggregation.

In this thesis, I studied the molecular mechanisms of CBCR signaling via c-di-GMP in *Thermosynechococcus*, focusing on photobiochemical properties and physiological functions of SesA, SesB and SesC. The aim of this study is

to reveal how multiple unique signaling proteins are coordinated in a cell and understand the general principle underlying such diversity from a molecular and physiological perspective.

Figures and Tables

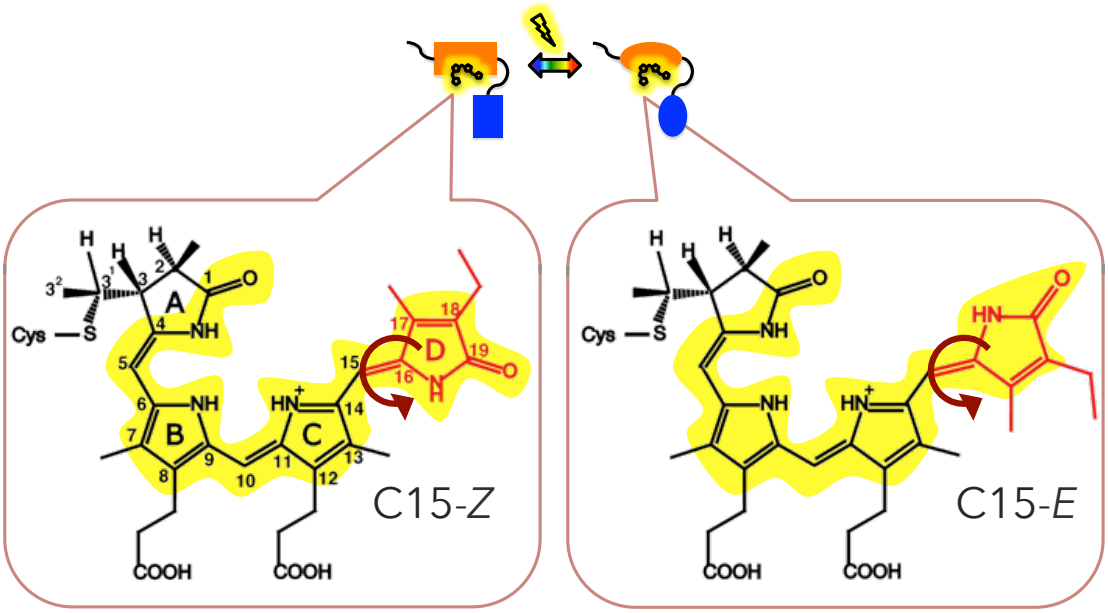

Fig. 0_1. Reversible photoconversion of CBCRs and phytochromes.
Both CBCRs and phytochromes covalently bind a linear tetrapyrrole (bilin) chromophore (here shows phycocyanobilin, PCB) autocatalytically at the conserved Cys residue and cradle it mainly in their GAF domain (colored in orange). They reversibly convert between two photo-induced states according to their bilin chromophore *Z*/*E* isomerization of the C15=C16 double bond between pyrrole rings C and D, namely between its C15-*Z* and C15-*E*. The photoisomerization induces a series of chromophore–protein rearrangements, altering the biochemical output activity of the output domain (colored in blue).

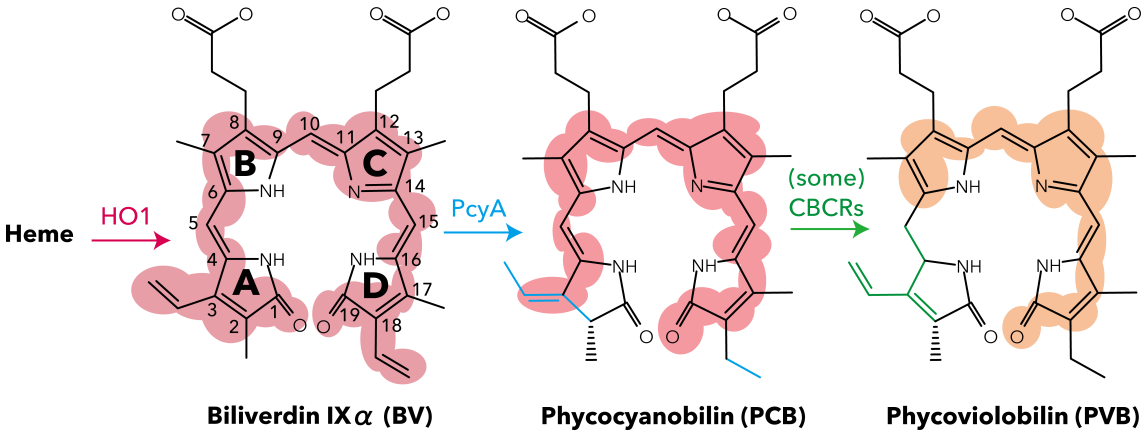

Fig. 0_2. Biosynthesis of linear tetrapyrrole (bilin) species that are relevant to CBCRs. The first step of the bilin biosynthesis pathway is the cleavage of heme by heme oxygenases 1 (HO1) to produce the first linear molecule, biliverdin IXα (BV). This reaction is ubiquitously found also in mammal cells. BV is then reduced by phycocyanobilin (PCB): ferredoxin oxidoreductase (PcyA), which is a member of ferredoxin-dependent bilin reductase family, to produce PCB. PCB is the major chromophore species of CBCRs. During assembly of the holoprotein of some of CBCRs, after PCB is incorporated to the apoprotein, PCB is autocatalytically isomerized to phycoviolobilin (PVB). The conjugated system becomes shorter as the reactions proceed.

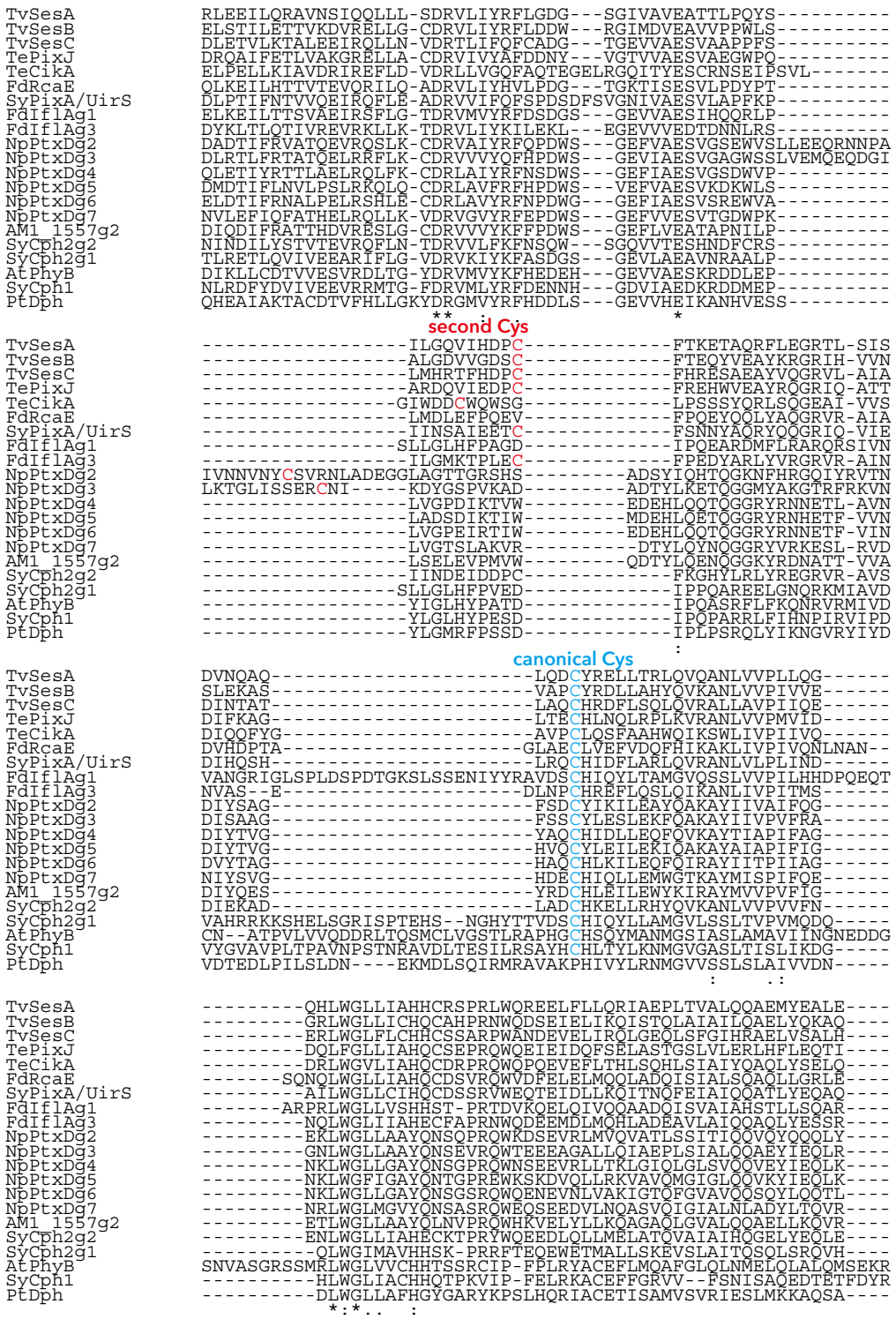

Fig. 0_3. Sequence alignment (CLUSTALX) of the chromophore-binding GAF domains of the experimentally confirmed CBCRs and phytochromes.

Multiple GAF domains in a single polypeptide are numbered from the N-terminus. For example, FdIflAg1 is the most N-terminal of the GAF domains of FdIflA. The canonical Cys is highlighted in blue and the second Cys is highlighted in red. Refer to **Table 0_1** for more details of each protein.

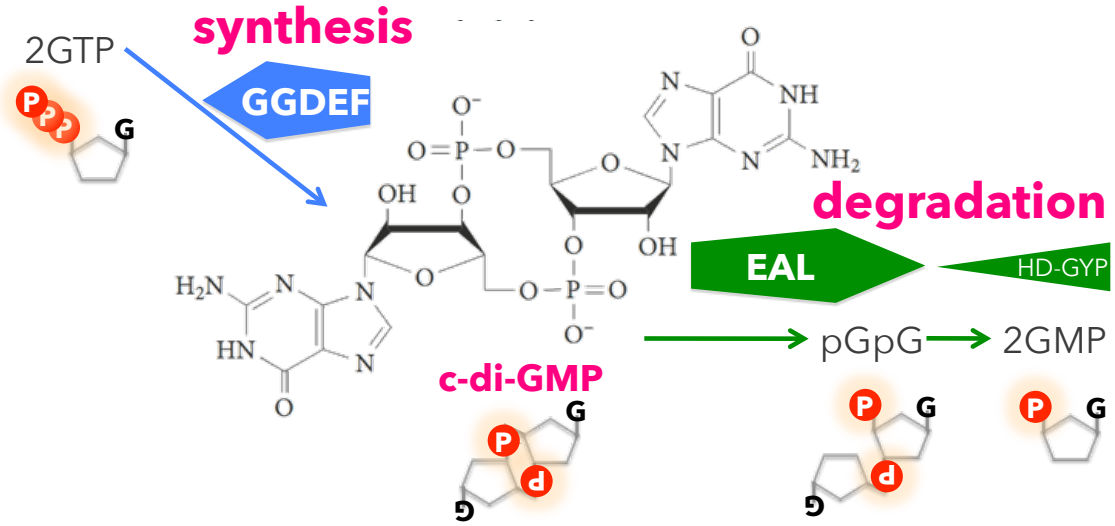

Fig. 0_4. Structure and synthesis/degradation of c-di-GMP.
bis-(3′-5′)-cyclic dimeric guanosine monophosphate (c-di-GMP) is synthesized by diguanylate cyclases (DGCs) that carry GGDEF domains and degraded by specific phosphodiesterases that carry EAL or HD-GYP domains. 5′-phosphoguanylyl-(3′-5′)- guanosine (pGpG) is a degradation intermediate of c-di-GMP.

Table 0_1. Summary of representatives of CBCRs and phytochromes (Phys) experimentally explored.

Protein Name	Domain architecture[1]	Absorption peak (nm) C15-*Z*	C15-*E*	Bilin[2]	Output activity[3]	Physiological function	Species	Reference
CBCRs								
SesA	4CBS-PAS-**GAF**-GGDEF	436	538	PVB	DGC	Cell aggregation	*Thermosynechococcus vulcanus*	This study
SesB	**GAF**-GGDEF-EAL	417	498	PVB	PDE	Cell aggregation	*Thermosynechococcus vulcanus*	This study
SesC	4PAS-**GAF**-PAS-GGDEF-EAL	415	522	PVB	DGC/PDE	Cell aggregation	*Thermosynechococcus vulcanus*	This study
PixJ	2TM-HAMP-**GAF**-HAMP-MA	433	531	PVB	Methylation?	Motility?	*Thermosynechococcus elongatus*	(Ishizuka *et al.*, 2006)
CikA	**GAF**-HK-HATP-REC	438	518	PCB	Histidine kinase?	Circadian rhythm?	*Thermosynechococcus elongatus*	Enomoto *et al.* Unpublished.
RcaE	PAS-**GAF**-PAS-HK-HATP	661	532	PCB	Histidine kinase	Chromatic acclimation	*Fremyella diplosiphon*	(Hirose *et al.*, 2013, Kehoe & Grossman, 1996)
PixA/UirS	TM-2PAS-**GAF**-HK-HATP	396	533	PVB	Protein-protein interaction?	Phototaxis	*Synechocystis* sp. PCC 6803	(Narikawa *et al.*, 2011, Song *et al.*, 2011b)
IflA	**GAF**-GAF-**GAF**	645 421	688 545	PCB? PCB	?	Growth at low cell density	*Fremyella diplosiphon*	(Bussell & Kehoe, 2013)
PtxD	GAF-6**GAF**-MA	382 398 646 640 648 608	446 588 530 N.D. 546 542	PCB PCB PCB PCB PCB PCB	Methylation?	Phototaxis	*Nostoc punctiforme*	(Campbell *et al.*, 2015, Rockwell *et al.*, 2011, Rockwell *et al.*, 2012c)
AM1_1557	GAF-**GAF**-HK-HATP-REC	697	622	BV	Histidine kinase?	?	*Acaryochloris marina*	(Narikawa *et al.*, 2015b)
CBCR/Phy								
Cph2	**GAF**-**PHY**-GGDEF-EAL-**GAF**-GGDEF	644 ~420	695 ~520	PCB PVB?	DGC PDE?	Phototaxis	*Synechocystis* sp. PCC 6803	(Savakis *et al.*, 2012, Anders *et al.*, 2011)
Phys								
PhyB	**PAS-GAF-PHY**-2PAS-HKRD	663	718	PØB	Protein-protein interaction?	Photomorphogenesis Circadian rhythm etc.	*Arabidopsis thaliana*	(Burgie *et al.*, 2014, Jones *et al.*, 2015)
Cph1	**PAS-GAF-PHY**-HK-HATP	654	706	PCB	Histidine kinase	?	*Synechocystis* sp. PCC 6803	(Yeh *et al.*, 1997)
Dph	**PAS-GAF-PHY**-HK-HATP-REC	700	750	BV	Histidine kinase	?	*Phaeodactylum tricornutum*	Fortunato, Jaubert, Enomoto *et al.* Submitted.

[1]Photosensory region (CBCR-GAF or phytochrome (PAS-)GAF-PHY) is highlighted in bold. Numbers leading domain names mean that there are the same domains consecutively in that number. For refer to domain abbreviations, see the abbreviation list on page 3.
[2]PCB, phycocyanobilin; PVB, phycoviolobilin; BV: biliverdin IXα; PØB, phytochromobilin.
[3]DGC, diguanylate cyclase to synthesize c-di-GMP; PDE, phosphodiesterase to degrade c-di-GMP.

~Chapter 1~

Thiol-based photocycle of the blue and teal light-sensing cyanobacteriochrome SesB

Abstract

Cyanobacteriochromes are a spectrally diverse photoreceptor family that binds a bilin chromophore. For some cyanobacteriochromes, in addition to the widely conserved cysteine to anchor the chromophore, its ligation with a second cysteine is responsible for a remarkable blue shift. Herein, I report a newly discovered cyanobacteriochrome SesB (Tlr1999) exhibiting reversible photoconversion between a blue-absorbing form at 418 nm (P418) and a teal-absorbing form at 498 nm (P498). Acidic denaturation suggests that P418 harbors C15-*Z* phycoviolobilin, whereas P498 harbors C15-*E* phycoviolobilin. When treated with iodoacetamide, which irreversibly modifies thiol groups, P418 is slowly converted to a green-absorbing photoinactive form denoted P552. The absorption spectrum of P498 appears to be unaffected by iodoacetamide, but when iodoacetamide modified, it is photoconverted to P552. These results suggest that a covalent bond exists between the second Cys and the phycoviolobilin in P418 but not in P498. Subsequent treatment with dithiothreitol converts P552 into P418, whereas dithiothreitol reduces P498 to yield P420, a photoinactive form. Site-directed mutagenesis shows that the second Cys is essential for assembly of the photoactive holoprotein and that the photoactivity of this inert mutant is partially rescued by β-mercaptoethanol. These results suggest that the covalent attachment and detachment of a thiol, although not necessarily that of the second Cys, is critical for the reversible spectral blue shift and the complete photocycle. I propose a thiol-based photocycle, in which the thiol-modified P552 and P420 are intermediate-like forms.

Introduction

The precise role of the second Cys in photochemistry of CBCRs remained to be clarified at the time of the study. There were two contradictory models concerning the role of the second Cys during photoconversion between a blue light-absorbing form (Pb) and a green light-absorbing form (Pg) represented by TePixJ and SesA (Ishizuka *et al.*, 2006, Rockwell *et al.*, 2008). The reversible attachment model (**Fig. 1_1**) (Ishizuka *et al.*, 2011, Rockwell *et al.*, 2008) suggests that Cys is covalently ligated to C10 of PVB in Pb, whereas it is not bound to the chromophore in Pg. The stable double linkage model (Ulijasz *et al.*, 2009) suggests that the second Cys is stably ligated to PVB-like chromophore in both Pb and Pg during the photoconversion. It is also suggested that the chromophore is distorted between rings A and B owing to the thioether linkage between the second Cys and C4 or C5. The Cys-ligated site has not yet been experimentally determined. Nonetheless, the second Cys may be involved in the Pb/Pg photocycle.

For the study reported herein, I expressed, purified, and characterized the spectral properties of the SesB (Tlr1999) GAF domain (SesB-GAF) of *Thermosynechococcus elongatus* and studied the role of its second Cys mainly by the chemical modification of thiols. Based on my results, I demonstrate the reversible attachment of Cys during photoconversion.

Results

Domain Architecture of SesB.

According to SMART (Letunic *et al.*, 2012), *T. elongatus* SesB contains a CBCR-GAF domain, a GGDEF domain, and an EAL domain (**Fig. 1_2*A***). By comparing the sequence of SesB with those of Pb/Pg-type CBCRs such as TePixJ and SesA, the canonical Cys and the second Cys were respectively assigned to Cys274 and Cys246, the latter of which is part of a [D/E]XCF motif (**Fig. 0_3**).

Photoconversion between the Blue- and Teal- Absorbing Forms.

SesB-GAF was purified from cyanobacterial cells as a nearly homogeneous, soluble protein (**Fig. 1_2*B***). The SDS-PAGE band corresponding to SesB-GAF intensely fluoresced when in the presence of Zn^{2+}, suggesting that SesB-GAF contains a covalently bound bilin chromophore. After irradiation with blue light, the absorption spectrum of SesB-GAF contained a sharp peak (λ_{max} = 498 nm). This 498 nm light-absorbing form was denoted P498. When P498 was irradiated with teal light, the peak at 498 nm disappeared and a broader, less intense peak centered at 418 nm increased. This form was denoted P418 (**Fig. 1_2*C,D***). Photoconversion between P418 and P498 was reversible (data not shown).

In the absorption spectra, there was a small absorption peak at ~552 nm that was not affected by green light (**Fig. 1_2*D***). A similar minor, photoinactive peak has been detected in the spectra of the Pb/Pg-type CBCRs TePixJ (Ishizuka *et al.*, 2006) and SesA (Rockwell *et al.*, 2008). When 1 mM DTT was included throughout the preparation procedure, the 552 nm peak was hardly detectable (data not shown), suggesting that the peak is associated with a form of SesB-GAF that contains an oxidized cysteine(s).

Another small peak at ~660 nm was assigned to a chlorophyll contaminant.

Roles of the Conserved Cys Residues.

The chromophore of SesB-GAF was studied by acidic urea denaturation (**Fig. 1_2*E***). The difference spectrum of denatured P498 minus denatured P418 (λ_{max} = 509 nm, λ_{min} = 602 nm; **Fig. 1_3**) strongly suggested that SesB-GAF covalently binds PVB and that its configuration is C15-*Z* in P418 and C15-*E* in P498, as was found for TePixJ (Ishizuka *et al.*, 2007).

I replaced the canonical Cys (Cys274) and the second Cys (Cys246) individually and together with alanines by site-directed mutagenesis to produce the mutants C274A, C246A, and C246A/C274. These mutants were expressed in and isolated from cyanobacterial cells (**Fig. 1_4**).

The C246A mutant covalently binds a bilin as shown by its Zn^{2+}-enhanced fluorescence (**Fig. 1_4*A***). C246A showed two absorption peaks at 585 and 616 nm (**Fig. 1_4*A***) but was photoinactive in both cases (data not shown). After denaturation, the spectrum of C246A had a peak at 666 nm (**Fig. 1_4*D***), suggesting that the $C3^1$ of C15-*Z* PCB is covalently anchored to Cys274, as was found for Cph1 (Ishizuka *et al.*, 2007).

The C274A mutant also covalently bound a bilin, but its absorption spectrum contained a broad peak centered at 545 nm (**Fig. 1_4*B***). This mutant was also photoinactive (data not shown). The spectrum of denatured C274A was quite different from PCB or PVB (**Fig. 1_4*E***). This may correspond to isophycocyanobilin, which was suggested as a ligation intermediate in the assembly of PCB to phycocyanin apoprotein (Tu *et al.*, 2009) or may be an aberrant ligation of PCB involving a site other than the authentic $C3^1$.

The C246A/C274A double mutant did not bind the chromophore, and its absorption spectrum was devoid of bands except for that associated with contaminated chlorophyll (**Fig. 1_4*C*,*F***).

Given their amino acid sequences, spectral properties, chromophore configurations, and our site-directed mutagenesis study, I concluded that SesB and the Pb/Pg-type CBCRs undergo the same type of photocycle and that the conserved Cys residues are involved in the photoconversion. However, the absorbance band for P498 was blue-shifted by ~35 nm compared with those of the Pg-type CBCRs (λ_{max} = 530−540 nm). Notably, this peak is the sharpest found so far for a CBCR. The absorption spectrum of P498 is similar to that of phycourobilin, which has saturated C-4/5 and C-15/16 bonds (Blot *et al.*, 2009), suggesting that the PVB D ring of P498 was heavily twisted with respect to the plane formed by the B and C rings, resulting in a shorter π-conjugated system similar to that of phycourobilin. The aqueous solution of P418 is yellow as are those of the Pb forms of TePixJ and SesA, whereas P498 is orange (**Fig. 1_2*C***), unlike the pink solutions found for the Pg forms of TePixJ (Ishizuka *et al.*, 2006) and SesA.

The absorption spectrum of SesB-GAF purified from *Escherichia coli* had an additional peak at ~616 nm (denoted P616) (**Fig. 1_3**). The absorption spectrum of denatured SesB-GAF purified from *E. coli* indicated that its chromophore was ~70% PVB (603 nm) and ~30% PCB (671 nm) (**Fig. 1_3**) (Ishizuka *et al.*, 2007). These results suggested that P616 derived from PCB. These features have also been observed in TePixJ purified from *E. coli* (Ishizuka *et al.*, 2011) and seem to be a common problem of PVB-harboring CBCRs. The ambience light during the protein expression may influence the PVB population as suggested recently (Rockwell *et al.*, 2012a). Therefore, experiments were performed using protein prepared from cyanobacterial cells, unless stated otherwise.

IAM Modification: P552 and P420.

To determine the roles of the Cys residues, especially that of the second Cys, I treated SesB-GAF with iodoacetamide (IAM), which irreversibly modifies

thiols (Hansen & Winther, 2009). When P418 was incubated with 50 mM IAM in the dark, the P418 peak was gradually disappeared (>21 h) as the peak at 552 nm increased (**Fig. 1_5*A***). Green-light irradiation did not affect the 552 nm peak, indicating that it is a photoinactive form (denoted P552). The spectrum of denatured P552 confirmed that C15-*Z* configuration of its PVB had been maintained during and after the modification with IAM (data not shown). The slow IAM-induced conversion of P418 into P552 suggested that the covalent linkage between Cys and the chromophore is not so stable; i.e., Cys exists in a dynamic equilibrium involving its ligated and free forms. Perhaps, IAM modified Cys to yield P552. After incubating P498 with 50 mM IAM in the dark for 5 min, the small peak near 420 nm (which I associated with a form of SesB-GAF denoted P420) had decreased and the peak at 498 nm had increased (**Fig. 1_5*B***). I assumed that P420 is a photo-inactive form of SesB-GAF because the 420 nm peak in the spectrum of P498 was unaltered by saturating blue-light irradiation. The IAM-induced conversion of P420 into P498 suggested that in P420 C15-*E* PVB is ligated to Cys and in P498 C15-*E* PVB is not ligated to Cys. Further incubation with IAM did not affect the spectrum of P498. However, teal-light irradiation converted P498 into P552 (**Fig. 1_5*B***). P498-derived P552 seems to be identical to P418-derived P552 because the PVB chromophore is in the C15-*Z* configuration in both forms, neither of which responds to a green-light irradiation. Because teal-light irradiation could induce C15-*E* → *Z* isomerization in IAM-modified P498, it seemed that the second Cys is not necessary for the isomerization. In summary, the results suggested that in P418 C15-*Z* PVB is ligated to the second Cys; in P552, C15-*Z* PVB and Cys are not ligated; in P420, C15-*E* PVB is ligated to the Cys; and in P498, C15-*E* PVB and Cys are not ligated. The 552 nm peak in the native protein may also be P552, which contains the oxidized second Cys.

Effects of DTT on P552 and P498.

After excess IAM had been removed by dialysis, treatment with 20 mM DTT in the dark reverted P552 into P418 within 1 min (**Fig. 1_6*A***). P418 could then be converted into P498 by the blue-light irradiation, together with reduction of P552. P552 itself, however, could not be converted into P498 by green-light irradiation. Perhaps, P552 was indirectly converted into P498 via P418 during the blue-light irradiation. Irradiation of IAM-modified P498 with teal light generated both P552 and P418 (**Fig. 1_6**). L-Cysteine had similar effects as DTT (**Fig. 1_7**). These results suggested that instead of the IAM-modified Cys, the thiol of DTT (and L-cysteine) reversibly ligated to the chromophore given that an IAM-modified thiol is unaffected by DTT (Hansen & Winther, 2009).

When SesB-GAF purified from *E. coli* was treated with IAM and then DTT, the amount of not only P552 but also P616 was increased by IAM and decreased by DTT (**Fig. 1_8**), suggesting that P616 contains a C15-*Z* PCB that was not ligated to a thiol just like C246A (**Fig. 1_4*A***). The presence of DTT decreased the amount of P616 to a lesser extent than it did P552, suggesting that thiols were ligated more easily to PVB than to PCB.

When an excess of DTT (1 M) was added in the dark to a solution of P498, the protein was completely converted to a photoinactive blue-absorbing form peaking around 420 nm in the dark (**Fig. 1_9**). Denaturation analysis confirmed that the configuration of its PVB (C15-*E*) was unaffected (data not shown). These results indicate that P420 carrying C15-*E* PVB ligated with the thiol of DTT was produced by 1 M DTT. Notably, although 20 mM DTT largely converted P552 to P418, little P420 was produced (**Fig. 1_6**).

Effects of β-Mercaptoethanol (βME) on C246A.

The DTT-induced blue spectral shift of P552 to P418 (**Fig. 1_6**) and P498 to

P420 (**Fig. 1_9**) prompted us to examine the effect of DTT on C246A, which possibly binds PCB at C3[1] with the canonical Cys274 (**Fig. 1_4*A***). DTT had little effect on the absorption spectrum of C246A (data not shown). However, when β ME, which is smaller compound than is DTT, was added to C246A, the absorbance at ~620 nm was decreased and the absorption at ~380−400 nm was increased slightly (**Fig. 1_10**). Blue-light irradiation reduced the 380 −400 and 620 nm absorption peaks and increased the absorbance at ~500 nm slightly. Subsequent teal-light irradiation reduced the 500 nm absorbance and increased the absorbance at ~380−400 and 620 nm. Namely, blue and teal light induced a reversible photoconversion. The spectrum of the denatured teal- absorbing form indicated that the protein contained C15-*E* PCB, but isomerization of PCB to PVB had not occurred (data not shown). These results suggested that the photoinactive peak at ~620 nm (C15-*Z* PCB, free from thiol) was converted into the photoactive blue-absorbing form (C15-*Z* PCB, thiol-ligated) by β ME and then photoconverted to the photoactive teal-absorbing form (C15-*E* PCB, free from thiol). These reactions (**Fig. 1_10**) are similar to the photoconversions shown in **Fig. 1_6**. Notably, the absorption-peak maximum of PCB C15-*E* form (~500 nm) was at nearly the same position as that of PVB (498 nm), suggesting that PCB is heavily twisted at C5, leading to a shorter π-conjugated system similar to that of PVB.

Discussion

Reversible Attachment of the Second Cys to PVB during Photoconversion.

For this report, I studied SesB, which is a new type of CBCR that contains a [D/E]XCF motif and undergoes a reversible photoconversion between a blue-absorbing form (P418) and a teal-absorbing form (P498). Modification of SesB-GAF with IAM in the dark converts P418 into P552 and P420 into P498, without C15-*Z*/*E* isomerization (**Fig. 1_5**). These results suggest that P418 and P420 contain a second Cys-PVB adduct, whereas P552 and P498 contain PVB free from Cys. This suggests that the covalent ligation of the second Cys to PVB is unstable; i.e., the ligated and free forms of Cys are in dynamic equilibrium. The possibility that the second Cys−chromophore bond is thermally labile has been discussed for SesA (Rockwell *et al.*, 2008). My study characterized four forms of SesB-GAF: photoactive P418 containing C15-*Z* PVB ligated to the second Cys [P418 (*Z*/S)], photoactive P498 containing C15-*E* PVB that is not ligated to Cys [P498 (*E*/−)], photoinactive P552 containing C15-*Z* PVB that is not ligated to Cys [P552 (*Z*/−)], and photoinactive P420 containing C15-*E* PVB ligated to Cys [P420 (*E*/S)] (**Fig. 1_11**).

For the [D/E]XCF-type CBCRs, there are two conflicting hypotheses concerning the role of the second Cys. One hypothesis is the reversible attachment model for which the second Cys is ligated to PVB in Pb, but free in Pg (**Fig. 1_1**) (Ishizuka *et al.*, 2011, Rockwell *et al.*, 2008). The other is the stable double linkage model for which the second Cys is ligated to PCB in both Pb and Pg, forming a stable PVB-type chromophore (Ulijasz *et al.*, 2009). By modification of SesB-GAF wild-type protein with IAM, I demonstrated that the second Cys reversibly binds PVB during the P418 (*Z*/S)/ P498 (*E*/−) photoconversion.

An Active Thiol, Not Necessarily That of Cys, Is Critical for the Spectral Blue Shift.

Once modified by IAM, a cysteine thiol cannot be regenerated by DTT (Hansen & Winther, 2009). However, treatment of the photoinactive P552 (*Z*/−) with DTT in the dark regenerated the photoactive blue-absorbing P418 (*Z*/S) (**Fig. 1_6**). Similarly, the photoactive P498 (*E*/−) was converted to the photoinactive blue-absorbing P420 (*E*/S) by the treatment with 1 M DTT in the dark (**Fig. 1_9**). These results suggest that DTT efficiently ligates the chromophore, instead of the second Cys thiol, causing the remarkable spectral blue shift. I also showed that the treatment of C246A with βME in the dark, but not with DTT, generates a small amount of a photoactive blue-absorbing form from a photoinactive red-absorbing form (**Fig. 1_10**). This may imply that βME, which is smaller than DTT, can access the chromophore-binding pocket and covalently ligate the chromophore. Although the thiol-ligation site on the chromophore has not been characterized, I assume that it is C10 of PVB as was suggested previously (Rockwell *et al.*, 2008), because the blue spectral shift found for the thiol adducts fits with rubinoid species that contain a disconnected π-conjugated system between rings B and C (Terry *et al.*, 1993, Küfer & Scheer, 1982) and the nucleophilic reactivity of the C10 of the chromophore (Tu *et al.*, 2009, Chen *et al.*, 2009).

Thiol Attachment/Detachment: A Thermal and Dark Reaction during the Photocycle.

Upon photoconversion, isomerization at C15 and covalent attachment/detachment of the thiol to PVB occur. IAM modification and treatment with DTT in the dark induced the thiol-attachment/detachment

reactions without isomerizing C15. Because a relatively small concentration of DTT converted P552 (*Z*/−) into P418 (*Z*/S) (**Fig. 1_6**), the conversion of the P552 (*Z*/−) into P418 (*Z*/S) seems to be a naturally occurring dark reaction. Because excess DTT was needed to cause the opposite reaction (P498 (*E*/−) into P420 (*E*/S)) (**Fig. 1_9**), the conversion of the P420 (*E*/S) into P498 (*E*/−) also seems to be naturally occurring dark reaction. The latter suggestion is consistent with the observation that IAM-induced conversion of P420 (*E*/S) into P498 (*E*/−), which occurs within a few minutes, is much faster than that of P418 (*Z*/S) into P552 (*Z*/ −) (>21 h) (**Fig. 1_5**). These reactions are summarized in **Fig. 1_11*A***. The photoconversion of P498 (*E*/−) to P418 (*Z*/S) can be split into two steps: the photoreaction P498 (*E*/−) → P552 (*Z*/−) and the dark reaction P552 (*Z*/−) → P418 (*Z*/S) when aided by IAM and DTT. I postulate that the reverse photoconversion of P418 (*Z*/S) to P498 (*E*/−) as in **Fig. 1_11*A***, although I could not demonstrate the efficient production of P420 (*E*/S) from P418 (*Z*/S) under reducing conditions.

In this context, it should be noted that the Pb/Pg-type CBCR, SesA, showed temperature-induced changes in equilibrium implicated in the dark reactions (Rockwell *et al.*, 2008). However, I did not observe such temperature-induced spectral changes in the equilibrium of P498 (*E*/−) and P420 (*E*/S) at 45 or 4 °C (data not shown). At present, I do not know the biochemistry that underlies the difference in the temperature dependency in the equilibrium of the dark reaction between SesB and Tlr0924. How or if temperature induces a change in the equilibrium positions of P498 (*E*/−) and P420 (*E*/S) awaits determination.

A Proposed Thiol-Based Photocycle.

Given the results, I can propose a complete photocycle for SesB (**Fig. 1_11*B***). I can assume a P552-like intermediate [P552′ (*Z*/−)] transiently exists during the photoconversion of P498 (*E*/−) to P418 (*Z*/S). Similarly, I can

assume that a P420-like intermediate [P420′ (*E*/S)] transiently exists during the photoconversion of P418 (*Z*/S) to P498 (*E*/−). Furthermore, I assume that the initial photoproducts (Ia and Ib) decay to the metastable P552′ (*Z*/−) and P420′ (*E*/S). A time-resolved photoconversion study of the related Pb/Pg-type CBCR, TePixJ, detected intermediates peaking at 560−570 nm after <50 ns and 870 μs of excitation of the Pg form [Fukushima, Y., and Itoh, S., personal communication]. These slightly red- shifted intermediates of TePixJ might be analogous to P552′ (*Z*/−) of SesB. Similarly, at least two intermediates (Ib and P420′) can be assumed to be present during the reverse photoconversion.

In the two-step dark reactions from Ia to P418 (*Z*/S), I can assume that only slight conformational changes occur in the apoprotein in the absence of thiol attachment, whereas large conformational changes coupled to the thiol attachment occurring during the P552′ (*Z*/−) → P418 (*Z*/S) reaction. These conformational changes in the apoprotein suppress the reverse photoreaction from P418 (*Z*/S) to P498 (*E*/−) via P552′ (*Z*/−). Instead, P418 (*Z*/S) can be photoconverted into Ib, which decays first to P420′ (*E*/S) and then to P498 (*E*/−) in the dark (**Fig. 1_11*B***).

In this study, I demonstrated that the thiol of the second Cys or an exogenous thiol such as those of DTT supports full photoconversion of SesB, suggesting that DTT promotes conformational changes similar to those induced by the Cys. SesB also contains GGDEF and EAL domains (**Fig. 1_2*A***), which may serve as a diguanylate cyclase (Ryjenkov *et al.*, 2005) or a phosphodiesterase (Schmidt *et al.*, 2005) for the bacterial second messenger bis(3′-5′)-cyclic dimeric guanosine monophosphate (c-di-GMP), respectively (Hengge, 2009, Schirmer & Jenal, 2009). Measuring these activities would determine if the DTT-adduct P418 (*Z*/S) acts in a manner equivalent to that of the native P418 (*Z*/S) during c-di-GMP signaling. It also would be interesting to compare the signaling activity of P552 (*Z*/−) and P498 (*E*/−)

after the IAM modification. By measuring these signaling activities, I can assess the effect of Cys and exogenous thiols on the protein conformational changes.

Materials and Methods

Computational Studies.

The SesB (Tlr1999) domain composition was determined using SMART (http://smart.embl- heidelberg.de/) (Letunic *et al.*, 2012). Sequence alignment of CBCR chromophore-binding GAF domains was by CLUSTAL_X (Larkin *et al.*, 2007).

Plasmid Construction.

The gene encoding the GAF domain of *T. elongatus* SesB (SesB-GAF, amino acid residues 191−342) was PCR amplified with Ex Taq DNA polymerase (TaKaRa, Ohtsu, Japan) and the primers 5′-AACATATGGAGCTTTCGACGATTCTC-3′ and 5′-GAGGATCCTATTGAGCTTTTTGATAGAGTT-3′ and was then cloned into a pT7blue T-Vector (Novagen, Madison, WI). After sequence confirmation, the DNA was excised with NdeI and BamHI and cloned into pTCH2031V (Ishizuka *et al.*, 2006) at the trc promoter site for expression in *Synechocystis* sp. PCC 6803. The gene was also cloned into pET28a (Novagen) for expression in *Escherichia coli*. The expressed protein was $(His)_6$ tagged at its N-terminus.

Site-Directed Mutagenesis.

The genes encoding the second Cys mutant (C246A), the canonical Cys mutant (C274A), and the Cys double mutant (C274A/C246A) were created using QuikChange site-directed mutagenesis kit reagents (Stratagene, La Jolla, CA) according to the manufacturer's instructions. Primers for the C246A construct were 5′-CGTGGGAGATTCCGCCTTTACGGAACAG-3′ and 5′-CTGTTCCGTAAAGGCGGAATCTCCCACG-3′. Primers for the C274A

construct were 5′-CTCAGTTGCCCCCGCCTATCGCGATTTGC-3′ and 5′-GCAAATCGCGATAGGCGGGGGCAACTGAG-3′. The sequences were confirmed by nucleotide sequencing.

Protein Expression in and Purification from Cyanobacterial Cells.

Cells of the cyanobacterium *Synechocystis* sp. PCC 6803 were transformed with the pTCH2031V derivatives according to ref (Midorikawa *et al.*, 2009). The recombinant cells were grown in 8 L of BG11 medium with 20 μg/mL chloramphenicol at 31 °C bubbled with air containing 1% (v/v) CO_2 in the light (intensity ca. 30 μmol photons m^{-2} s^{-1}). Cells were harvested by centrifugation, suspended in disruption buffer (20 mM HEPES-NaOH (pH 7.5), 100 mM NaCl, 10% (w/v) glycerol), and then frozen at −80 °C. After thawing, cells were disrupted with a French press (no. 5501-M, Ohtake, Japan) three times at 1500 kg cm^{-2}. The homogenate was centrifuged twice at 12000*g* for 10 min and twice at 194100*g* for 30 min. The final supernatant was loaded onto a nickel-affinity His-Trap chelating column (GE Healthcare, Piscataway, NJ). Proteins were eluted with a linear gradient of 30−430 mM imidazole in disruption buffer. EDTA (1 mM) was added to the peak fractions, which were then held at 4 °C for 1 h. Pooled protein fractions were dialyzed against 20 mM HEPES-NaOH (pH 7.5), 500 mM NaCl, 10% (w/v) glycerol.

Protein Purification from *E. coli*.

The *E. coli* strain C41 (DE3) (Miroux & Walker, 1996) harboring the SesB-GAF expression plasmid and the pKT271 plasmid for PCB (Mukougawa *et al.*, 2006) was precultured overnight at 37 °C in the dark in Luria−Bertani medium containing 20 μg/mL kanamycin and 20 μg/mL chloramphenicol. Fresh medium (1 L) was then inoculated with 10 mL of the culture. After incubation at 37 °C for 2 h, 1 mM isopropyl β-D-1-

thiogalactopyranoside was added. The culture was incubated at 37 °C for an additional 3 h. Cells were collected by centrifugation, suspended in disruption buffer, and stored at −80 °C. Cells were thawed on ice and lysed with a French press three times at 1500 kg cm^{-2}. The homogenate was centrifuged at 194100*g* for 30 min at 4 °C. The protein was purified by His-Trap chromatography as described above.

SDS-PAGE and Zinc-Enhanced Fluorescence Assay.

Purified protein was solubilized in 2% (w/v) lithium dodecyl sulfate, 60 mM dithiothreitol (DTT), and 60 mM Tris-HCl (pH 8.0) and then subjected to SDS-PAGE through a 12% (w/ v) polyacrylamide gel. For the zinc-enhanced fluorescence assay (Berkelman & Lagarias, 1986), the gel was soaked in 20 μM zinc acetate at room temperature for 30 min in the dark, and fluorescence was detected through a 605 nm filter with excitation at 532 nm (FMBIO II, TaKaRa). The gel was then stained with Coomassie Brilliant Blue R-250 (Bio-Rad, Richmond, CA).

Chemical Modification and Spectral Analysis.

To modify cysteine thiols irreversibly, iodoacetamide (IAM) was added into protein solutions at a final concentration of 50 mM (Hansen & Winther, 2009), and the mixtures were then incubated for 60 min at room temperature in the dark. Excess IAM was removed by dialysis before treatment with DTT.

Absorption spectra were recorded at room temperature using a UV-2400PC spectrophotometer (Shimadzu, Kyoto, Japan). For blue-light irradiation, light-emitting diodes (λ_{max} = 392 nm, half-bandwidth = 12 nm) were used. For teal-light irradiation, light from a halogen lamp was passed through an interference filter with λ_{max} = 514 nm and a half-bandwidth = 8.5 nm. For green irradiation, light from a halogen lamp was passed through

an interference filter with λ_{max} = 567.5 nm and a half-bandwidth = 13 nm. Proteins were denatured in 8 M urea (pH 2.0) at room temperature in the dark.

Figures and Tables

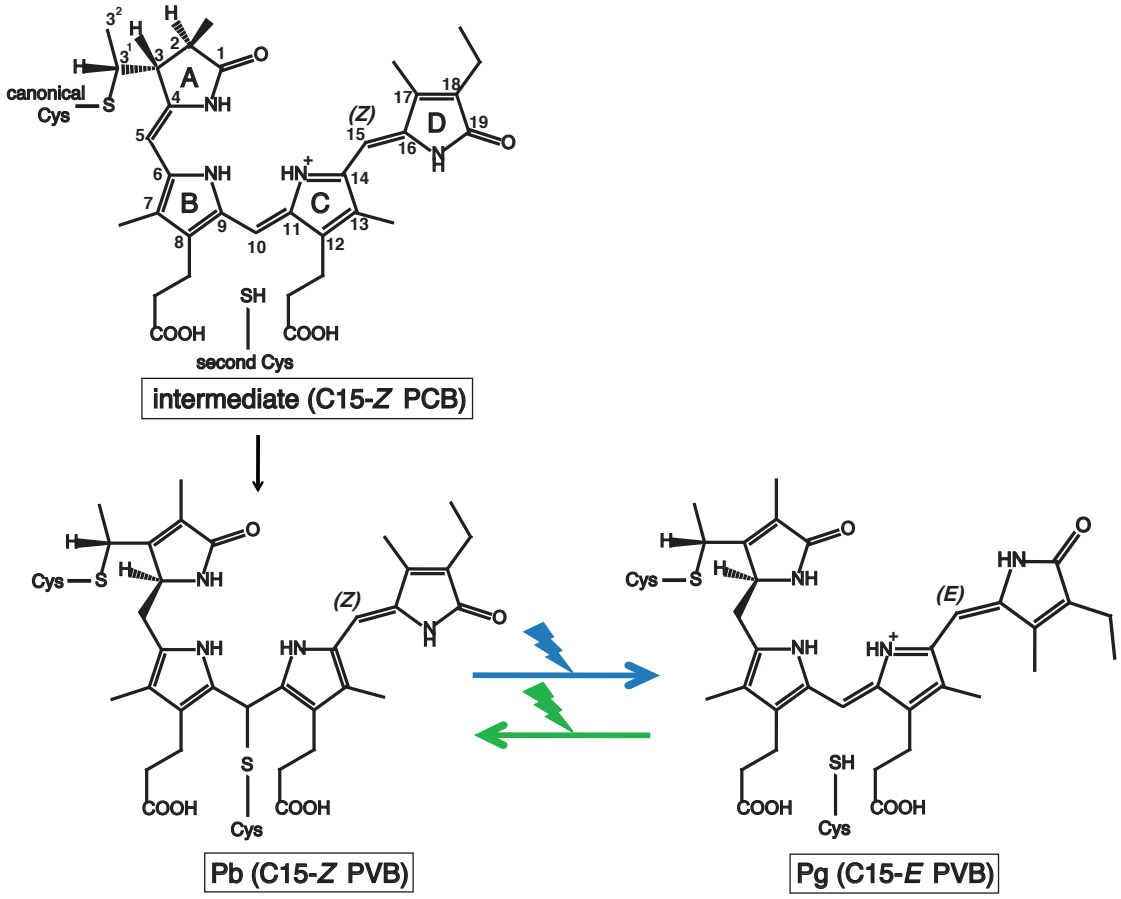

Fig. 1_1. The chromophore structure and the reversible Cys attachment model of Pb/Pg photoconversion.
Upper left, the assembly intermediate (C15-*Z* PCB), lower left, the Pb form (C15-*Z* PVB with an additional thioether linkage between the second Cys and C10), and lower right, the Pg form (C15-*E* PVB without the additional linkage). The chromophore is anchored to the canonical Cys via thioether linkage at $C3^1$ of ring A. PCB is isomerized to PVB by auto-isomerase activity.

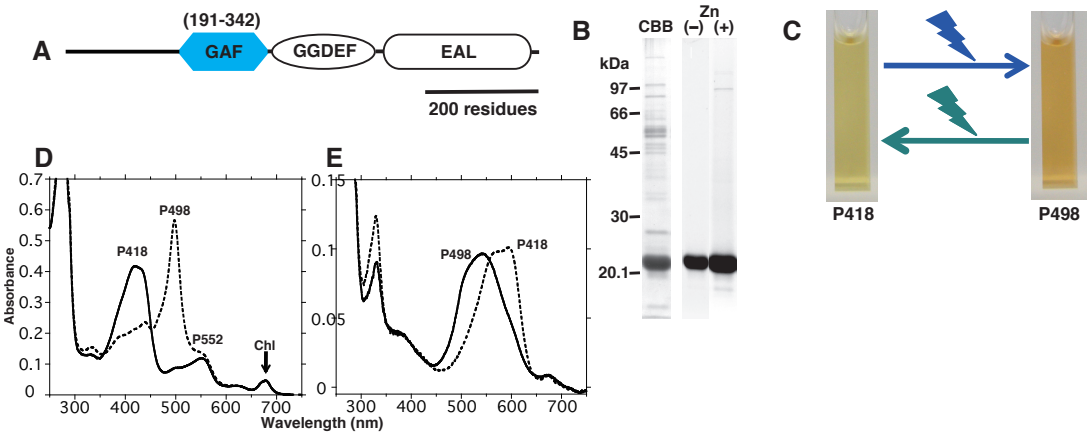

Fig. 1_2. SesB-GAF.
(***A***) Domain architecture of SesB (Tlr1999) according to the motif analysis made by SMART. (***B***) SDS-PAGE gels of His-tagged SesB-GAF (residues 191−342) purified from cyanobacterial cells. Left lane: CBB, after Coomassie Brilliant Blue staining. Fluorescence emission by SesB-GAF before (−, middle lane) and after (+, right lane) soaking the gel in Zn^{2+}. (***C***) Photographs of P418 and P498 in solution. (***D***) Absorption spectra of P418 (solid line) and P498 (broken line). Chl: absorbance peak associated with a chlorophyll contaminant. (***E***) Absorption spectra of denatured P498 (solid line) and P418 (broken line).

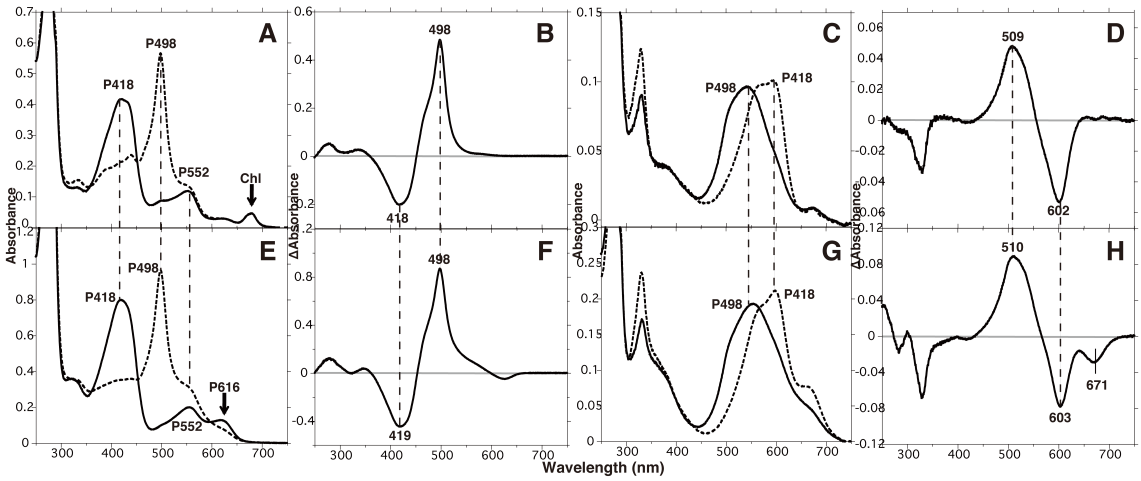

Fig. 1_3. Absorption and difference spectra of SesB-GAF purified from cyanobacterial cells (*A*~*D*) and *E. coli* (*E*~*H*).

(***A***,***E***) Absorption spectra of P418 (solid line) and P498 (broken line). (***B***,***F***) The difference spectra of P498 minus P418. (***C***,***G***) Absorption spectra of denatured P498 (solid line) and denatured P418 (broken line). (***D***,***H***) The difference spectra of the denatured P498 minus denatured P418. For comparison, the panel ***A*** and panel ***C*** were reproduced from **Fig. 1_2*D*** and ***E***, respectively.

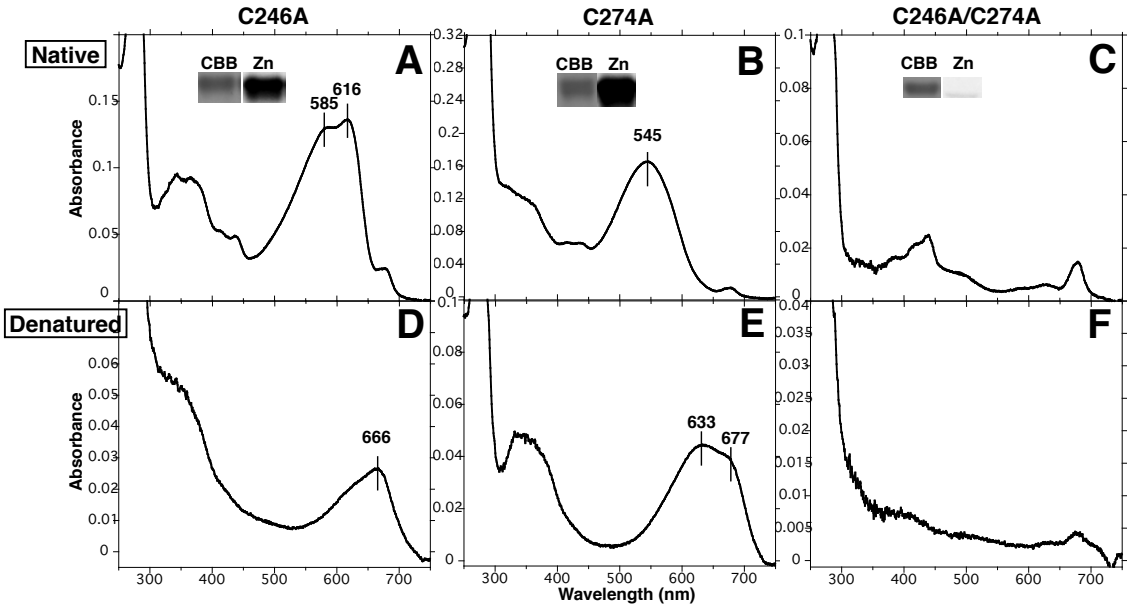

Fig. 1_4. Absorption spectra of SesB-GAF Cys → Ala mutants expressed in and purified from cyanobacterial cells.

Absorption spectra of native (***A***) C246A, (***B***) C274A, and (***C***) C246A/C274A. Absorption spectra of denatured (***D***) C246A, (***E***) C274A, and (***F***) C246A/C274A. Insets: protein in SDS-PAGE gels after Coomassie Brilliant Blue (CBB) staining (left panels) and fluorescence after soaking the gel in a Zn^{2+} solution (right panels).

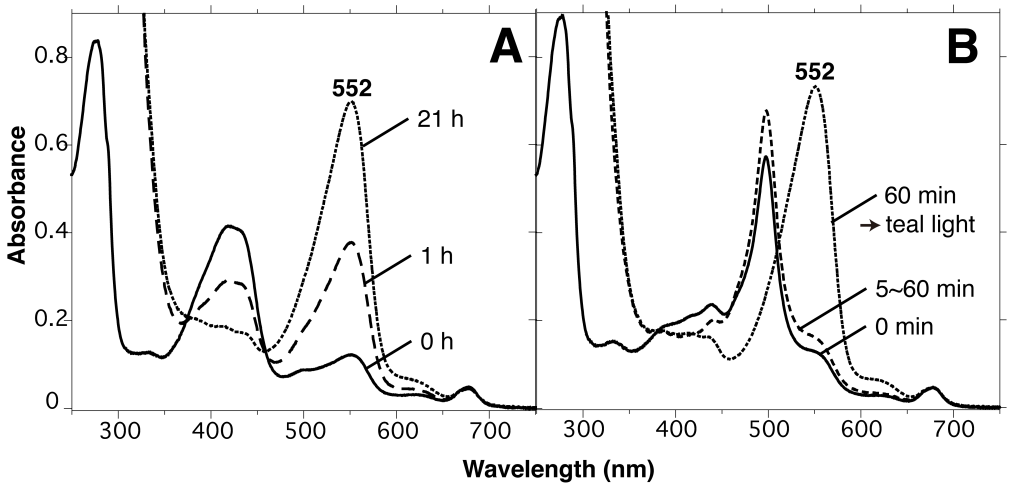

Fig. 1_5. Absorption spectra of IAM-modified SesB-GAF.
(***A***) 0 h (solid line), 1 h (broken line), and 21 h (dotted line) after reaction of P418 with 50 mM IAM. (***B***) 0 min (solid line) and 5 min (broken line) after reaction of P498 with 50 mM IAM. No further change in the absorption spectrum was observed after 5 min. After incubation for 1 h, P498 was irradiated with teal light (dotted line).

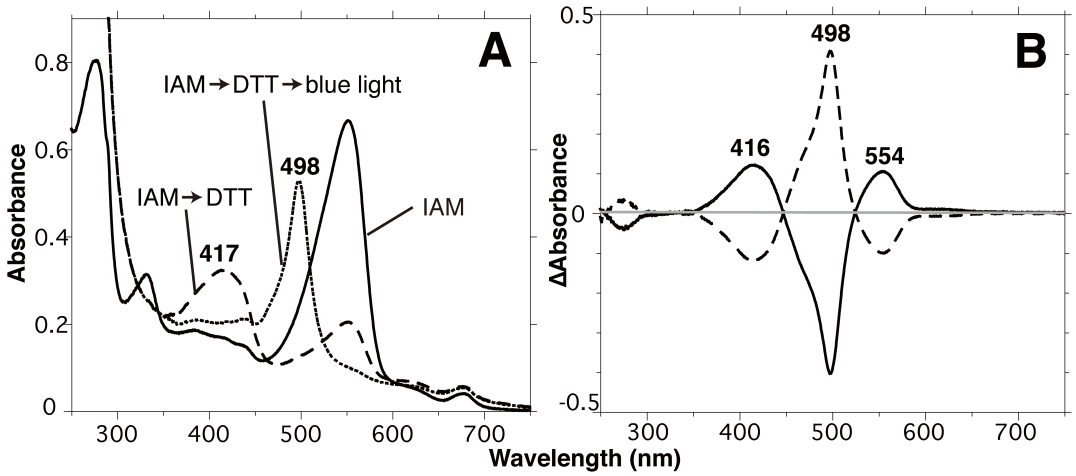

Fig. 1_6. Effects of DTT on IAM-modified SesB-GAF.
(***A***) Absorption spectra. Dialyzed, IAM-modified SesB-GAF (solid line) was treated with 20 mM DTT (broken line), irradiated with blue light (dotted line), and then irradiated with teal light (spectrum not shown, but it was almost the same as that shown by the broken line). (***B***) Difference spectra. The photoconversion by blue light shown in (***A***) (solid line) and the subsequent photoconversion with teal light (broken line). The spectra were shown as before −after light irradiation.

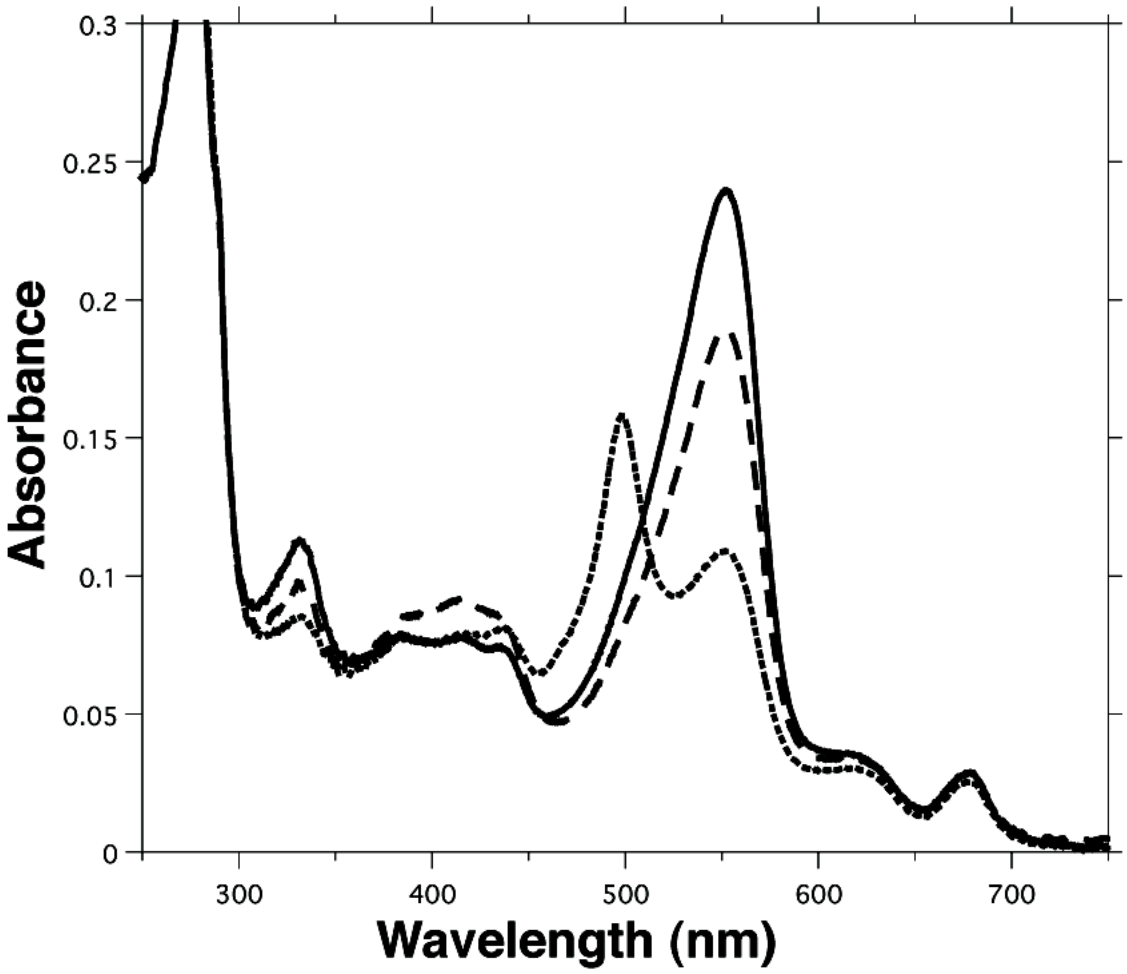

Fig. 1_7. Treatment of IAM-modified SesB-GAF with L-cysteine.
Absorption spectra. The IAM-modified SesB-GAF after dialysis (solid line) was treated with 30 mM L-cysteine (broken line) and then irradiated with blue light (dotted line).

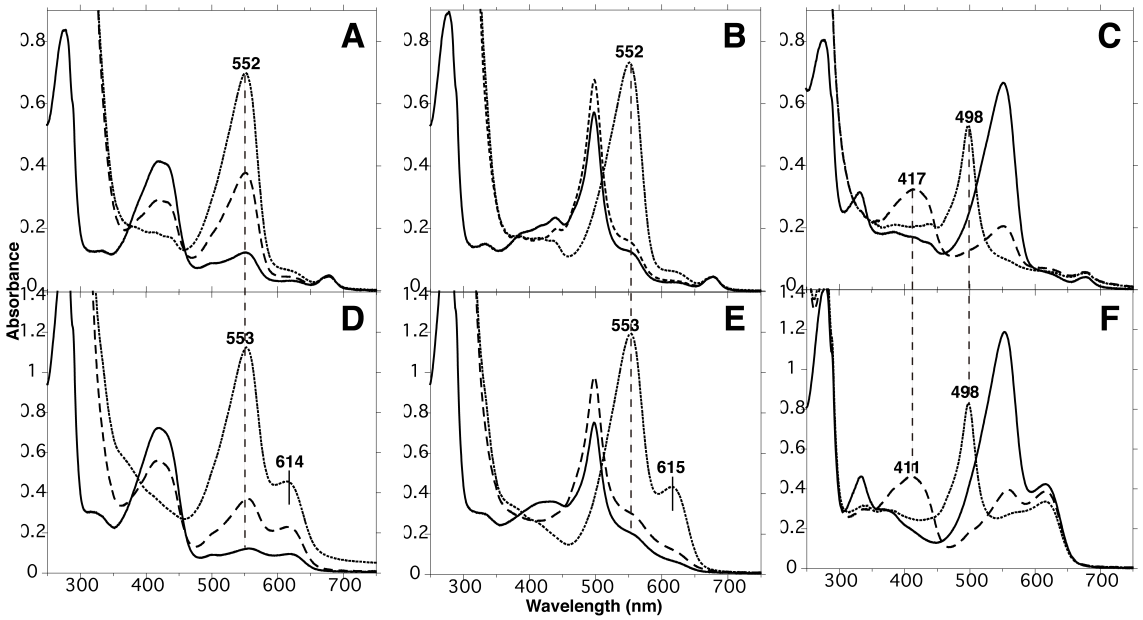

Fig. 1_8. Effects of IAM and DTT on SesB-GAF from *E. coli* in comparison with those from cyanobacterial cells.

Absorption spectra. (***A***~***C***) Protein prepared from cyanobacterial cells; (***D***~***F***) Protein prepared from *E. coli*. (***A***,***D***) 0 h (solid line), 1 h (broken line), and 21 h (dotted line) after reaction of P418 with 50 mM IAM. (***B***,***E***) 0 h (solid line) and 5 min (broken line) after reaction of P498 with 50 mM IAM. No further change in the absorption spectrum was observed after 5 min. After incubation for 1 h, P498 was irradiated with teal light (dotted line). (***C***,***F***) Dialyzed, IAM-modified SesB-GAF (solid line) was treated with 20 mM DTT (broken line), irradiated with blue light (dotted line). For comparison, the panel ***A***, ***B***, and ***C*** were reproduced from **Fig. 1_5*A***, ***B***, and **Fig. 1_6*A***, respectively.

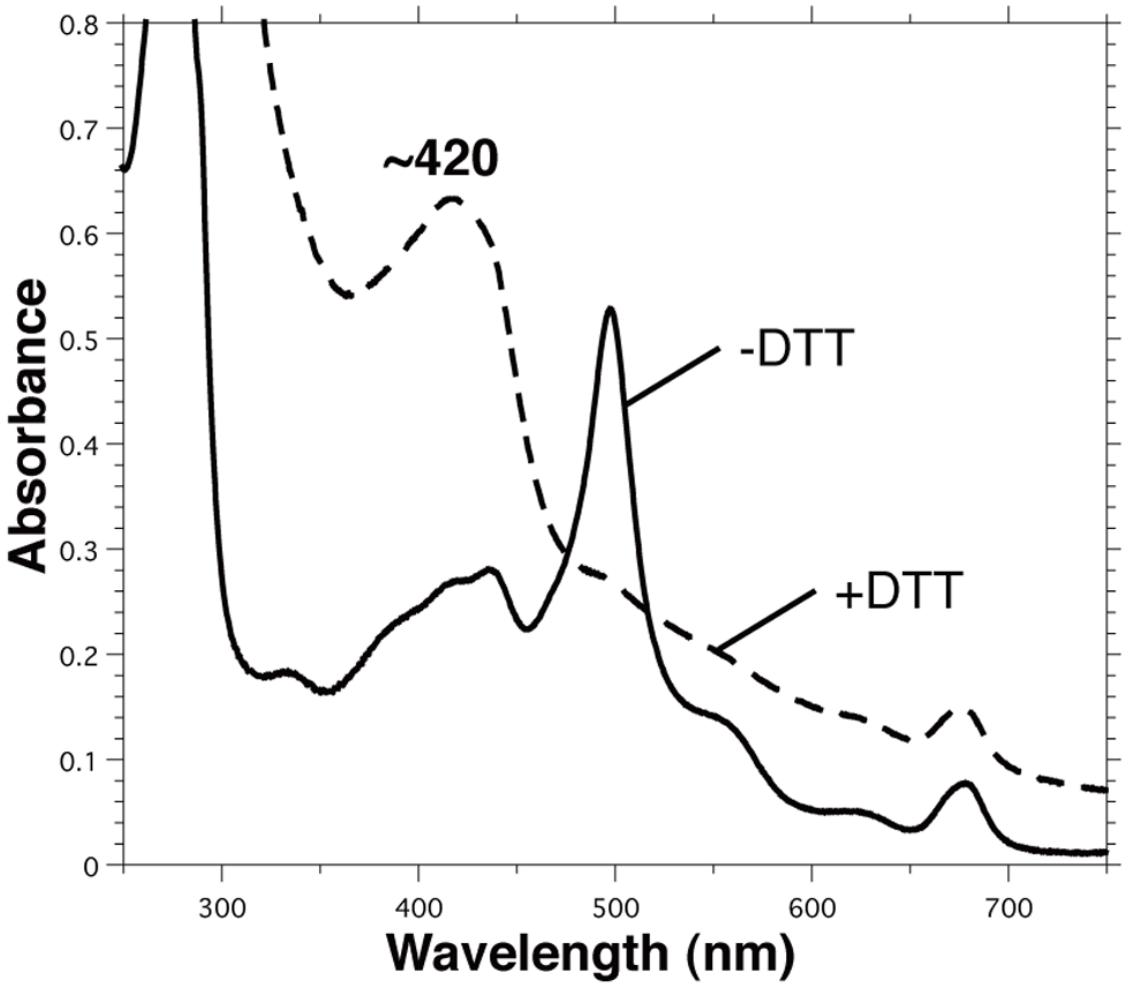

Fig. 1_9. Treatment of unmodified P498 with 1 M DTT.
Absorption spectra before (solid line) and after (broken line) DTT treatment.

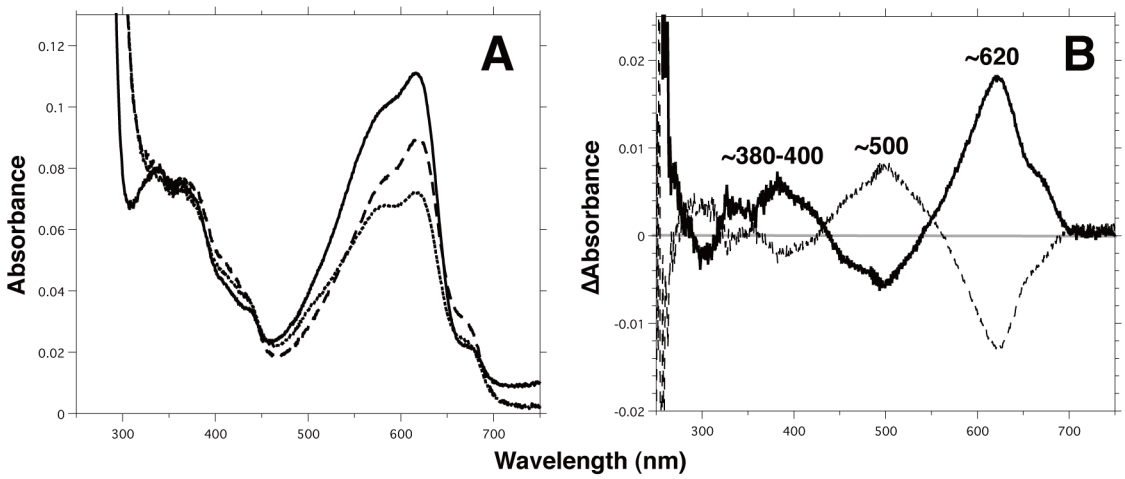

Fig. 1_10. Treatment of C246A with β ME.
(***A***) Absorption spectra of C246A (solid line) after treatment with 1% β ME (broken line) followed by blue-light irradiation (dotted line) and then teal-light irradiation (spectrum not shown, but it was almost the same as that shown by the broken line). (***B***) Difference spectra. The photoconversion by blue light shown in (***A***) (solid line) and the subsequent photoconversion with teal light (broken line). The spectra were shown as before−after light irradiation.

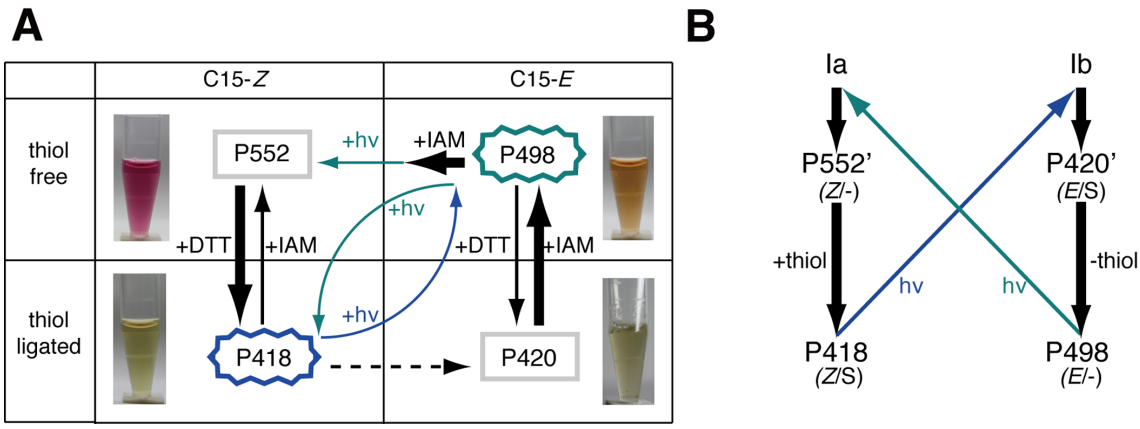

Fig. 1_11.

(***A***) Summary of IAM modification and DTT treatment of SesB-GAF. Blue/teal arrows indicate photoconversions. Thick black arrows indicate dark reactions that occur rapidly, and thin black arrows indicate dark reactions that occur slowly or are unfavorable. Note that P418 and P498 are photoactive species, whereas P552 and P420 are photoinactive species. (***B***) A model for the SesB-GAF photocycle. *Z* or *E*, C15-*Z* or C15-*E*, respectively; S or −, thiol-ligated or thiol-free PVB, respectively. See text for descriptions of Ia, Ib, P552′, and P420′.

~Chapter 2~

Three cyanobacteriochromes work together to form a light color-sensitive input system for c-di-GMP signaling of cell aggregation

Abstract

Cyanobacteriochromes (CBCRs) are cyanobacterial photoreceptors that have diverse spectral properties and domain compositions. Although large numbers of CBCR genes exist in cyanobacterial genomes, no studies have assessed whether multiple CBCRs work together. Our laboratory recently showed that the diguanylate cyclase (DGC) activity of the CBCR SesA from *Thermosynechococcus elongatus* is activated by blue-light irradiation and that, when irradiated, SesA, likely via its product cyclic dimeric GMP (c-di-GMP), induces aggregation of *Thermosynechococcus vulcanus* cells at a temperature that is sub-optimum for single-cell viability. For this report, I first characterize the photobiochemical properties of two additional CBCRs, SesB and SesC. Blue/teal light-responsive SesB has only c-di-GMP phosphodiesterase (PDE) activity, which is up-regulated by teal light and GTP. Blue/green light-responsive SesC has DGC and PDE activities. Its DGC activity is enhanced by blue light, whereas its PDE activity is enhanced by green light. A Δ*sesB* mutant cannot suppress cell aggregation under teal-green light. A Δ*sesC* mutant shows a less sensitive cell-aggregation response to ambient light. Δ*sesA*/Δ*sesB*/Δ*sesC* shows partial cell aggregation, which is accompanied by the loss of color dependency, implying that a nonphotoresponsive DGC(s) producing c-di-GMP can also induce the aggregation. The results suggest that SesB enhances the light color dependency of cell aggregation by degrading c-di-GMP, is particularly effective under teal light, and, therefore, seems to counteract the induction of cell aggregation by SesA. In addition, SesC seems to improve signaling specificity as an auxiliary backup to SesA/SesB activities. The coordinated action of these three CBCRs highlights why so many different CBCRs exist.

Introduction

The functions of SesB and SesC to our knowledge had not been characterized before this report, but the presence of a CBCR-GAF domain in these two proteins implied that they might also be involved in the light-regulated cell aggregation.

For this study, I first characterized the photobiochemical properties of SesA, SesB, and SesC from the thermophilic cyanobacteria *T. vulcanus* and *T. elongatus* that had been expressed in and purified from a cyanobacterial expression system, and then investigated the effects of disruption of *sesA*, *sesB*, and *sesC* separately and in combination with the temperature-sensitive aggregation of *T. vulcanus*. I also performed heterologous expression of *E. coli*-derived DGC and PDE to reveal the role of c-di-GMP.

I found coordinated regulation of cell aggregation by SesA, SesB, and SesC via c-di-GMP signaling, which partially explains why multiple CBCR and c-di-GMP synthesis/degradation proteins are present in cyanobacteria.

Results

Photobiochemical Properties of SesA.

Previously, Our laboratory reported the physiological role of *T. vulcanus sesA* together with the photobiochemical properties of SesA protein from the closely related *T. elongatus* (Enomoto *et al.*, 2014). Here, I prepared the full-length *T. vulcanus* SesA holoprotein (~90.5 kDa) from a cyanobacterial expression system and confirmed that it is indeed a blue light-induced DGC (**Fig. 2_1** and **2_2*A***).

Spectral Properties.

I isolated the full-length *T. vulcanus* SesB holoprotein (~93.6 kDa; **Fig. 2_3*A***) from a cyanobacterial expression system (**Fig. 2_3*B***) and showed that it reversibly photoconverts between a blue light-absorbing form (Pb; λ_{max} 417 nm) and a teal light-absorbing form (Pt; λ_{max} 498 nm) (**Fig. 2_3*C*** and **2_2*B***). The light-induced difference spectrum of urea/acid-denatured SesB shows that its chromophore is phycoviolobilin (PVB). These results are consistent with my previous analyses on the CBCR-GAF domain of *T. elongatus* SesB (Chapter 1).

I also prepared the full-length *T. vulcanus* SesC holoprotein (~145.7 kDa; **Fig. 2_4*A***) from cyanobacterial cells (**Fig. 2_4*B***) and showed that it reversibly photoconverts between a blue light-absorbing form (Pb; λ_{max} 415 nm) and a green light-absorbing form (Pg; λ_{max} 522 nm) (**Fig. 2_4*C*** and **2_2*C***). The bound chromophore is PVB.

Although there are one and three amino acid differences in the *T. vulcanus* and *T. elongatus* SesB and SesC homologs, respectively (**Fig. 2_5**), *T. elongatus* SesB and SesC showed spectral properties similar to the corresponding ones in *T. vulcanus* (**Fig. 2_6** and **2_7**). When prepared in *E.*

coli, all three CBCR proteins (SesA, SesB, and SesC) contain both PVB and phycocyanobilin (PCB) (**Fig. 2_8**) (Chapter 1) (Rockwell *et al.*, 2012a), and SesA and SesC show two independent photoconversions (**Fig. 2_9**) (Rockwell *et al.*, 2012b). Conversely, when these CBCRs are expressed in cyanobacteria their chromophore is PVB, and they have only a single photoconversion cycle that occurs in a similar spectral window, although their effective wavelengths are distinct.

DGC and PDE Activities.

SesB and SesC have GGDEF-type DGC and EAL-type PDE domains that might be involved for signal (c-di-GMP) output. I measured the DGC and PDE activities of the full-length *T. vulcanus* SesB and SesC holoproteins from the cyanobacterial expression system and found that SesB has no DGC activity under blue- or teal-light conditions but has PDE activity that is enhanced under teal light rather than under blue light (**Fig. 2_3*D***), indicating that SesB degrades c-di-GMP mainly when exposed to teal light. Therefore, SesB represents a previously unidentified type of CBCR, that is, one that can degrade c-di-GMP. Addition of GTP further substantially enhances this newly uncovered PDE activity of SesB under blue and teal light (**Fig. 2_3*D***), whereas ATP has no effect (**Fig. 2_2*D***). In SesB, the consensus GGDEF motif (Römling *et al.*, 2013) is replaced with GSDEF (**Fig. 2_5*A***). As mentioned above, SesB does not show DGC activity, suggesting that its degenerate GGDEF domain may act instead as a GTP-binding domain to regulate its PDE activity, which would be functionally similar to that of the degenerate GGDEF domain in CC3396 (PdeA) from *Caulobacter crescentus*, which has the noncanonical motif GEDEF (Christen *et al.*, 2005). The teal-on/blue-off PDE activity of SesB is compatible with the blue-on/green-off DGC activity of SesA (Enomoto *et al.*, 2014), in that c-di-GMP is increased under blue light and decreased under teal and green

light.

SesC has DGC activity that is enhanced under blue light and decreased under green light (**Fig. 2_4*D***). It also has PDE activity that is enhanced under green light and decreased under blue light (**Fig. 2_4*E***), which indicates that SesC is a blue/green sensor/regulator of c-di-GMP levels. SesC is, therefore, the first protein, to our knowledge, whose photosensory CBCR-GAF domain appears to regulate two distinct output activities—c-di-GMP synthesis and degradation. Interestingly, the spectral dependency of SesC is also compatible with the aforementioned regulation of c-di-GMP levels by light color.

I confirmed that the SesB and SesC homologs from *T. elongatus* have photobiochemical properties similar to the corresponding ones in *T. vulcanus*. *T. elongatus* SesB is a teal light- and GTP-activated PDE (**Fig. 2_6**), and *T. elongatus* SesC is a blue light-induced DGC/green light-induced PDE bifunctional protein (**Fig. 2_7**).

Single-Gene Mutagenesis.

In contrast to the very closely related *T. elongatus*, *T. vulcanus* shows cellulose-dependent cell aggregation under blue light and at a low temperature (31 °C) that is not optimal for viability and replication (Kawano *et al.*, 2011, Enomoto *et al.*, 2014). To assess the roles of *T. vulcanus* SesA, SesB, and SesC in cell aggregation, I disrupted those genes to create strains that lack *sesA* and/or *sesB* and/or *sesC* (Δ*sesA*, Δ*sesB*, and Δ*sesC*, respectively). I cultured these strains at 31 °C for 48 h under violet (λ_{max} 404 nm), blue (λ_{max} 448 nm), teal-green (λ_{max} 507 nm), or red light (λ_{max} 634 nm) at a photon flux density of 5 μmol photon·m^{-2}·s^{-1} (**Fig. 2_10**). In all cases, the strains were also irradiated with red light (30 μmol photon·m^{-2}·s^{-1}) to support phototrophic viability without affecting the activities of SesA, SesB, and SesC. To determine the effect of disrupted Ses genes, I calculated

the relative number of aggregated to total cells (reported as the aggregation index; %) (Kawano *et al.*, 2011) (**Fig. 2_11*A***). I also present the aggregation indexes for the mutants as a function of light wavelength (**Fig. 2_11*B***).

Aggregation of wild-type *T. vulcanus* is strictly dependent on violet- and blue-light irradiation, and no aggregation occurred under teal-green and red light. Δ*sesA* did not aggregate under any of the light conditions, which is a finding consistent with a previous report in my laboratory (Enomoto *et al.*, 2014). Δ*sesB* showed apparently enhanced cell aggregation under all light conditions, which was significantly different from that of wild type when cells were exposed to teal-green light. These results indicate that SesB is a negative regulator of cell aggregation and fine-tune the effective light range allowed for cell aggregation upon blue/violet-light irradiation. For Δ*sesC*, the dependency of cell aggregation on the specific color of light appeared to be weakened but not significantly different from that for wild type. However, the Δ*sesC* aggregation index fluctuated compared with that of wild type, indicating that SesC improves the specificity of the c-di-GMP signal in the cell-aggregation system.

Double- and Triple-Gene Mutagenesis.

Δ*sesA*/Δ*sesB* restored cell aggregation (**Fig. 2_12**, violet line), even though Δ*sesA* could not aggregate under any light-color conditions (**Fig. 2_11**). The restored cell aggregation was up-regulated by blue light and down-regulated by teal-green light. Because the cell-aggregation results for Δ*sesA*/Δ*sesB* are consistent with the observation that SesC is a dual sensor/regulator of c-di-GMP levels, I hypothesized that SesC in Δ*sesA*/Δ*sesB* was responsible for cell aggregation. This hypothesis was strengthened by assessing the effect of Δ*sesA*/Δ*sesB*/Δ*sesC* on cell aggregation. Disruption of all three genes resulted in partial cell aggregation, which was accompanied by the loss of color dependency (**Fig. 2_12**, brown line). The uncoupling of the light-color and

cell aggregation for Δ*sesA*/Δ*sesB*/Δ*sesC* also implies that no other photoreceptor is involved in cell aggregation. Moreover, because Δ*sesA*/Δ*sesB*/Δ*sesC* can still aggregate, a light-independent, parallel c-di-GMP signaling pathway(s) operating on an unidentified target(s) appears to be present. Thus, SesC improves the specificity of the c-di-GMP signal that induces cell aggregation, possibly by sequestering c-di-GMP from a parallel c-di-GMP pathway(s). In addition to *sesA*, *sesB*, and *sesC*, six other genes exist in the *T. vulcanus* genome that encode a GGDEF domain, and some may be involved in a parallel pathway(s).

Because neither Δ*sesA*/Δ*sesC* (**Fig. 2_12**, orange line) nor Δ*sesA* (**Fig. 2_11*B***, red line) aggregated, it appears that in the absence of SesC, only SesA is capable of triggering cell aggregation and that SesB can only negatively regulate cell aggregation to counteract the effects of SesA, although I cannot rule out that the expression of *sesC* might be impaired in Δ*sesA*, as described for RcaE/IflA (Bussell & Kehoe, 2013). Cell aggregation of Δ*sesB*/Δ*sesC* is increased under blue light and decreased under teal-green light (**Fig. 2_12**, dark green line), which is consistent with the presence of SesA providing DGC activity. Under teal-green or red light, however, SesA appears to work as a negative regulator of cell aggregation (compare the results for Δ*sesB*/Δ*sesC* and Δ*sesA*/Δ*sesB*/Δ*sesC* in **Fig. 2_12**), which implies that SesA might bind and sequester c-di-GMP in the allosteric product-inhibition site of its GGDEF domain (Chan *et al.*, 2004) that is produced by a parallel pathway(s). In summary, none of the mutants displayed the cell aggregation-related wild-type color sensitivity, which, therefore, underscores my proposal that all three photoreceptors are needed for color-sensitive cell aggregation.

Heterologous Expression of DGC and PDE.

To confirm that c-di-GMP is an activating factor for cell aggregation, I

created two heterologous expression mutants, one that expressed DGC-encoding *ydeH* (Zahringer *et al.*, 2013) and one that expressed PDE-encoding *yhjH* (Pesavento *et al.*, 2008), both from *E. coli* in wild-type *T. vulcanus*. The mutant that expressed *ydeH* showed strong cell aggregation under all light colors (**Fig. 2_13**). Conversely, the mutant that expressed *yhjH* showed greatly decreased cell aggregation compared with that of wild type under all light colors (**Fig. 2_13**). These results demonstrate that c-di-GMP is, indeed, a critical factor that can trigger cell aggregation and that the dependency of light color on cell aggregation at low temperature(s) is regulated by the c-di-GMP levels produced/degraded by SesA, SesB, and SesC.

Discussion

For this report, I identified and characterized a color-sensitive, cyanobacterial c-di-GMP signaling system composed of three CBCRs: (*i*) SesA, a blue light-activated DGC; (*ii*) SesB, a teal light- and GTP-activated PDE; and (*iii*) SesC, a bifunctional CBCR with DGC activity induced by blue light and PDE activity induced by green light (**Fig. 2_14*A***). A large number of photoreceptors have been found in cyanobacteria, and the results herein demonstrate that some may work in concert. Multiple blue-light receptors, such as PixA (Narikawa *et al.*, 2011, Song *et al.*, 2011b), PixJ (Yoshihara & Ikeuchi, 2004), PixD (Okajima *et al.*, 2005), and Cph2 (Savakis *et al.*, 2012), are known to regulate *Synechocystis* phototaxis, but their combined effects have not been evaluated. In moss and ferns, chloroplast relocation is regulated by a phytochrome or neochrome photoreceptor with activity regulated by a red/far-red photocycle and a blue light-receptor phototropin (Hughes, 2013). However, the effects of these light colors likely cannot be discriminated by moss and ferns, because the activities of the two photoreceptors have been assumed to work under very low light intensity (Kawai *et al.*, 2003).

SesA is the main trigger of cell aggregation in *T. vulcanus*, because Δ*sesA* did not aggregate under any of the tested light conditions (**Fig. 2_11**). SesB serves to counteract the activity of SesA, because the presence of SesB appears to be necessary for cell-aggregation suppression under all light-color conditions in Δ*sesA* (**Fig. 2_11**) and Δ*sesA*/Δ*sesC* (**Fig. 2_12**). More specifically, SesB prevents cell aggregation of the teal-green light–irradiated wild-type strain by degrading c-di-GMP, as shown in Δ*sesB* (**Fig. 2_11**). Thus, I concluded that SesB is a light color-specificity enhancer. It is of note that SesB Pt has the narrowest absorption peak, owing to the trapped-twist form of its chromophore (**Fig. 2_3*C***, teal line) (Rockwell *et al.*, 2014b, Rockwell *et*

al., 2012b). Even though teal light-absorbing CBCRs are commonly found, their physiological roles have not been delineated. It is very likely that, because the SesB Pt peak is sharp and blue-shifted compared with the Pg peaks, SesB can confine the cell-aggregation response to irradiation by shorter wavelengths of light, resulting in color specificity.

I concluded that SesC is a signaling-specificity enhancer because Δ*sesC* is less sensitive in cell-aggregation responses under all tested light colors (**Fig. 2_11**). SesC seems to have an auxiliary backup-type role in comparison with the SesA/SesB pair, because the contribution of SesC to cell aggregation is most noticeable only when *sesA* and *sesB* are disrupted (**Fig. 2_12**). SesC may help sequester c-di-GMP generated in the cell aggregation-signaling pathway from another parallel c-di-GMP signaling pathway(s). SesC responds to a wider range of light wavelengths than do SesA and SesB (**Fig. 2_14*B***). SesC produces c-di-GMP under shorter-wavelength conditions than does SesA. SesC also degrades c-di-GMP under longer-wavelength conditions than does SesB. Because of these properties, SesC should broaden the effective range of light wavelengths without deteriorating color specificity. The coordination of the three CBCRs is, therefore, crucial for light wavelength-sensitive cell aggregation. This study provides the first clue, to our knowledge, as to why many CBCRs and c-di-GMP synthesis/degradation proteins are needed in a simple bacterial cell.

Physiologically, photosynthesis is driven by visible light, but blue light also damages the manganese cluster of the oxygen-evolving complex of photosystem II in plants and cyanobacteria (Nishiyama *et al.*, 2011). Cell aggregation is effective in protection against blue light-induced damage by self-shading especially at relatively low temperature (suboptimal conditions for damage repair), whereas cell aggregation should be avoided to perform photosynthesis effectively under other light conditions. Thus, survival and photosynthetic production could be optimized by the complex light

color-sensitive regulatory system.

SesB and SesC as Targets of Intramolecular Signaling.

The SesB GGDEF domain seems to respond to the presence of GTP, and its CBCR-GAF domain responds to blue and teal light. Although further work is needed to confirm the binding of GTP to the GGDEF domain of SesB, both domains seem to regulate its single signal-output domain, which is the EAL domain (**Fig. 2_3*D***). In SesC, a single CBCR-GAF domain regulates the DGC activity of the GGDEF domain and the PDE activity of the EAL domain in an opposing manner (**Fig. 2_4*D*,*E***). Many GGDEF and EAL domains are present in tandem in a single polypeptide chain (approximately one-third of all GGDEF domains and approximately two-thirds of all EAL domains) (Römling *et al.*, 2013). In certain of these hybrid proteins, either a GGDEF or EAL domain is the enzymatically active domain; although the other domain is inactive, it may modulate the activity of the neighboring domain. For example, in *C. crescentus* CC3396 (PdeA), the inactive GGDEF domain still binds GTP and, thereby, enhances the activity of the EAL domain (Christen *et al.*, 2005). SesB is a composite protein, with an inactive GGDEF domain that can still bind GTP and an N-terminal photosensory CBCR-GAF domain that, under blue and teal light, regulates the PDE activity of its C-terminal EAL domain.

There are a few other GGDEF/EAL hybrid proteins known to have DGC and PDE activities (Römling *et al.*, 2013). *Shewanella woodyi* DGC and, probably, *Vibrio parahaemolyticus* ScrC, regulate both their GGDEF and EAL domain activities independently but with the aid of interacting partner proteins (Liu *et al.*, 2012, Ferreira *et al.*, 2008). Notably, SesC is the first example, to our knowledge, of a protein containing GGDEF and EAL domains that regulates the activities of these domains via an intramolecular photosensory domain. Generally, proteins containing active GGDEF and

EAL domains are dimeric and their dimerization interfaces often modulate their DGC and PDE activities (Barends *et al.*, 2009, Zahringer *et al.*, 2013, Chan *et al.*, 2004). GAF domains including those of CBCRs often transduce the input signal via a rotary movement of a connecting α-helix toward a neighboring output domain (Narikawa *et al.*, 2013, Gasser *et al.*, 2014). Further characterization of SesB and SesC should clarify their intramolecular signaling and any possible intermolecular signaling with interacting proteins, which then might be used to design chimeric sensor proteins.

C-Di-GMP Signaling Specificity.

A major feature of c-di-GMP signaling is redundancy; many c-di-GMP synthesis/degradation domains (GGDEF/EAL/HD-GYP) are found in bacterial genomes, including those of cyanobacteria. A second feature of c-di-GMP signaling is its specificity; c-di-GMP produced or degraded by an individual DGC or PDE regulates a subset of all possible c-di-GMP–regulated responses, even though canonical second messengers, such as c-di-GMP, are thought to be a diffusible intracellular pool of molecules (Römling *et al.*, 2013). The great specificity of c-di-GMP signaling may be accomplished by intracellular compartmentalization of the various DGC/PDE and c-di-GMP receptor proteins, so that these proteins would have available only a local supply of c-di-GMP (Tuckerman *et al.*, 2011). *Thermosynechococcus* spp. may be a suitable system for elucidating the basis for c-di-GMP signaling specificity, because the number of *Thermosynechococcus* spp. c-di- GMP synthesis/degradation genes is only 10; the cell has a large, elongated rod-like shape, which is suitable for localization studies, and it is thermally stable, which is suitable for biochemical studies.

Materials and Methods

Plasmid Constructions.

Primers used are listed in **Table 2_1**. Plasmids were constructed using the In-Fusion System (TaKaRa). To express *Thermosynechococcus elongatus* or *Thermosynechococcus vulcanus* SesA, SesB, and SesC individually in *E. coli* C41 (DE3) or in the cyanobacterium *Synechocystis* sp. PCC 6803, protein-encoding DNA was cloned into pET28a (Novagen) or pTCH2031V, respectively. The protease recognition site in each original plasmid for removal of the N-terminal His tag was replaced with one for tobacco etch virus (TEV) protease, which could be used for future purification. The *E. coli rrnB* terminator sequence was inserted after the C terminus of the protein-encoding region incorporated into pTCH2031V.

For disruption of *sesB* (*tlr1999*) in the thermophilic cyanobacterium *T. vulcanus* strain RKN (equivalent to National Institute for Environmental Studies 2134) that shows positive phototaxis, a kanamycin-resistance cassette was inserted at the EcoRV site inside the protein-coding region. For disruption of *sesC* (*tlr0911*) in *T. vulcanus*, most of the protein-encoding region was deleted and a spectinomycin/streptomycin-resistance cassette was inserted in its place. The protocol for disruption of *sesA* (*tlr0924*) in *T. vulcanus* has been reported (Enomoto *et al.*, 2014). For expression of *E. coli ydeH* encoding DGC in *T. vulcanus*, the DNA construct included the *psaA* promoter (–4 to –622 of *psaA* of *T. vulcanus*), *ydeH* protein-encoding region, and *E. coli rrnB* terminator sequence and was introduced downstream of *tlr2443* as a neutral site. For expression of *E. coli* PDE *yhjH* in *T. vulcanus*, a similar construct was used except that the synthetic promoter *trc* replaced the *psaA* promoter.

Cyanobacterial Strains and Cultures.

The thermophilic cyanobacterium *T. vulcanus* strain RKN that shows positive phototaxis was cultured at 45 °C or 31 °C in BG11 medium as described (Enomoto *et al.*, 2014). Culture density was monitored at 730 nm. Transformations of *T. vulcanus* were performed according to ref. (Enomoto *et al.*, 2014). The antibiotic concentration in BG11 medium for selection of transformants was 5 μg·mL^{-1} chloramphenicol, 80 μg·mL^{-1} kanamycin, or 10 μg·mL^{-1} spectinomycin plus 5 μg·mL^{-1} streptomycin.

Protein Purification.

E. coli and *Synechocystis* protein-expressing cells were harvested by centrifugation at 4,450 × *g* for 10 min, suspended in 50 mM Hepes·NaOH (pH 7.5), 300 mM NaCl, 10% (wt/vol) glycerol, 0.5 mM Tris(2-carboxylethyl)phosphine, and then frozen at −80 °C. After thawing, cells were subjected to three rounds of disruption using a French press (5501-M; Ohtake) at 1,500 kg·cm^{-2}. The homogenate from the cyanobacterial cells was centrifuged at 12,000 × *g* for 10 min and then at 194,100 × *g* for 30 min. The *E. coli* homogenate was centrifuged at 194,100 × *g* for 30 min. Each supernatant was filtered and then loaded onto a nickel-affinity His-Trap chelating column (GE Healthcare). Proteins were eluted with a linear gradient of 30–430 mM imidazole in 20 mM Hepes·NaOH (pH 7.5), 300 mM NaCl, 10% (wt/vol) glycerol, 0.5 mM Tris(2-carboxylethyl)phosphine. EDTA (1 mM) was added to the pooled peak fractions, which were then dialyzed against 20 mM Hepes·NaOH (pH 7.5), 300 mM NaCl, 10% (wt/vol) glycerol, 1 mM DTT.

SDS/PAGE and Spectroscopy.

SDS/PAGE, followed by Zn^{2+}-enhanced fluorescence detection and

Coomassie Brilliant Blue staining, of recombinant SesB and SesC was performed as described (Chapter 1). The zinc-induced fluorescence from a protein band in SDS/PAGE gels indicates that a linear tetrapyrrole (bilin) is covalently bound to the protein. Absorption spectra were recorded using a UV-2600PC spectrophotometer (Shimadzu). For the photoconversion of SesB, a blue-light light-emitting diode (LED) (λ_{max} 392 nm; half-bandwidth, 12 nm) and a teal-light LED (λ_{max} 512 nm; half-bandwidth, 34 nm) were used. For the photoconversion of SesC, a blue-light LED and a green-light LED (λ_{max} 539 nm; half-bandwidth, 36 nm) were used. To determine the covalently bound chromophore compositions, the Pt form of SesB and Pg form of SesC proteins (C15-*E* forms) were first denatured in 8 M urea (pH 2.0) at room temperature in the dark and then irradiated with white light for 3 min. The difference spectra allow distinguishing PVB (negative peak at ~600 nm) from PCB (negative peak at ~660 nm) (Ishizuka *et al.*, 2007).

DGC and PDE Activity Assays.

The reaction mixture for *T. elongatus* SesB contained 50 mM Tris·HCl (pH 8.0), 10 mM $MgCl_2$, 0.5 mM EDTA, 50 mM NaCl, 100 μM GTP (Sigma-Aldrich) for DGC or 100 μM c-di-GMP (Biolog) for PDE. For some of the PDE assays, 100 μM GTP or ATP was added. Each reaction was initiated by addition of preirradiated protein (final concentration ~3 μM) to a prewarmed reaction mixture and incubated at 45 °C under blue or teal light. Each reaction was stopped by addition of EDTA (final concentration 20 mM) and immediately heated at 95 °C for 5 min, followed by centrifugation at 20,400 × *g* for 5 min. Each supernatant was subjected to HPLC. Reaction mixtures for *T. elongatus* SesC (0.2 μM), *T. vulcanus* SesA (0.1 μM), *T. vulcanus* SesB (0.3 μM), and *T. vulcanus* SesC (0.1 μM) contained 50 mM Tris·HCl (pH 8.0), 10 mM $MgCl_2$, 50 mM NaCl, 1 mM DTT, 100 μM GTP for DGC or 100 μM c-di-GMP for PDE. DGC activities of *T. elongatus* and *T.*

vulcanus SesC were measured at pH 6.8.

Nucleotides were separated by reversed-phase HPLC through a C18 column (150 mm × 6 mm i.d.; DAISOPAK SP-120-5-ODS-AP; Daiso). Samples (20 μL) were injected and eluted at 1.4 mL·min^{-1} using buffer A (100 mM potassium phosphate, 4 mM tetrabutylammonium hydrogen sulfate, pH 6.0) and buffer B (75% buffer A, 25% methanol) (Ryjenkov *et al.*, 2005) and the gradient protocol: 0.0, 0; 2.5, 0; 5.0, 30; 14.0, 40; 25.0, 100; 32.0, 100; 33.0, 50; and 34.0, 0 [the first of each set of values is the time (min) and the second in each set is the percentage of buffer B]. Nucleotides were detected at 254 nm. The internal standard NAD (final concentration 50 μM) was added to each sample just before an injection.

Cell-Aggregation Assays.

Cultures of wild-type *T. vulcanus* and its disrupted mutants were incubated at 45 °C (OD_{730} 0.5–2) and then diluted to give a culture OD_{730} of 0.2. These samples were then incubated at 31 °C for 48 h under photosynthetic red light (λ_{max} 634 nm; 30 μmol photon·m^{-2}·s^{-1}; Valore Corp.; **Fig. 2_10**) and, at the same time, some samples were irradiated with violet, blue, or teal-green light (λ_{max} 404, 448, or 507 nm, respectively; 5 μmol photon·m^{-2}·s^{-1}; Valore; **Fig. 2_10**). The results of the cellulose-dependent cell-aggregation assay, described as follows, are reported as an aggregation index (%) (Kawano *et al.*, 2011). Briefly, after the irradiation period, cell suspensions were thoroughly mixed and aliquots were transferred to cuvettes. The samples were held at room temperature for 30 min, during which time most of the aggregated cells had precipitated to the bottom of the cuvettes. Then the OD_{730} of each sample was measured (denoted OD_{NA}; i.e., OD_{730} of nonaggregated cells remaining in the culture medium). Next, cellulase (12.5 U·mL^{-1}; Worthington Biochemical) was added to each cuvette sample, which were then incubated for 30 min at 37 °C to completely disperse the aggregated

cells. The OD_{730} of each sample (denoted OD_{total}) was then measured. The aggregation index (%) is defined as $((OD_{total} - OD_{NA})/OD_{total}) \times 100$.

Figures and Tables

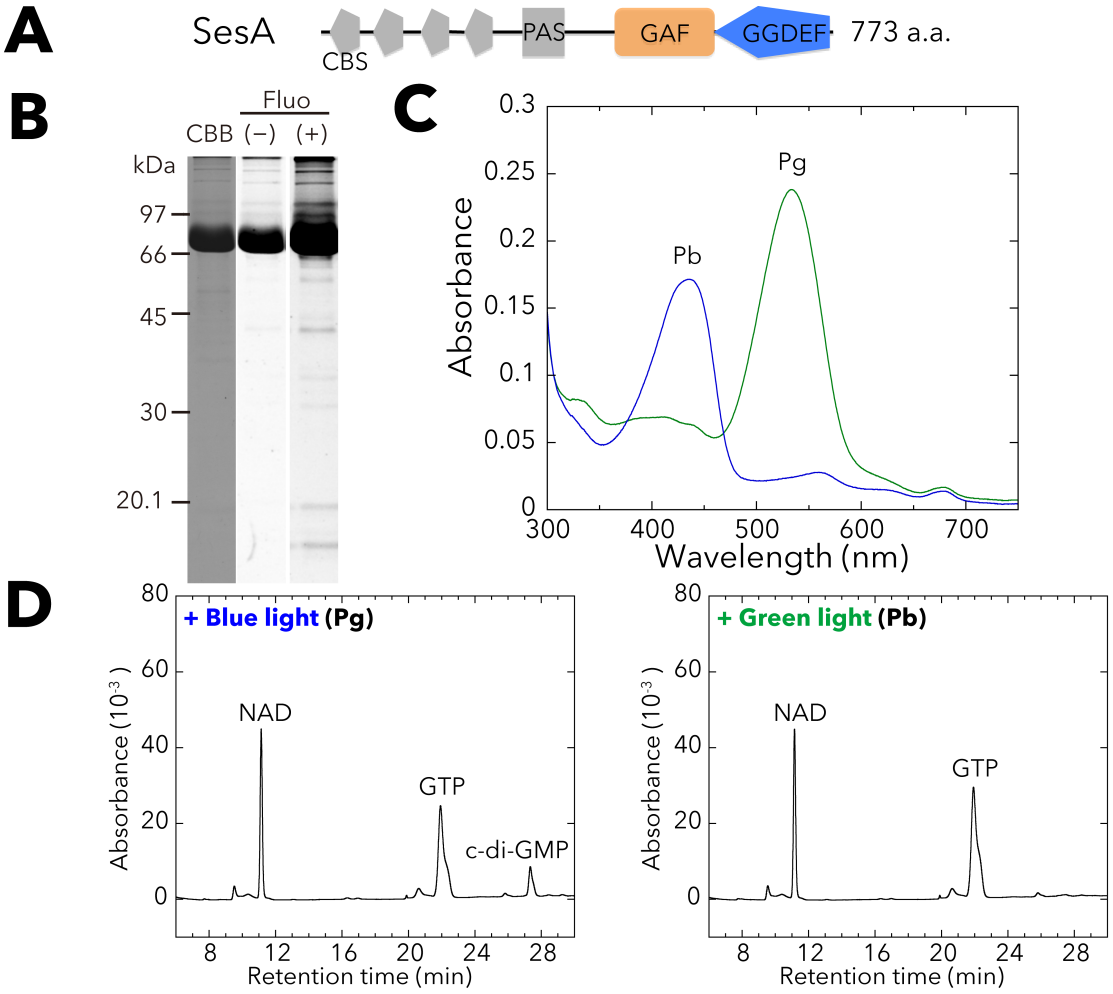

Fig. 2_1. Photobiochemical properties of *T. vulcanus* SesA.
The full-length SesA holoprotein was prepared in and purified from the cyanobacterial expression system. (***A***) Domain architecture of SesA (Tlr0924) deduced by SMART (smart.embl-heidelberg.de). CBS, cystathionine beta synthase; PAS, Per/ARNT/Sim. (***B***) SDS/PAGE of SesA after Coomassie Brilliant Blue (CBB) staining and fluorescence (Fluo) in the gel before (-) and after (+) Zn^{2+} addition. (***C***) Absorption spectra of native SesA Pb (blue line) after irradiation with green light, and SesA Pg (green line) after irradiation with blue light. (***D***) HPLC chromatograms assessing SesA DGC activity (GTP→c-di-GMP). NAD served as the internal control. Reaction mixtures, including 100 μM GTP, were incubated for 5 min under blue light (Left) or green light (Right).

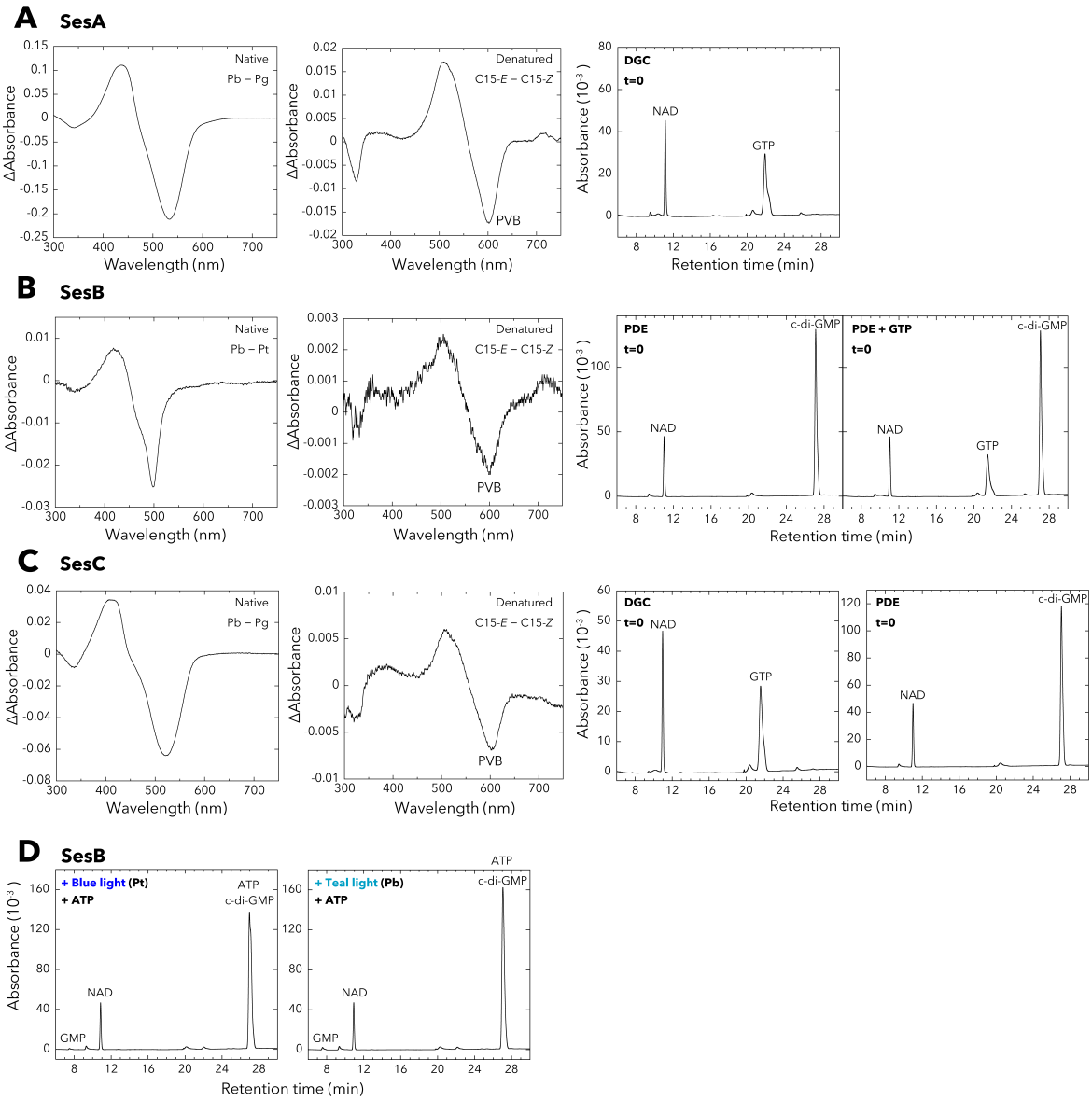

Fig. 2_2. Properties of the full-length *T. vulcanus* SesA, SesB, and SesC holoproteins expressed in and purified from the cyanobacterial expression system.
(***A***, Left) Difference spectrum of the absorption spectra of native SesA Pb and Pg. (Middle) White light-induced difference spectrum of the chromophore (C15-*E* – C15-*Z*) for the urea/acid-denatured SesA. (Right) Control HPLC chromatogram for the DGC assay of SesA (incubation: 0 min). NAD served as the internal control. (***B***, Left) Difference spectrum of the absorption spectra of native SesB Pb and Pt. (Middle) White light-induced difference spectrum of the chromophore (C15-*E* – C15-*Z*) for the urea/acid-denatured SesB. (Right) Control HPLC chromatograms for the PDE assays of SesB (incubation: 0 min). NAD served as the internal control. (***C***, Left) Difference spectrum of the absorption spectra of native SesC Pb and Pg. (Middle) White light-induced difference spectrum of the chromophore (C15-*E* – C15-*Z*) for the urea/acid-denatured SesC. (Right) Control HPLC chromatograms for the DGC/PDE assays of SesC (incubation: 0 min). NAD served as the internal control. (***D***) SesB is a PDE (c-di-GMP→pGpG) that is not affected by ATP. NAD served as the internal control. Reaction mixtures including 100 μM c-di-GMP with 100 μM ATP were incubated for 10 min under blue light (Left) or teal light (Right).

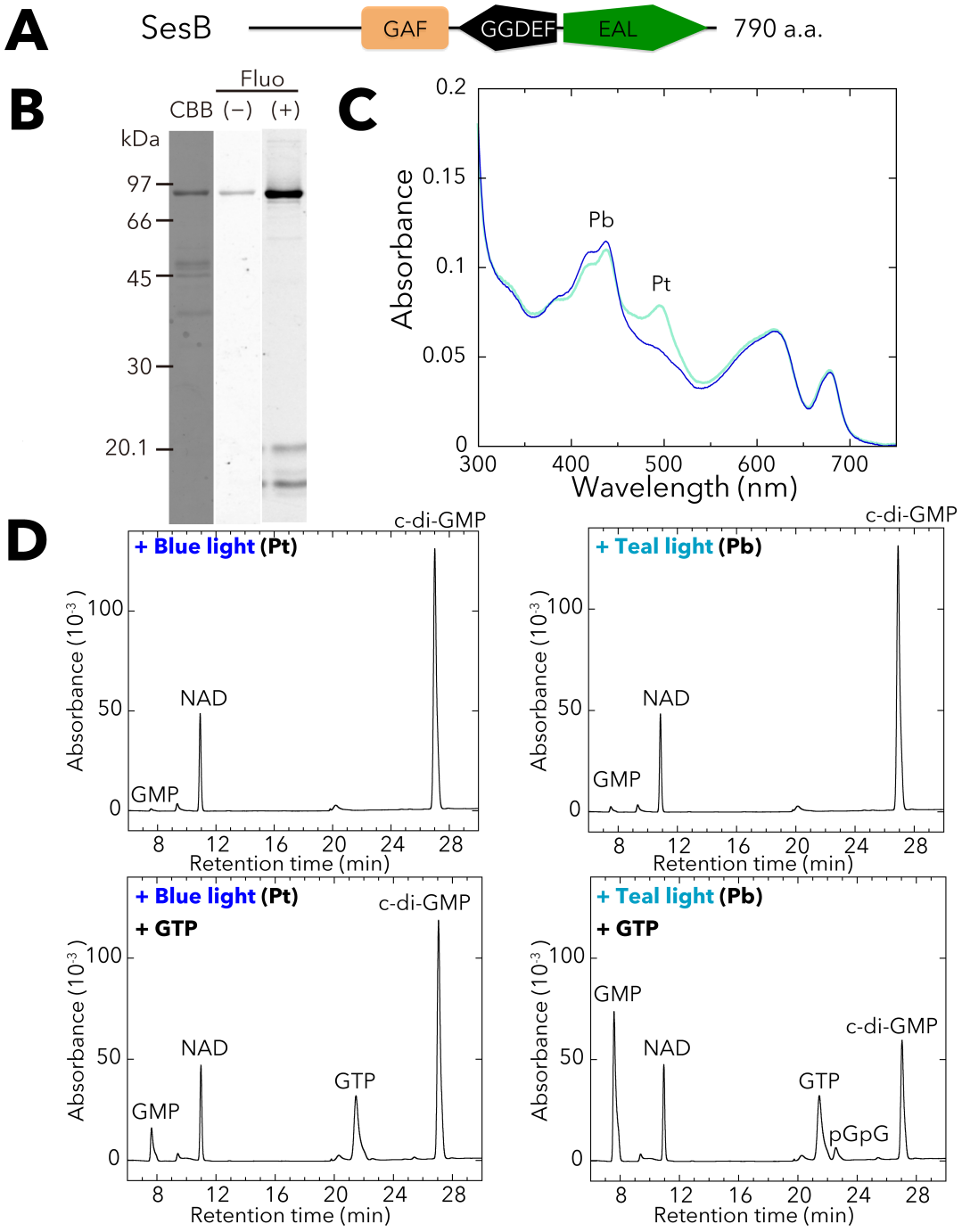

Fig. 2_3. Photobiochemical properties of *T. vulcanus* SesB.
The full-length SesB holoprotein was prepared in and purified from the cyanobacterial expression system. (***A***) Domain architecture of SesB (Tlr1999) deduced by SMART. (***B***) SDS/PAGE of SesB after CBB staining and the fluorescence in the gel before (–) and after (+) Zn^{2+} addition. (***C***) Absorption spectra of native SesB Pb (blue line) after irradiation with teal light, and SesB Pt (teal line) after irradiation with blue light. (***D***) HPLC chromatograms assessing SesB PDE activity (c-di-GMP→pGpG→GMP). NAD served as the internal control. The reaction mixtures including 100 μM c-di-GMP (substrate) were incubated for 10 min under blue light (Left) or teal light (Right). Addition of 100 μM GTP (Lower) under both light conditions enhanced PDE activity, compared with reactions performed without GTP (Upper).

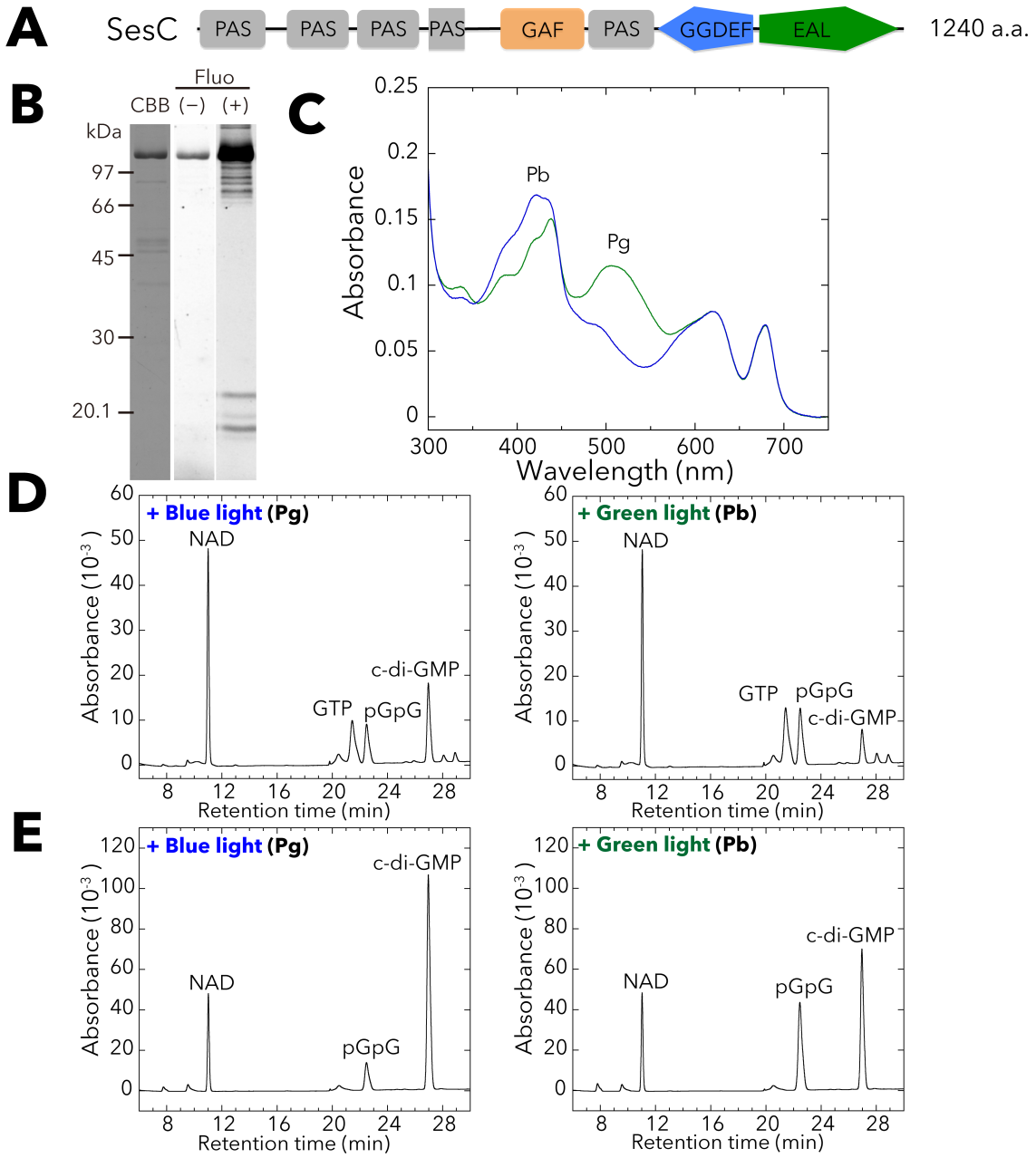

Fig. 2_4. Photobiochemical properties of *T. vulcanus* SesC.
The full-length SesC holoprotein was prepared in and purified from the cyanobacterial expression system. (***A***) Domain architecture of SesC (Tlr0911) deduced by SMART. (***B***) SDS/PAGE of SesC after CBB staining and the fluorescence in the gel before (–) and after (+) Zn^{2+} addition. (***C***) Absorption spectra of native SesC Pb (blue line) after irradiation with green light, and SesC Pg (green line) after irradiation with blue light. (***D***) HPLC chromatograms assessing SesC DGC activity (GTP→c-di-GMP). NAD served as the internal control. Reaction mixtures, including 100 μM GTP, were incubated for 10 min under blue light (Left) or green light (Right). pGpG was produced from c-di-GMP, the DGC product, via the accompanying SesC PDE activity. (***E***) HPLC chromatograms assessing SesC PDE activity (c-di-GMP→pGpG→GMP). NAD served as the internal control. The reaction mixtures, including 100 μM c-di-GMP, were incubated for 10 min under blue light (Left) or green light (Right).

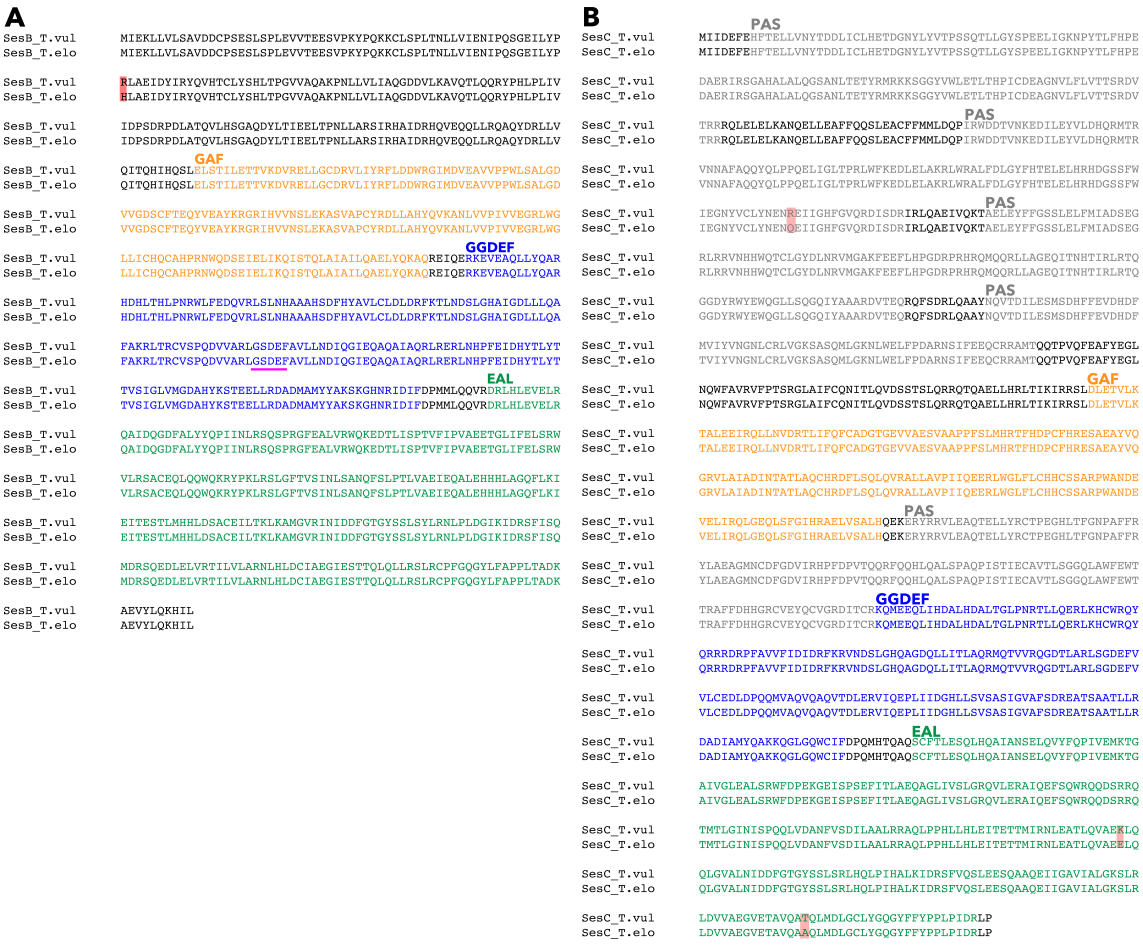

Fig. 2_5.
(***A***) Amino acid sequence alignment of *T. vulcanus* and *T. elongatus* SesB. The degenerate motif in the GGDEF domain of SesB is underlined in magenta. The residue that differs in the two sequences is shaded in red. (***B***) Amino acid sequence alignment of *T. vulcanus* and *T. elongatus* SesC. The residues that differ in the two sequences are shaded in pale red.

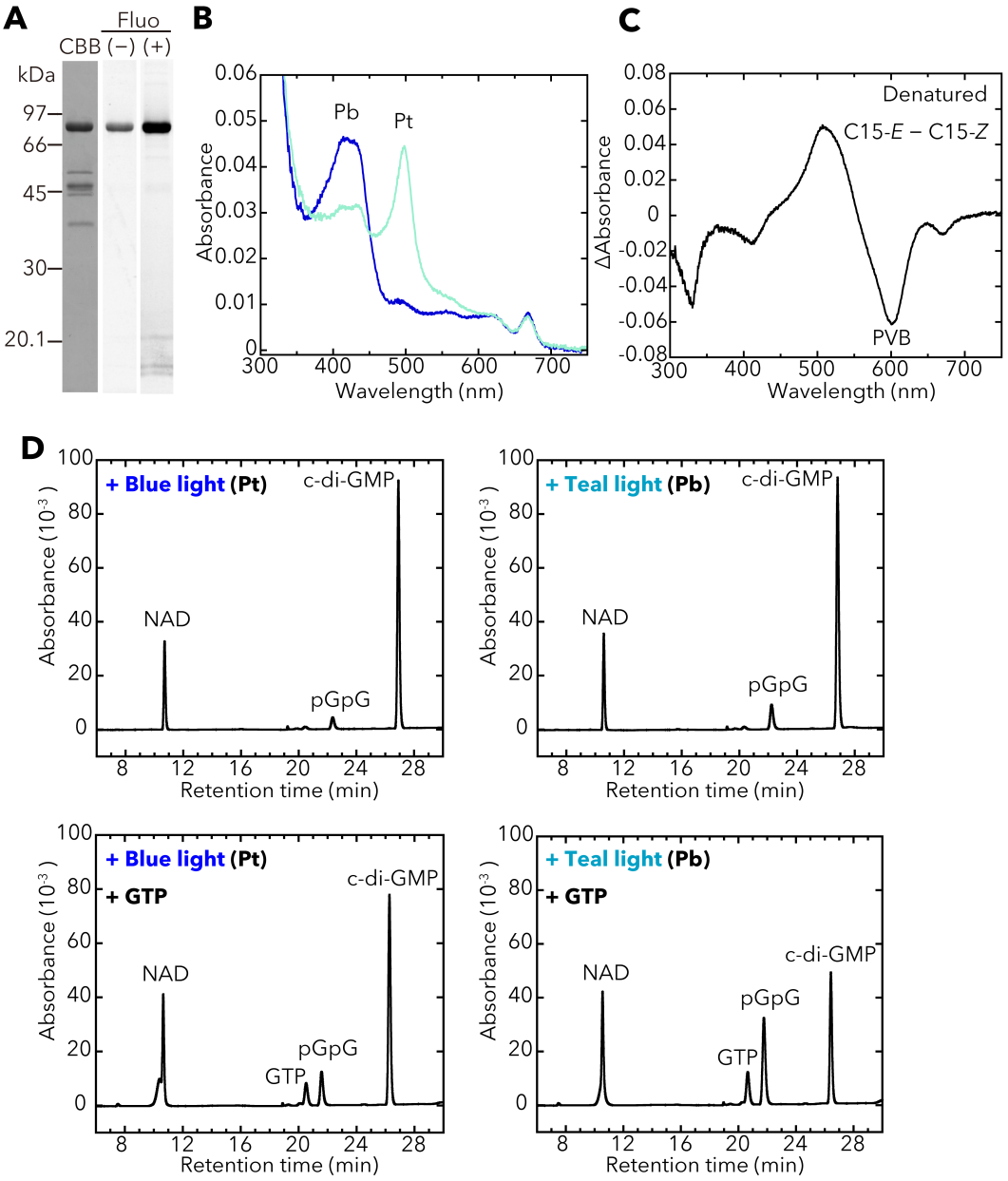

Fig. 2_6. Photobiochemical properties of the full-length *T. elongatus* SesB holoprotein expressed in and purified from the cyanobacterial expression system.
(***A***) SDS/PAGE. CBB, Coomassie brilliant blue stain; Fluo, fluorescence before (–) and after (+) Zn^{2+} addition. (***B***) Photoconversion. The SesB Pb absorption spectrum induced by irradiation with teal light is shown in blue. The SesB Pt absorption spectrum induced by irradiation with blue light is shown in teal. (***C***) The white light-induced difference spectra of the chromophore (C15-*E* − C15-*Z*) for the urea/acid-denatured SesB. (***D***) SesB is a PDE (c-di-GMP→pGpG) activated by teal light and GTP. NAD served as the internal control. Reaction mixtures, including 100 μM c-di-GMP, were incubated for 10 min under blue light (Left) or teal light (Right). Addition of 100 μM GTP (Lower) under both light conditions enhanced PDE activity, compared with reactions performed without GTP (Upper).

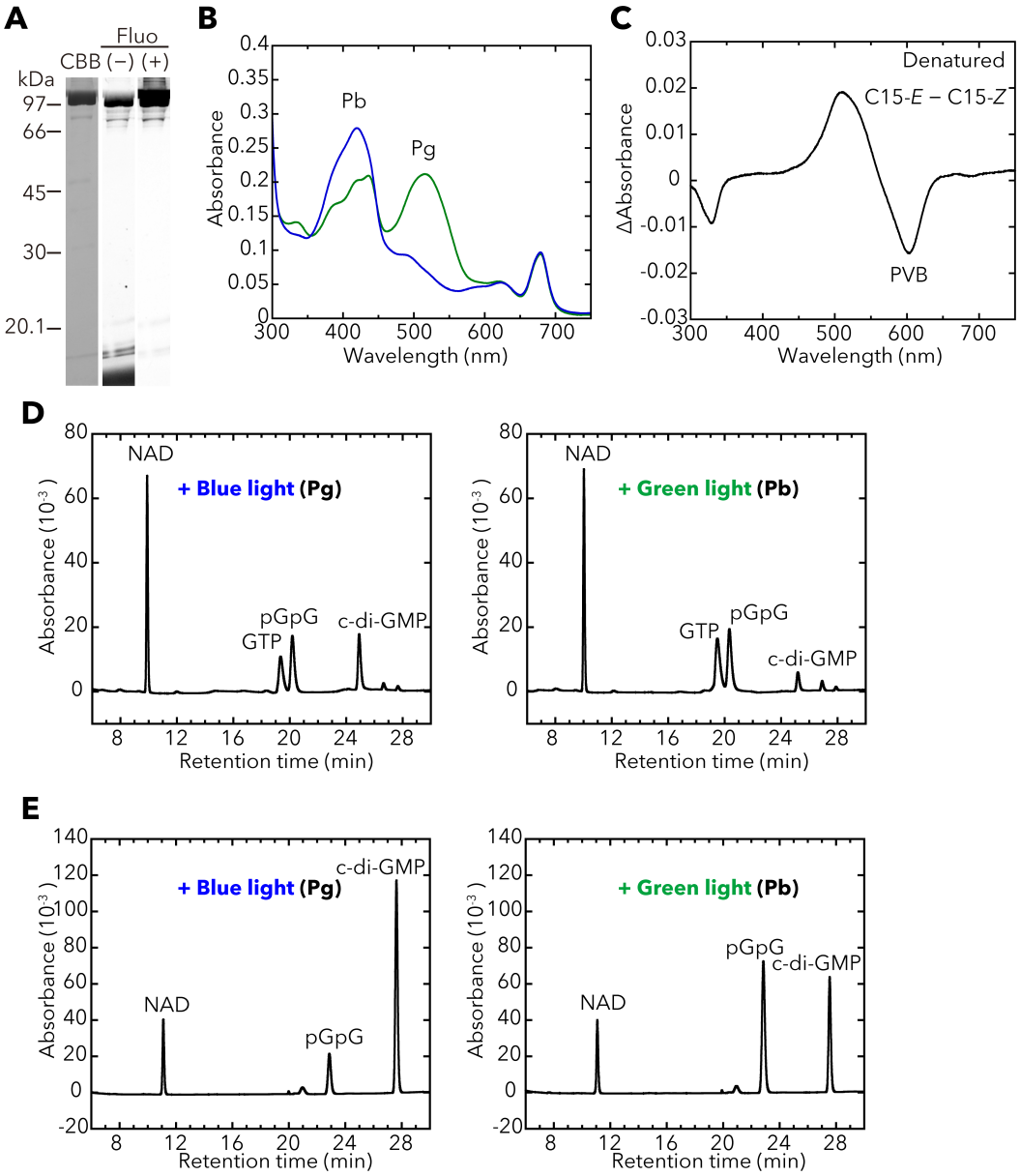

Fig. 2_7. Photobiochemical properties of the full-length *T. elongatus* SesC holoprotein expressed in and purified from the cyanobacterial expression system.
(***A***) SDS/PAGE. (***B***) Photoconversion. The SesC Pb absorption spectrum induced by irradiation with green light is shown in blue. The SesC Pg absorption spectrum induced by blue-light irradiation is shown in green. (***C***) The white light-induced difference spectra of the chromophore (C15-*E* − C15-*Z*) for the urea/acid-denatured SesC. (***D***) SesC is a DGC (GTP→ c-di-GMP) activated by blue light. NAD served as the internal control. Reaction mixtures, including 100 μM GTP, were incubated for 10 min under blue light (Left) or green light (Right). pGpG was produced from the DGC product, c-di-GMP, via SesC PDE activity. (***E***) SesC is a PDE (c-di-GMP→pGpG) activated by green light. NAD served as the internal control. The reaction mixtures, including 100 μM c-di-GMP, were incubated for 10 min under blue light (Left) or green light (Right).

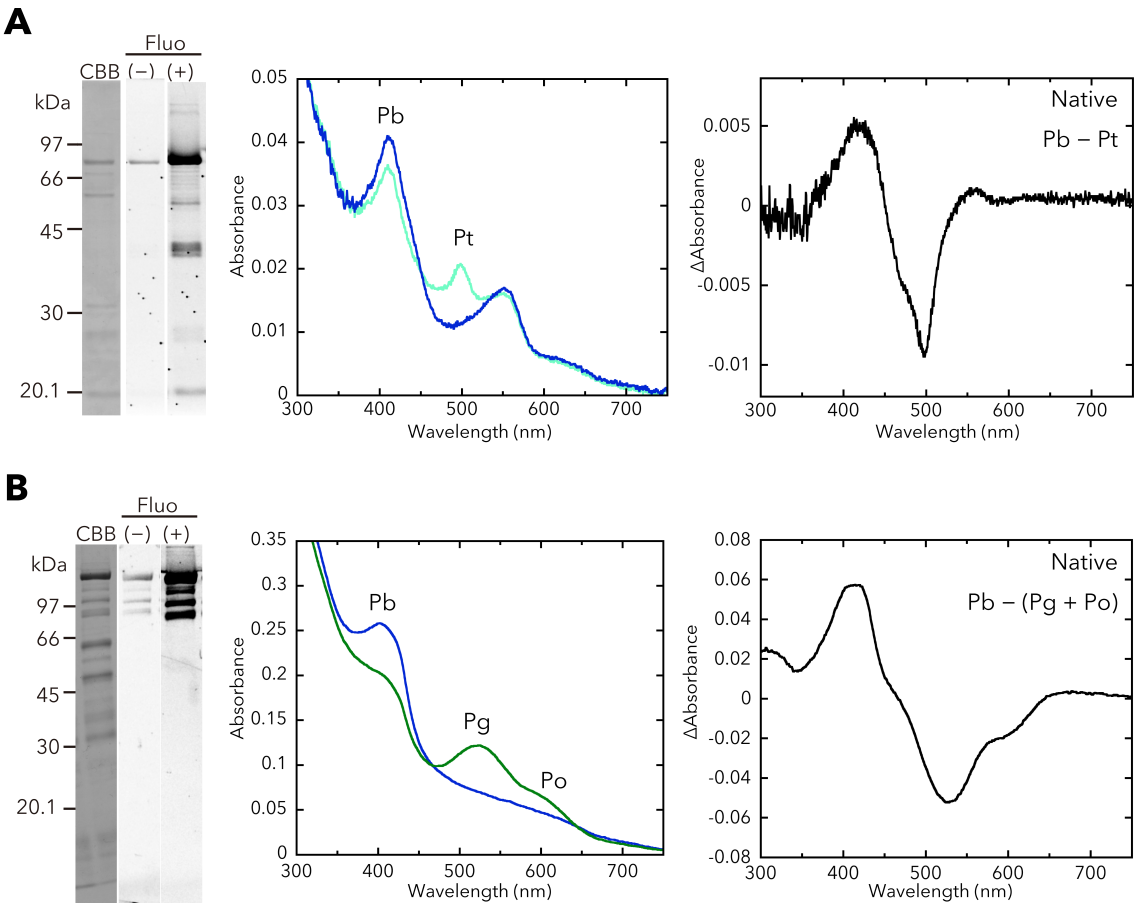

Fig. 2_8. Spectral properties of the full-length *T. elongatus* SesB and SesC holoproteins prepared in and purified from the *E. coli* expression system.
(***A***) SesB. (Left) SDS/PAGE of SesB after CBB staining and fluorescence before (–) and after (+) Zn^{2+} addition. (Middle) Absorption spectra of native SesB Pb (blue line) after irradiation with teal light, and SesB Pt (teal line) after irradiation with blue light. (Right) Difference spectrum for SesB Pb and Pt. (***B***) SesC. (Left) SDS/PAGE of SesC after CBB staining and fluorescence before (–) and after (+) Zn2+ addition. (Middle) Absorption spectra of native SesC Pb (blue line) after irradiation with green and orange light, and SesC Pg and an orange light-absorbing form (Po) (green line) after irradiation with blue light. (Right) Difference spectrum for SesC Pb and Pg plus Po

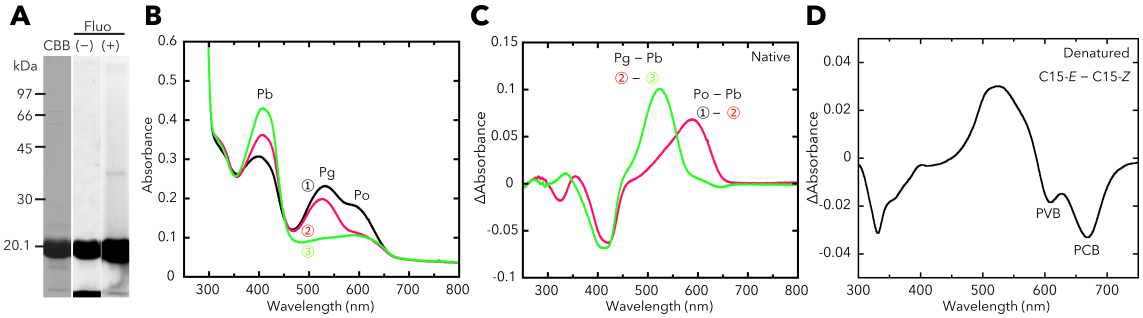

Fig. 2_9. Two independent photoconversions of SecC PCB and PVB.
The SesC-GAF protein was prepared in and purified from the E. coli expression system. (***A***) SDS/PAGE of SecC-GAF after CBB staining and fluorescence before (–) and after (+) Zn^{2+} addition. (***B***) Absorption spectra of native SesC-GAF after irradiation with blue light (black line; 1), then orange light (red line; 2), and finally green light (green line; 3). (***C***) Difference spectrum for the native SesC-GAF Pb and Po absorption spectra (red line), representing photoconversion of the PCB-bearing population, and the difference spectrum for the SesC-GAF Pb and Pg absorption spectra (green line), representing photoconversion of the PVB-bearing population. (***D***) The white light-induced difference spectra of the chromophore (C15-*E* – C15-*Z*) for the urea/acid-denatured SesC-GAF, representing the chromophore composition (PCB vs. PVB).

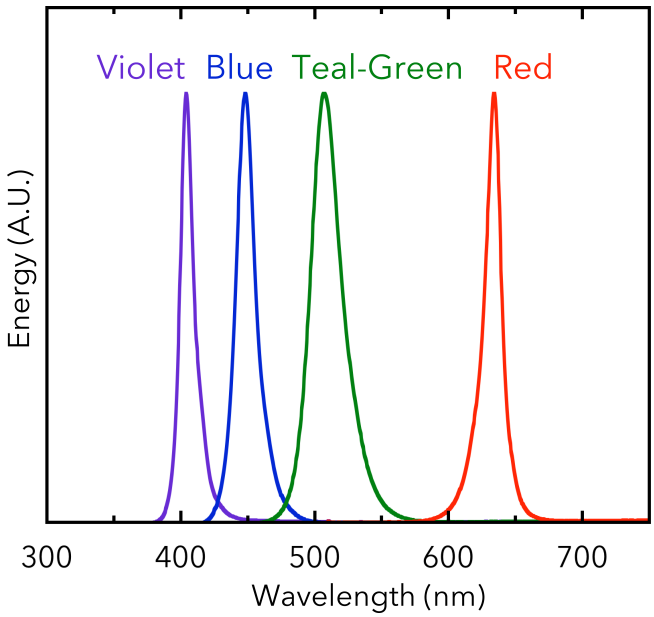

Fig. 2_10.
Energy spectra of the LEDs used for the cell-aggregation assays. A.U., arbitrary units.

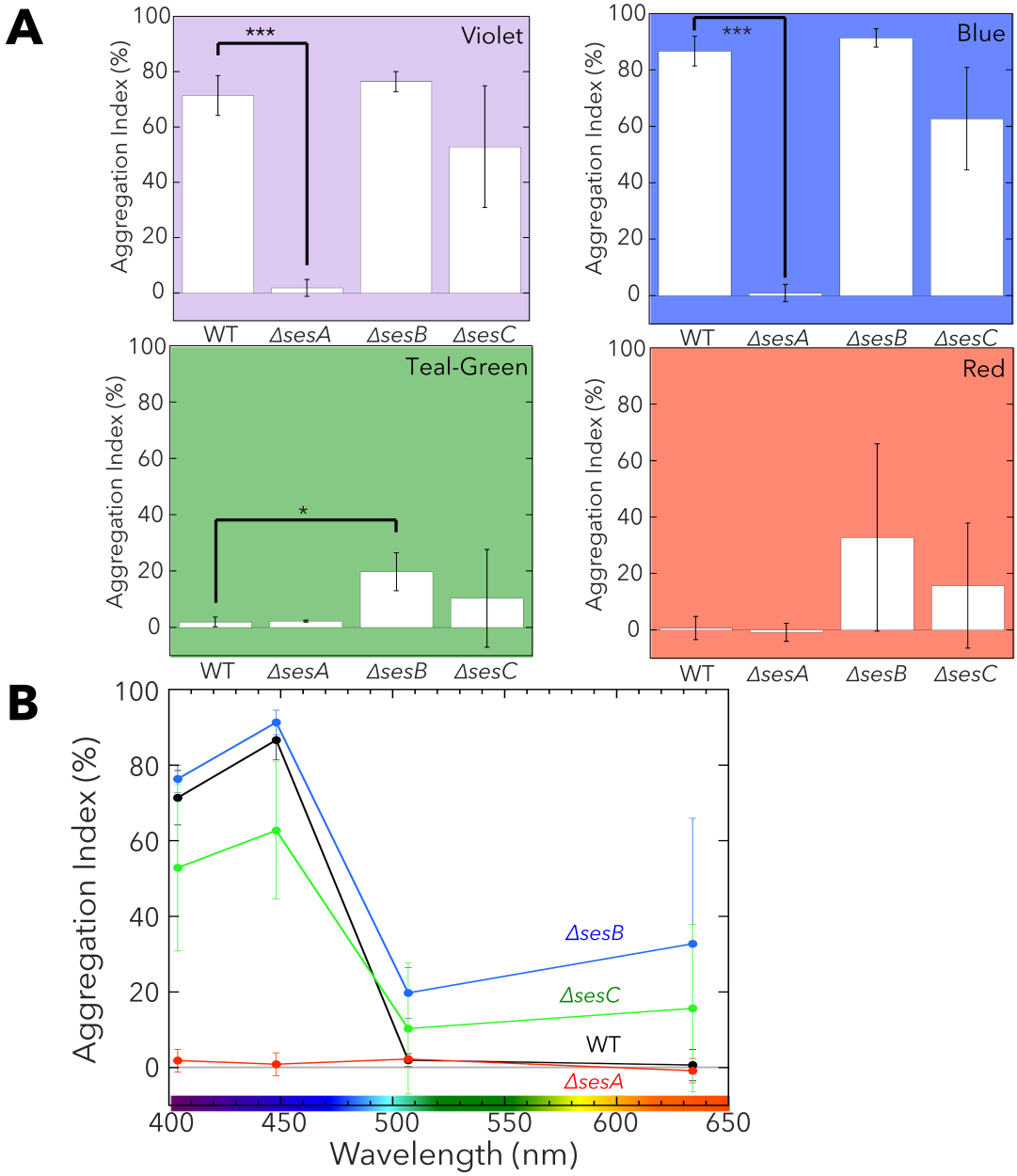

Fig. 2_11. Light-induced cell aggregation of the *T. vulcanus* single gene-disrupted mutants.

(***A***) Aggregation index values for wild type (WT) and its single gene-disrupted mutants (Δ*sesA*, Δ*sesB*, and Δ*sesC*) (error bars report the SDs for three biological replicates). Cells were cultured at 31 °C for 48 h under light of a single wavelength (violet light, Upper Left; blue light, Upper Right; teal-green light, Lower Left). The cells were also cultured under only photosynthetic red light (Lower Right). Statistical significance was determined using Student's *t* tests (**P* < 0.05; ****P* < 0.001). (***B***) Aggregation indexes for the single gene-disrupted mutants as a function of light wavelength using the data shown in ***A***.

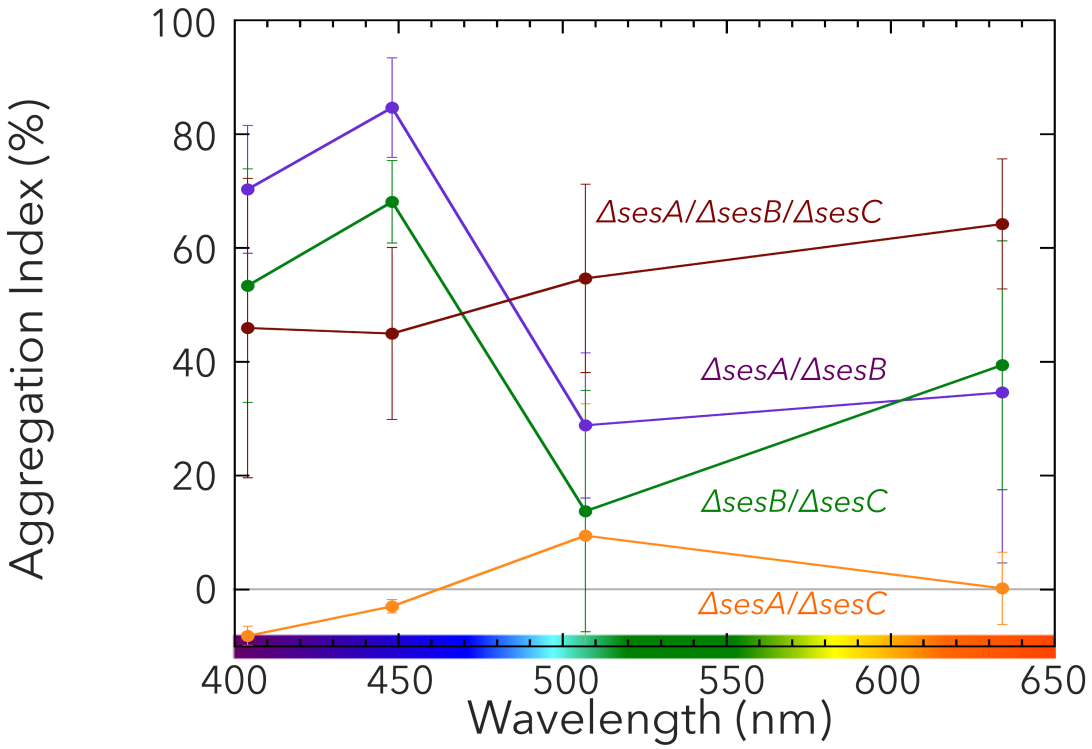

Fig. 2_12. Aggregation indexes for the *T. vulcanus* double (Δ*sesA*/Δ*sesB*, Δ*sesA*/Δ*sesC*, and Δ*sesB*/Δ*sesC*) and triple (Δ*sesA*/Δ*sesB*/Δ*sesC*) gene-disrupted mutants as a function of light wavelength.

Experiments were performed and the data are plotted as described in the legend for **Fig. 2_11.**

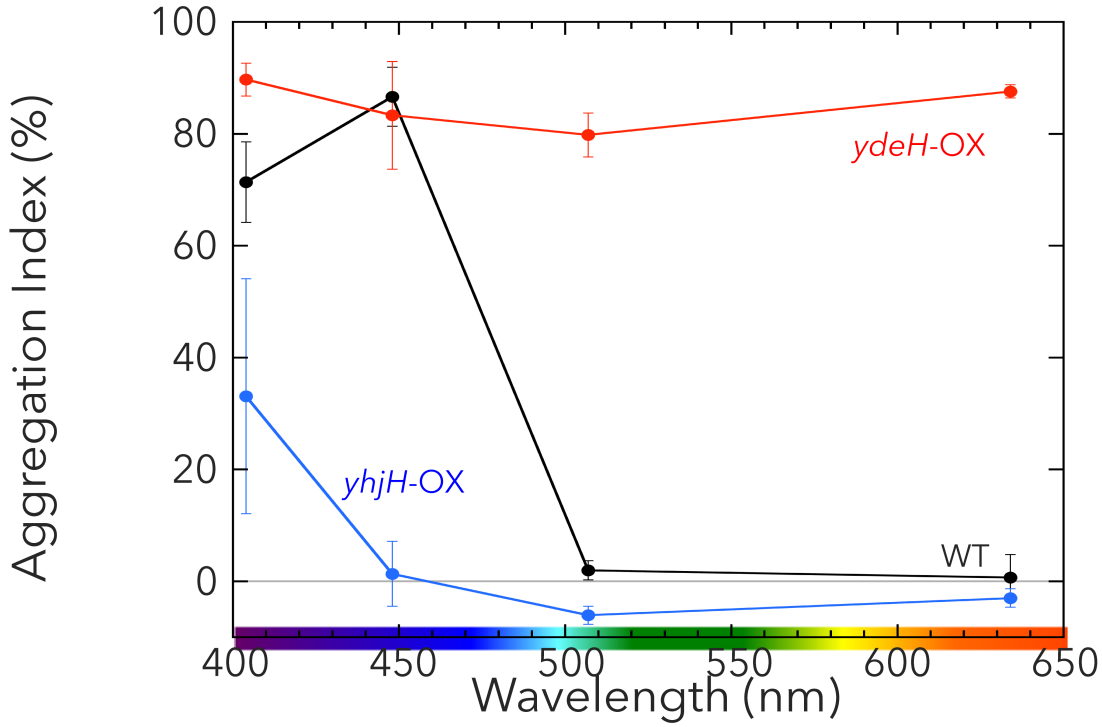

Fig. 2_13. Aggregation indexes for the heterologous DGC/PDE expression mutants (*ydeH*-OX and *yhjH*-OX) as a function of light wavelength.
ydeH-OX, the *T. vulcanus* mutant expressing the *E. coli* DGC, *ydeH*. *yhjH*-OX, the *T. vulcanus* mutant expressing the *E. coli* PDE, *yhjH*. The data for wild type are shown as a black line for comparison. Experiments were performed and the data are plotted as described in the legend for **Fig. 2_11.**

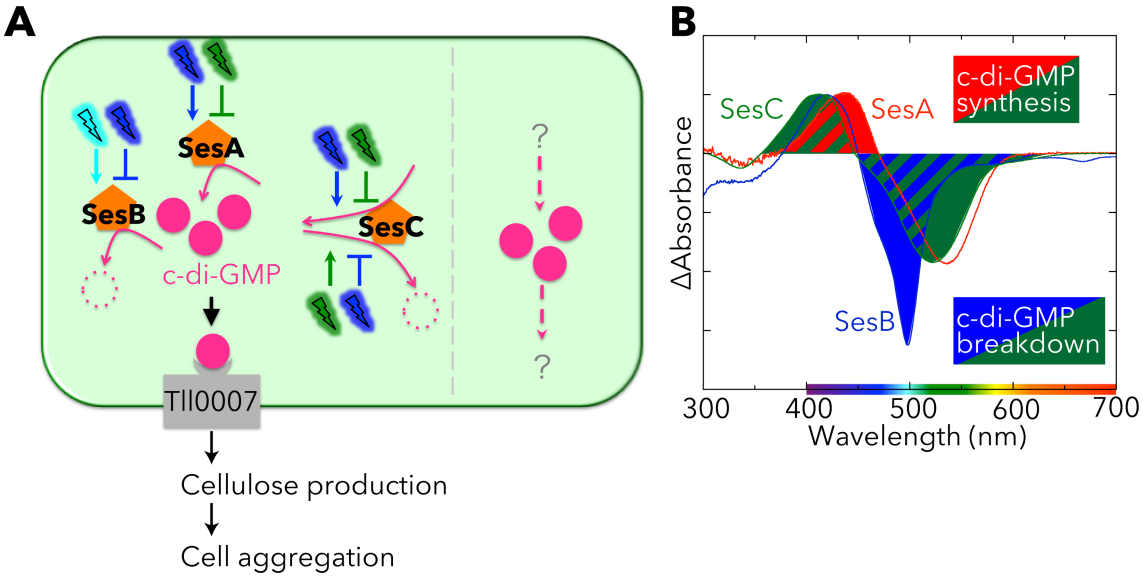

Fig. 2_14. Coordination of the CBCRs SesA, SesB, and SesC that form a color-sensitive, highly specific c-di-GMP signaling system.
(***A***) A signaling model for cell aggregation of *Thermosynechococcus* modulated SesA, SesB, and SesC. Under blue light, the DGC activities of SesA and SesC increase and the PDE activities of SesB and SesC decrease, leading to an increase in c-di-GMP levels. C-di-GMP binds to the PilZ domain of cellulose synthase Tll0007 and activates it, resulting in cell aggregation. Under teal-green light, the DGC activities of SesA and SesC are decreased and the PDE activities of SesB and SesC are increased, leading to a decrease in c-di-GMP levels. In the absence of c-di-GMP, the cellulose-synthesizing activity of Tll0007 is silenced and cell aggregation is not triggered. *Thermosynechococcus* probably contains a light-independent c-di-GMP signaling pathway(s), which has not been characterized. (***B***) The difference spectra for the photostates of SesA, SesB, and SesC. SesA produces c-di-GMP under blue light but SesB degrades it under teal light, thereby confining the wavelength range that induces an increase in c-di-GMP levels to shorter wavelengths. SesC produces c-di-GMP at shorter wavelengths than does SesA, and degrades it at longer wavelengths than does SesB. SesC can, therefore, broaden the effective wavelength range without impacting the color specificity of c-di-GMP net synthesis.

Table 2_1. Primers used in this study.

Purpose	Sequence
SesB (FL)	CACATATGATTGAGAAACTCCTTGT
	TAGGATCCGGTTTGATTGGCAGCACT
SesC (GAF)	GCCATATGGATCTTGAAACCGTTCTC
	CTGGATCCTAATGTAGCGCACTCACTAAT
SesC (FL)	CACATATGATCATTGACGAATTTG
	ATGGATCCAGCAAATCCTAAGGCAGG
Introduction of the TEV recognition site into pTCH2031V	TTGAAAATACAAATTTTCCCGACCCATTTGCTGTCCACCA
	AATTTGTATTTTCAATCCATGATTGAGAAACTCCTTGTTT
Introduction of the TEV recognition site into pET28a	TGAAAATACAGATTTTCGCCGCTGCTGTGATGATGATGA
	AAATCTGTATTTTCAGAGCCATATGATTGAGAAACTCC
rrnB terminator	CGCAGAAGCGGTCTGATAAA
	GCGTTCACCGACAAACAACA
ΔsesB	TCTCTATCGCGATTTCGC
	TGTTGAGGGTGATGATGC
ΔsesC	TCGTCAATGATCATTCCTG
	TGCCTATGAATTTGCGGG
	GTGTTAACGGAACTGCAACAATTGGG
	ATCTACGGCCAAAGTGAG
ydeH-OX	AGGAGAGACCATATGATCAAGAAGACAACGG
	GTGTTCAAACGCAAGTTAAACTCGGTTAATCACAT
yhjH-OX	GAGGAATAAACCATGATAAGGCAGGTTATCC
	GAGGTTAACAGATCTTTATAGCGCCAGAACCGC

FL, full length; GAF, GAF domain; OX, overexpression

~Chapter 3~

The two-step regulation of c-di-GMP signaling system for orchestrating cell aggregation

Abstract

In a thermophilic cyanobacterium *Thermosynechococcus vulcanus*, cell aggregation is regulated at low temperature in a light-responsive manner by three cooperating cyanobacteriochromes (SesA, SesB, and SesC) via c-di-GMP signaling. The cellulose synthase, Tll0007, is essential for the cell aggregation and has a putative PilZ domain, which may serve as a c-di-GMP binding module. However, experimental validation of c-di-GMP binding is lacking. Here, I show that Tll0007-PilZ domain indeed binds c-di-GMP by fluorescence resonance energy transfer (FRET)-based biosensor assays. The affinity towards c-di-GMP of Tll0007-PilZ is relatively low (K_d = 63.9 ± 5.1 μM), suggesting that the high amount of c-di-GMP is needed for the activation of Tll0007. I also show that SesA, the main trigger of the cell aggregation, is subject to product feedback inhibition with high affinity (IC50 = 1.07 ± 0.13 μM). The results suggest that Tll0007 may not be a direct target of c-di-GMP produced by SesA. I systematically analyzed the contributions of all of the ten c-di-GMP synthesis/degradation domain proteins of *T. vulcanus*, and found that *tlr0627* gene is also crucial for the cell aggregation. Tlr0627 may work as a c-di-GMP amplifier to act downstream of SesA and directly activate Tll0007. Such two step regulation of c-di-GMP signaling seems to be reasonable because the light regulation of the "first" c-di-GMP pool by SesA/B/C will be quick and energy-efficient in the μM range of c-di-GMP concentration. Cellulose, produced by Tll0007 after amplification of the "second" c-di-GMP pools possibly by Tlr0627, may work as a matrix to enclose gathered cells at later stages of cell aggregation.

Introduction

In chapter 2, I showed that the three CBCRs (SesA, SesB, and SesC) synthesize/degrade c-di-GMP in response to lights in blue-to-green window, and cooperatively regulate cell aggregation in a light color-sensitive manner in *T. vulcanus*. c-di-GMP is an inducer of the cellulose-dependent cell aggregation (Chapter 2). The cellulose synthase Tll0007 and its putative c-di-GMP binding PilZ domain are necessary for the cell aggregation (Enomoto *et al.*, 2014, Kawano *et al.*, 2011). These results strongly suggested that Tll0007 binds c-di-GMP via its PilZ domain and upregulates its cellulose synthase activity, like other bacterial cellulose synthases (Morgan *et al.*, 2014, Ross *et al.*, 1987), resulting in cell aggregation. However, the experimental evidence was lacking. Furthermore, there are seven other genes that encode GGDEF/EAL/HD-GYP domains in *T. vulcanus*, but their individual functions and overall organization are totally elusive.

In chapter 3, I analyzed the biochemical properties of c-di-GMP signaling system in *T. vulcanus* (PilZ domain of Tll0007 and the product feedback inhibition of the main trigger SesA), revealing the gap in the c-di-GMP concentration between the affinity of the PilZ domain of Tll0007 and the final c-di-GMP levels brought by SesA. To identify the DGC(s) that elevate the c-di-GMP levels sufficient for activation of the PilZ domain, I systematically analyzed cell aggregation of single gene disruption mutants of each of the ten genes encoding c-di-GMP synthesis/degradation domain in *T. vulcanus*. I found that *tlr0627* gene is also crucial for the cell aggregation. I proposed the two-step c-di-GMP signaling model composed of the light-input system and a following signal-amplification system.

Results

The Cellulose Synthase Tll0007 Binds C-Di-GMP with Relatively Low Affinity.

To confirm and assess the c-di-GMP binding of Tll0007, I designed the fluorescence resonance energy transfer (FRET)-based c-di-GMP biosensor proteins by concatenating two fluorescent proteins (mCyPet and mYPet, which are monomerized variants of CFP and YFP, respectively) and the PilZ domain of Tll0007 in between (**Fig. 3_1*A***) (Pultz *et al.*, 2012, Christen *et al.*, 2010). For purified biosensor proteins, the addition of c-di-GMP results in a corresponding increase in FRET efficiency, whereas that of GTP does not (**Fig. 3_1*B***). The concentration-responsive curve of the FRET efficiency for c-di-GMP suggested that the dissociation constant (K_d) was 63.9 ± 5.1 μM at 31ºC (**Fig. 3_1*C***). The affinity of Tll0007 is lower than known c-di-GMP binding proteins including other PilZ domain proteins (Pultz *et al.*, 2012, Chou & Galperin, 2016). The curve fitting indicated that the Hill coefficient was 0.90 ± 0.14, which also contrasts with other PilZ domains that usually show positive cooperativity in c-di-GMP binding (Benach *et al.*, 2007, Pultz *et al.*, 2012).

RXXXR motif in PilZ domain is necessary for binding c-di-GMP (Christen *et al.*, 2007, Whitney *et al.*, 2015, Ko *et al.*, 2010). I created R605A (Arg605, the latter Arg of RxxxR motif, was mutated to Ala) and assessed the binding of c-di-GMP. The R605A biosensor protein lost corresponding increase in FRET efficiency upon c-di-GMP addition (**Fig. 3_1*C***). These results indicated that the biosensor protein binds c-di-GMP, which depends on Arg605 in RXXXR motif of the PilZ domain. The R605A biosensor showed a little higher FRET efficiency than wild-type protein without the nucleotides, suggesting that the R605A protein have the locked conformation that is slightly activated. Taken together, Tll0007 indeed binds c-di-GMP via its

PilZ domain, although the affinity is relatively low.

The DGC Activity of SesA Exhibits Product Inhibition with Relatively High Affinity.

The DGC activities of many GGDEF proteins are negatively regulated by their product, c-di-GMP (Römling *et al.*, 2013, Christen *et al.*, 2006). To assess the product inhibition of SesA, I measured the initial rate of the DGC reactions in the presence of various concentrations of c-di-GMP using the pyrophosphate assay kit, which monitors the production of the byproduct of DGC reaction, pyrophosphate. The SesA protein was pre-irradiated with blue light so that it was kept in the active form, Pg, during the assay. In the absence of c-di-GMP, SesA showed high pyrophosphate production activity at first, and then the activity was decreased and eventually almost stopped around 5 μM c-di-GMP concentration (**Fig. 3_2*A***). In the presence of 10 μM c-di-GMP, the DGC activity of SesA is strongly inhibited from the beginning. These results indicated product feedback inhibition in the DGC activity of SesA.

The concentration-responsive curve of the DGC activity for the amount of added c-di-GMP suggested that the IC50 value was 1.07 ± 0.13 μM at 31ºC (**Fig. 3_2*B***). The product inhibition site of SesA had comparably high affinity for c-di-GMP compared with previously investigated DGC proteins such as DgcA (IC50 = 0.96 μM) and PleD (IC50 = 5.8 μM) (Christen *et al.*, 2006). The DGC activity of SesA in the absence of c-di-GMP (20.5 ± 2.1 μmol pyrophosphate/ μmol protein/ min, namely the turnover number (k_{cat}) ~10 min^{-1}) was relatively high compared with those of other DGC proteins reported previously (Zahringer *et al.*, 2013, Savakis *et al.*, 2012). The curve fitting also indicated that the Hill coefficient was 3.0 ± 0.3, indicating the high cooperativity of c-di-GMP binding to SesA.

Upon the product inhibition of DGCs, c-di-GMP binds to the allosteric

product inhibition site, which is located near the active site of GGDEF domains (Chan *et al.*, 2004, De *et al.*, 2009, Wassmann *et al.*, 2007). RXXD motif is the core c-di-GMP binding site for the allosteric product inhibition (Christen *et al.*, 2006). I replaced Arg676 of the RXXD motif of SesA with Ala and assessed the product inhibition. SesA (R676A) showed high pyrophosphate production activity regardless of the presence of 10μM c-di-GMP, and the activity is not inhibited during the assay for 600 sec (**Fig. 3_2*A***). The concentration-responsive curve indicated that SesA (R676A) maintained its high DGC activity even in the presence of 100 μM c-di-GMP (**Fig. 3_2*B***), indicating that RXXD motif is necessary for the product inhibition of SesA. The R676A protein showed slightly higher DGC activity than wild-type protein even in the absence of c-di-GMP, suggesting that R676A mutation alone could confer the preference of active protein conformation. The protein oligomerization may be changed by R676A mutation as reported in the same mutation in the GGDEF domain of TM1788 of *Thermotoga maritima* (Rao *et al.*, 2009, Deepthi *et al.*, 2014). Taken together, SesA is subject to product feedback inhibition with relatively high affinity.

Involvement of Other DGC/PDEs in the Regulation of Cell Aggregation.

Given the results of this study, c-di-GMP produced by SesA (IC50 ~ 1 μM) may not be sufficient for the activation of Tll0007 (K_d ~ 64 μM). The discrepancy prompted me to analyze the contributions of other c-di-GMP synthesis/degradation proteins in the regulation of cell aggregation. In *Thermosynechococcus*, there are 10 genes that encode GGDEF/EAL/HD-GYP domains (**Fig. 3_3**). The protein sequence alignment of the GGDEF domains revealed that the amino acids necessary for DGC activity (Schirmer & Jenal, 2009) are all conserved except for SesB (**Fig. 3_4**) (Chapter 2). The RXXD motif of GGDEF domain is conserved in SesA, SesC, Tlr1210, Tlr0627,

Tll1049, and Tll1859, suggesting that some of them may be subject to product inhibition. All the EAL domains in *Thermosynechococcus* appeared to be active based on the protein sequence alignment (**Fig. 3_5**) (Schirmer & Jenal, 2009, Sundriyal *et al.*, 2014).

Previous studies in our laboratory reported that the single gene disruption mutants of *tlr1210* showed no phenotype on cell aggregation (Tamura, 2012). I created other five gene disruption mutants (*tlr1158*, *tll1049*, *tll1859*, *tll0627*, and *tlr1612*) of *T. vulcanus* and analyzed cell aggregation under blue or teal-green light at 31ºC (**Fig. 3_6**).

Under teal-green light, all the analyzed mutants but Δ*sesB* (Chapter 2) showed little cell aggregation like wild type, suggesting that SesB is the primary PDE to repress cell aggregation under such condition. Under blue light, Δ*tlr0627* showed decreased cell aggregation compared with strong cell aggregation of wild type, indicating that Tlr0627 is important for cell aggregation. Δ*tlr0485* showed strong cell aggregation similar to wild type, which is consistent with previous report in our laboratory (Kamiya, 2015). Δ*tlr1158*, Δ*tll1049*, Δ*tll1859*, and Δ*tlr1612* showed less cell aggregation than wild type, but their relevance to cell aggregation was not obvious, given their large variation of aggregation index values.

Discussion

Affinity for C-di-GMP of Tll0007.

Tll0007 is the first cyanobacterial c-di-GMP receptor protein that is experimentally validated, corroborating that the intracellular c-di-GMP signaling network is present in cyanobacteria. The affinity of Tll0007 to c-di-GMP (K_d = 63.9 ± 5.1 μM) was relatively low compared with other c-di-GMP receptors such as PlzD (K_d = 0.2 μM), VpsT (K_d = 3.2 μM), and Alg44 (K_d = 12.7 μM) (Pultz *et al.*, 2012, Chou & Galperin, 2016, Krasteva *et al.*, 2010). Under my chimeric constructs, the full-length YcgR of *E. coli* showed affinity of 0.42 ± 0.08 μM (**Fig. 3_7**), which is similar to that reported in the previous study (K_d = 0.84 ± 0.16 μM) (Ryjenkov *et al.*, 2006), ensuring the reliability of the assay. Although I cannot exclude the possibility that the affinity for c-di-GMP is higher *in vivo* in the full-length Tll0007 protein, BcsA, which is the homologous protein of Tll0007 in *Salmonella* Typhimurium, showed higher affinity (K_d = 8.4 μM) than Tll0007 even in the similar construct and assay (Pultz *et al.*, 2012), indicating that Tll0007 should have lower affinity for c-di-GMP than the homologous BcsA. Taken together, the results suggest that the relatively high amount of c-di-GMP is necessary to activate Tll0007. The intracellular concentration of c-di-GMP in *T. vulcanus* may be high compared to other bacteria and cyanobacteria and I will address it in the future.

The Hill coefficient of Tll0007 was 0.90 ± 0.14, which contrasts with other PilZ domains that usually show positive cooperativity in c-di-GMP binding (Benach *et al.*, 2007, Pultz *et al.*, 2012). PilZ domains usually bind c-di-GMP dimer (Morgan *et al.*, 2014, Ko *et al.*, 2010, Habazettl *et al.*, 2011, Whitney *et al.*, 2015), whereas binding of c-di-GMP monomer was also reported (Benach *et al.*, 2007). Interestingly, a recent report showed that the binding of c-di-GMP dimer to a PilZ domain protein, Alg44, could induce functional

output, whereas binding of c-di-GMP monomer could not, indicating that a specific form of c-di-GMP is necessary for activation (Whitney *et al.*, 2015). Thus, the high cooperativity of other PilZ domains seems to reflect the preference of binding of c-di-GMP dimer. Conversely, Tll0007 might be activated by c-di-GMP monomer.

Product Inhibition of DGC Activity of SesA.

SesA, the major trigger of cell aggregation of *T. vulcanus,* was subject to the product feedback inhibition. The high cooperativity of product inhibition permits SesA to respond in an all-or-none fashion over a narrow range of c-di-GMP concentrations (Oliveira *et al.*, 2015).

The DGC activity of SesA (k_{cat} ~10 min^{-1}) is relatively high compared to known DGC proteins such as TM1788(R158A) (k_{cat} ~2.6 min^{-1}) (Rao *et al.*, 2009) and YdeH (k_{cat} ~1.6 min^{-1}) (Boehm *et al.*, 2009), and comparable with Cph2 (k_{cat} ~10.6 min^{-1}) (Savakis *et al.*, 2012). The high DGC activity will be important for SesA to produce rapidly the enough amount of c-di-GMP upon blue light exposure. Interestingly, *Synechocystis* cells that over-express SesA (R676A) for protein preparation was unviable under white light irradiation, while under green/red light, the cells are normally viable (data not shown). This finding suggests that the high and unlimited DGC activity of SesA (R676A) protein induced by blue light was toxic to the *Synechocystis* cells, probably via exhaustion of GTP and/or over-activation of c-di-GMP signaling. Thus, it seems that the product feedback inhibition is necessary to prevent the uncontrollable overflow of the high DGC activity of SesA. The product inhibition is assumed to be common in GGDEF domains and intensely investigated *in vitro* (Whiteley & Lee, 2015, De *et al.*, 2009, Christen *et al.*, 2006, Chan *et al.*, 2004). In spite of the prevalence, however, the physiological importance of the product inhibition of DGCs has not been elucidated, to my knowledge. The effect of R676A mutation in SesA on

cellular processes is now under investigation.

RXXD motif in GGDEF domains is essential for building an allosteric product inhibition site (Christen *et al.*, 2006, Chan *et al.*, 2004). The RXXD motif is, however, not sufficient for the physiologically relevant product inhibition because my preliminary experiments suggested that SesC and Tlr1210 seemed not to be subject to the feedback inhibition by c-di-GMP up to 50 μM (data not shown) despite that they carry apparently intact RXXD motif (**Fig. 3_4**). The product inhibition site is located often in boundary between a GGDEF domain and Van adjacent domain (Wassmann *et al.*, 2007, De *et al.*, 2008, Chan *et al.*, 2004). It is difficult to predict whether a GGDEF domain protein is subject to product inhibition or not.

Light-Input and Downstream C-Di-GMP Signal Amplification.

In this study, I suggested that SesA-produced c-di-GMP might not be sufficient for activation of the cellulose synthase Tll0007. In *Salmonella*, cellulose synthesis is regulated by two insulated c-di-GMP signaling systems. In response to unknown environmental cues, four DGC/PDEs (STM3388, STM2123, STM1703, and STM4264) regulate a c-di-GMP pool that activates the expression of a transcriptional regulator CsgD. CsgD induces expression of another DGC protein AdrA that produces higher levels of c-di-GMP, which, in turn, directly activates the cellulose synthesis via its PilZ domain (Kader *et al.*, 2006, Caly *et al.*, 2015).

In *Thermosynechococcus*, the two-step c-di-GMP signaling composed of a light-input system and a signal-amplification system may work (**Fig. 3_8**) in an analogous fashion to that of *Salmonella*. The light-input system composed of SesA, SesB, and SesC, may respond quickly to the ambient blue light to accumulate c-di-GMP at μM levels. Perhaps the light-input system including PDE activities (of SesB and SesC) also degrades the μM levels of c-di-GMP reversibly under green or teal light condition. Namely, the light-input

system quickly regulates some reversible responses leading to sessility. Type IV pili-dependent motility, which is driven by ATPases (Mattick, 2002, Wilde & Mullineaux, 2015, Guzzo *et al.*, 2009), might be a plausible target for such reversible regulation. The second signaling system may be a c-di-GMP-amplifier; c-di-GMP signal at μM levels which is brought by the light-input system, in turn, activates or induces another DGC to elevate the c-di-GMP levels sufficient for activation of the low affinity PilZ domain of the cellulose synthase Tll0007. Cellulose accumulation and cell aggregation are rather irreversible long-term responses. Given that cellulose production may be activated at a later step of cell aggregation, cellulose seems to work as biofilm matrix to enclose the gathered cells and give protective barrier and structural rigidity, rather than as cellular adhesin to attach multiple cells at early stages of biofilm formation (Flemming & Wingender, 2010, Römling & Galperin, 2015, Ha *et al.*, 2015). The promising candidate of the amplifier of the c-di-GMP signaling is Tll0627 because disruption of *tll0627* markedly decreased cell aggregation (**Fig. 3_6**). An epistasis analysis will provide a clue on how SesA/B/C and Tll0627 are integrated in the control of cellulose synthesis of Tll0007 and cell aggregation.

Materials and Methods

Plasmid Constructions.

Primers used are listed in **Table 3_1**. Plasmids were constructed using the In-Fusion System (TaKaRa). For constructing FRET biosensors, fluorescent proteins are cloned from pCyPet-His and pYPet-His (Addgene). I created monomerized variants of CyPet (mCyPet) and YPet (mYPet) by introducing A206K (Christen *et al.*, 2010, Zacharias *et al.*, 2002). The DNA encoding the chimeric protein consisting of mCyPet, Tll0007-PilZ (or the full-length YcgR of *E. coli*), and mYPet was cloned into pET28V, in which the protease recognition site in original pET28a plasmid (Novagen) for removal of the N-terminal His tag was replaced with one for tobacco etch virus (TEV) protease (Chapter 2). Site-directed mutagenesis was performed using PrimeSTAR Max Basal Mutagenesis kit reagents (TaKaRa). For producing the SesA protein in the cyanobacterium *Synechocystis* sp. PCC 6803, pTCH2031V vector carrying the protein-encoding DNA was used. The protease recognition site for removal of the N-terminal His tag was replaced with one for tobacco etch virus (TEV) protease, which could be used for future purification. The *E. coli rrnB* terminator sequence was inserted after the C terminus of the protein-encoding region incorporated into pTCH2031V (Chapter 2). For disruption of *tlr1158*, *tll1049*, *tll1859*, *tll0627*, and *tlr1612* in *T. vulcanus*, a spectinomycin/streptomycin-resistance cassette was inserted in the start codon of the genes. The protocols for disruption of *tlr1210* and *tlr0485* have been reported (Tamura, 2012, Kamiya, 2015).

Protein Purification.

E. coli and *Synechocystis* protein-expressing cells were harvested by centrifugation at 4,450 × g for 10 min, suspended in 50 mM Hepes·NaOH

(pH 7.5), 300 mM NaCl, 10% (wt/vol) glycerol, 30 mM imidazole, 0.5 mM Tris(2-carboxylethyl)phosphine, and then frozen at −80 °C. After thawing, cells were subjected to three rounds of disruption using a French press (5501-M; Ohtake) at 1,500 kg·cm^{-2}. The homogenate from the cyanobacterial cells was centrifuged at 12,000 × g for 10 min and then at 194,100 × g for 30 min. The *E. coli* homogenate was centrifuged at 194,100 × g for 30 min. Each supernatant was filtered and then loaded onto a nickel-affinity His-Trap chelating column (GE Healthcare). Proteins were eluted with a linear gradient of 30–430 mM imidazole in 20 mM Hepes·NaOH (pH 7.5), 300 mM NaCl, 10% (wt/vol) glycerol, 0.5 mM Tris(2-carboxylethyl)phosphine. EDTA (1 mM) was added to the pooled peak fractions, which were then dialyzed against 20 mM Hepes·NaOH (pH 7.5), 300 mM NaCl, 10% (wt/vol) glycerol, 1 mM DTT. For purify FRET-based biosensor proteins, the reducing agents (Tris(2-carboxylethyl)phosphine and DTT) were omitted.

Fluorescence Spectra.

Fluorescence spectra were recorded at 31 °C by a RF-5300PC spectrofluorometer (Shimadzu, excitation at 425 nm, 5 nm excitation and 3 nm emission slit widths, emission scan from 450 to 600 nm) using 50 nM proteins in 20 mM Hepes·NaOH (pH 7.5), 100 mM NaCl, 10% (wt/vol) glycerol. Binding affinity was determined by adding increasing concentrations of c-di-GMP (10 nM – 1 mM) or GTP (1 μM – 10 mM) and measuring the resulting YFP/CFP emission ratio (emission at 527 nm/ emission at 475 nm). The curve fitting was performed with the program KaleidaGraph (Synergy Software).

Kinetic Measurements of Diguanylate Cyclase Activity.

For the kinetic measurements of DGC activity, the amount of inorganic

pyrophosphate, a by-product of c-di-GMP synthesis, was monitored at 360 nm by a UV-2600PC spectrophotometer using EnzChek pyrophosphate assay kit reagents (Invitrogen) (Enomoto *et al.*, 2014, De *et al.*, 2008). The kit includes inorganic pyrophosphatase, which catalyzes conversion of inorganic pyrophosphate into 2 eq of inorganic phosphate. In the presence of inorganic phosphate, the substrate 2-amino-6-mercapto-7-methylpurine ribonucleoside was enzymatically converted to ribose 1-phosphate and 2-amino-6-mercapto-7-methylpurine, which shows the absorption at 360 nm. Each reaction contained 50 mM Tris-HCl, pH 7.5, 20 mM $MgCl_2$, and 0.2 μM SesA protein in the presence of various amount of c-di-GMP. The reactions were started by the addition of 100 μM GTP, incubated at 31°C, and monitored for 600 seconds.

Cell Aggregation Assay.

The thermophilic cyanobacterium *T. vulcanus* strain RKN (equivalent to National Institute for Environmental Studies 2134) that shows positive phototaxis was cultured at 45 °C in BG11 medium (Stanier *et al.*, 1971). Culture density was monitored at 730 nm. Transformations of *T. vulcanus* were performed according to (Iwai *et al.*, 2004). The antibiotic concentration in BG11 medium for selection of transformants was 5 $\mu g \cdot mL^{-1}$ chloramphenicol, 80 $\mu g \cdot mL^{-1}$ kanamycin, or 10 $\mu g \cdot mL^{-1}$ spectinomycin plus 5 $\mu g \cdot mL^{-1}$ streptomycin. Complete segregation of mutant allele (i.e. the wild-type loci were replaced by the mutant loci in all of the multiple copies of the cyanobacterial chromosome) was verified via PCR.

For cell aggregation assay, cultures of *T. vulcanus* wild-type and its disrupted mutants grown at 45 °C (OD_{730} 0.5–2) was diluted to give a culture OD_{730} of 0.2. These samples were then incubated at 31 °C for 48 h under photosynthetic red light (λ_{max} = 634 nm; 30 μmol photon$\cdot m^{-2} \cdot s^{-1}$; Valore Corp.) with blue or teal-green light (λ_{max} =448 or 507 nm, respectively; 5

μmol photon·m^{-2}·s^{-1}; Valore Corp.). The results of the cellulose-dependent cell-aggregation assay described as follows are reported as an aggregation index (%) (Kawano *et al.*, 2011). Briefly, after the irradiation period, cell suspensions were thoroughly mixed and aliquots were transferred to cuvettes. The samples were held at room temperature in the dark for 30 min, during which time most of the aggregated cells had precipitated to the bottom of the cuvettes. Then the OD_{730} of each sample was measured (denoted OD_{NA} ; i.e., OD_{730} of NonAggregated cells remaining in the culture medium). Next, cellulase (12.5 U·mL^{-1}; Worthington Biochemical) was added to each cuvette sample, which was then incubated for 30 min at 37 °C to completely disperse the aggregated cells. The OD_{730} of each sample (denoted OD_{total}) was then measured. The aggregation index (%) is defined as $((OD_{total} - OD_{NA})/OD_{total}) \times 100$.

Figures and Tables

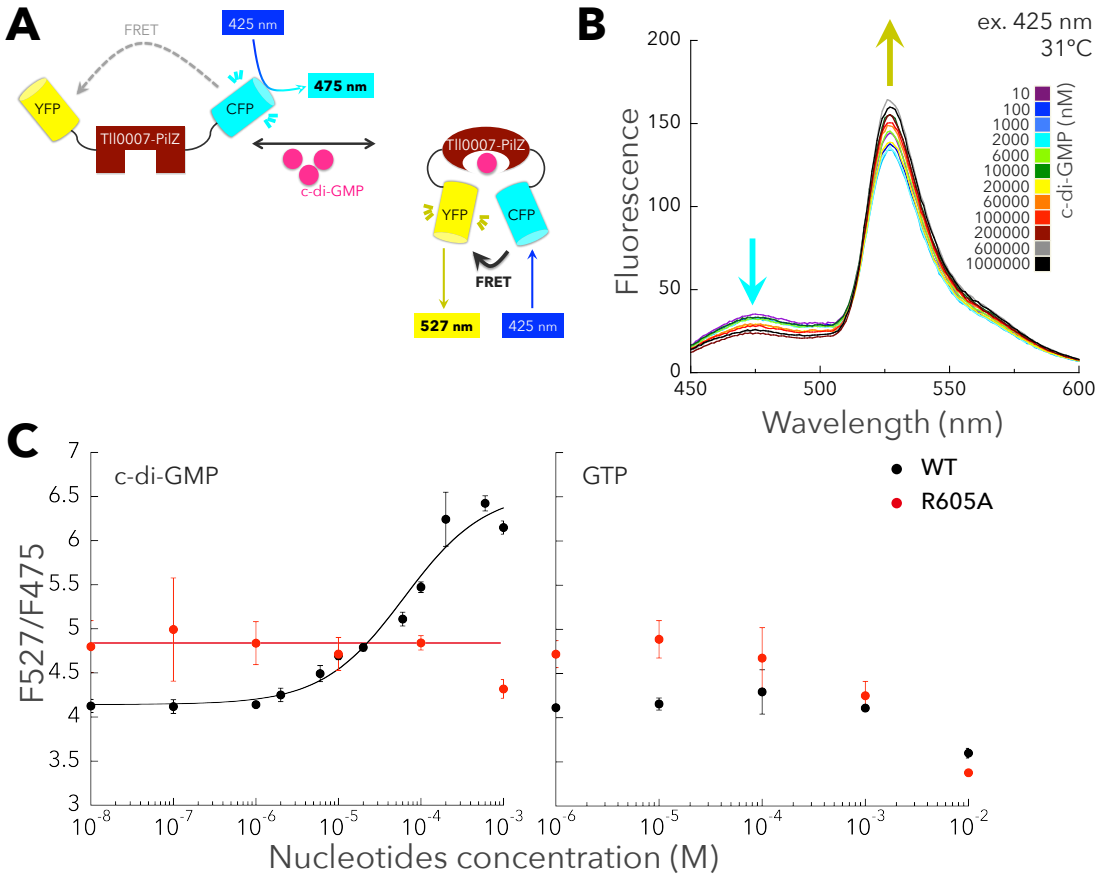

Fig. 3_1. FRET-based biosensor assay for assessment of c-di-GMP binding of the Tll0007-PilZ domain.

(***A***) A scheme illustrating how binding of c-di-GMP to a target protein domain (here Tll0007-PilZ) leads to a change in FRET efficiency between attached mCyPet (CFP) and mYPet (YFP). (***B***) Fluorescence emission spectra of the biosensor protein in the presence of indicated c-di-GMP concentrations. A representative of three independent experiments is shown. (***C***) The nucleotide concentration-responsive curve of the FRET efficiency (YFP emission at 527 nm/ CFP emission at 475 nm) for c-di-GMP (left) and GTP (right). Error bar represents the SD of the average of at least three independent experiments. Black, WT; red, R605A.

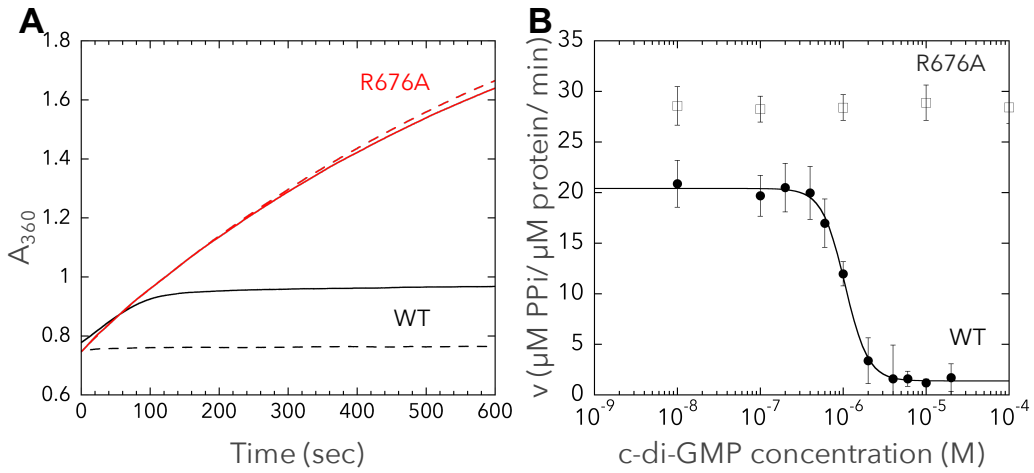

Fig. 3_2. Pyrophosphate assay for assessment of the product inhibition of SesA.
(***A***) SesA proteins (0.2 μM) were incubated at 31°C in reaction solution in the absence of c-di-GMP (solid line) or in the presence of 10 μM c-di-GMP (broken line), and pyrophosphate production was measured by continuously monitoring absorbance at 360 nm. Representative results of three independent experiments are presented. Black lines, WT; red lines, R676A. (***B***) The c-di-GMP concentration-responsive curve of the initial velocity of the DGC reaction of SesA (μM PPi/ μM protein/ min). Error bar represents the SD of the average of three independent experiments. Filled circle, WT; empty square, R676A.

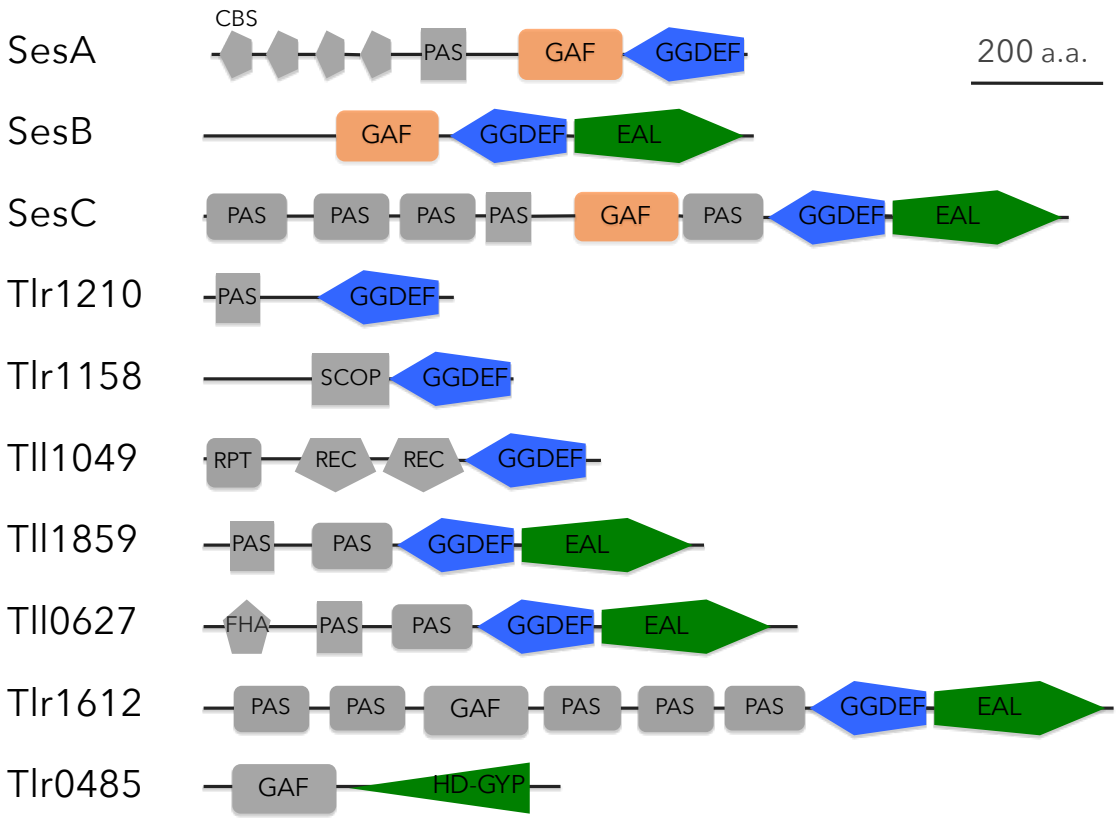

Fig. 3_3. Domain architectures of the 10 proteins that encode GGDEF/EAL/HD-GYP domains in *Thermosynechococcus*.
CBCR-GAF domain is highlighted in orange. GGDEF domain is highlighted in blue whereas EAL and HD-GYP domain is in green.

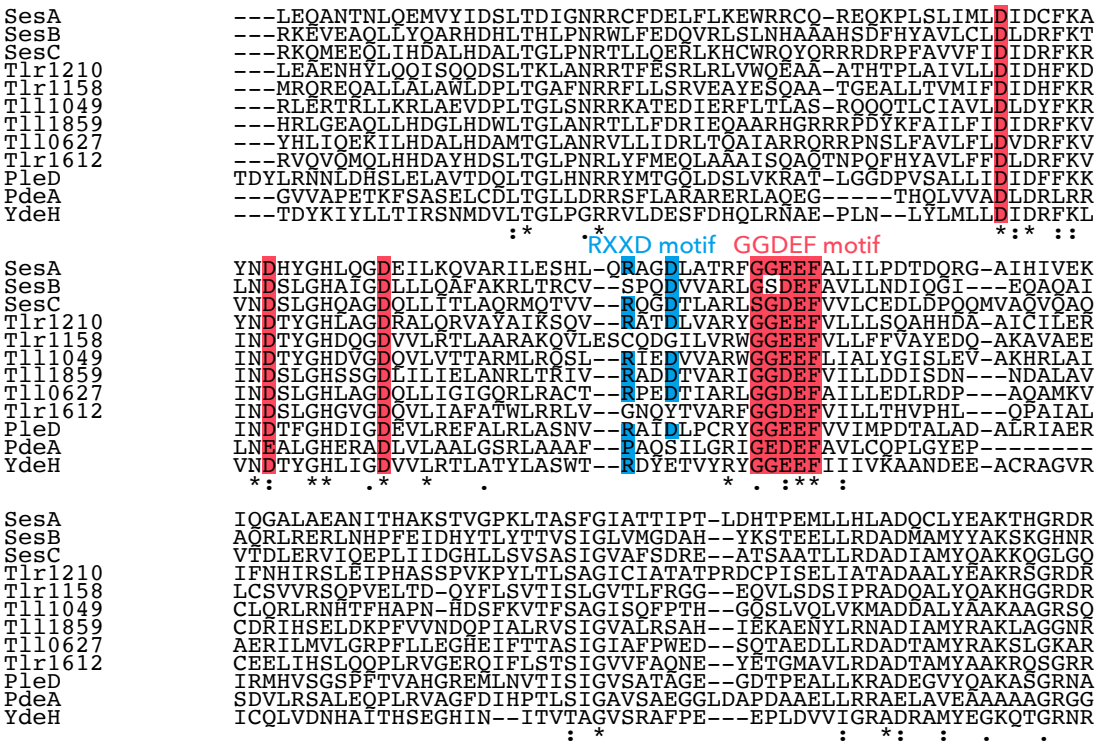

Fig. 3_4. The amino acid sequence alignment of the GGDEF domains in *Thermosynechococcus vulcanus*.
The conserved amino acids in the active site are shaded in red. The conserved Arg and Asp residues in RXXD motif that are necessary for allosteric product inhibition are shaded in blue. PleD and PdeA of *Caulobacter crescentus*, and YdeH of *E. coli* are included for comparison.

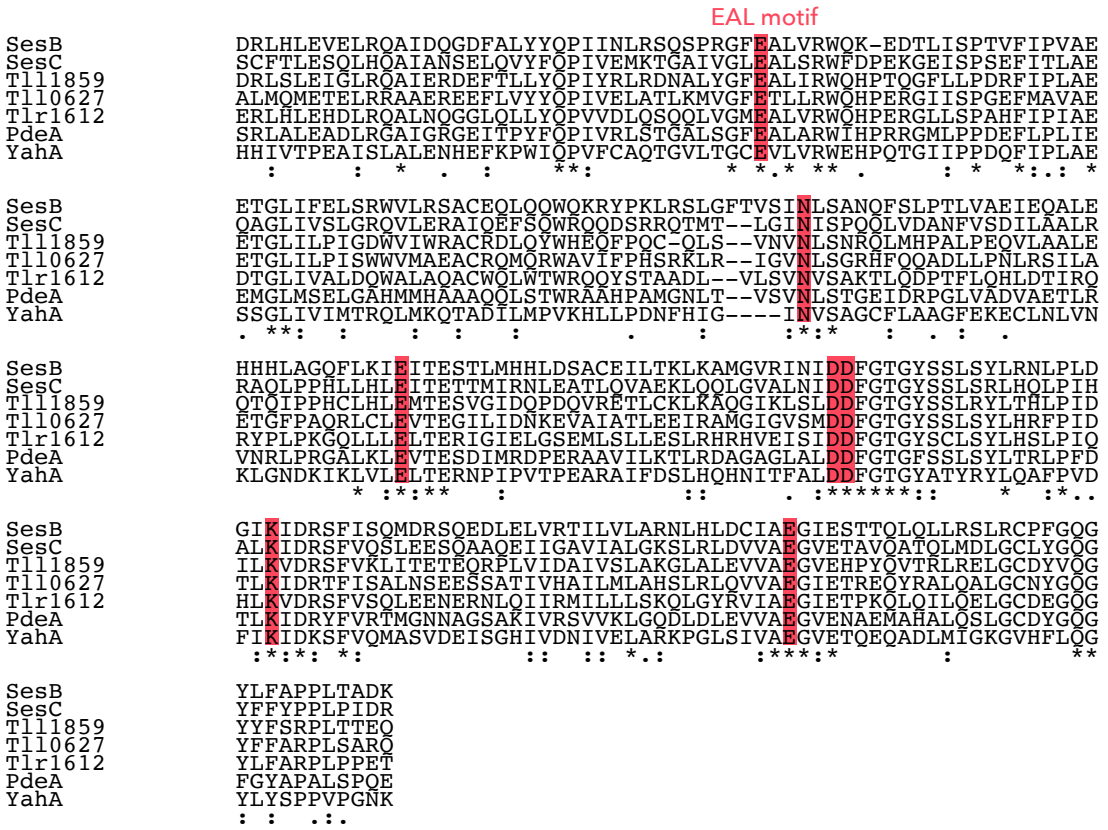

Fig. 3_5. The amino acid sequence alignment of the EAL domains in *Thermosynechococcus vulcanus*.
The conserved amino acids in the active site are shaded in red. PdeA of *Caulobacter crescentus*, and YahA of *E. coli* are included for comparison.

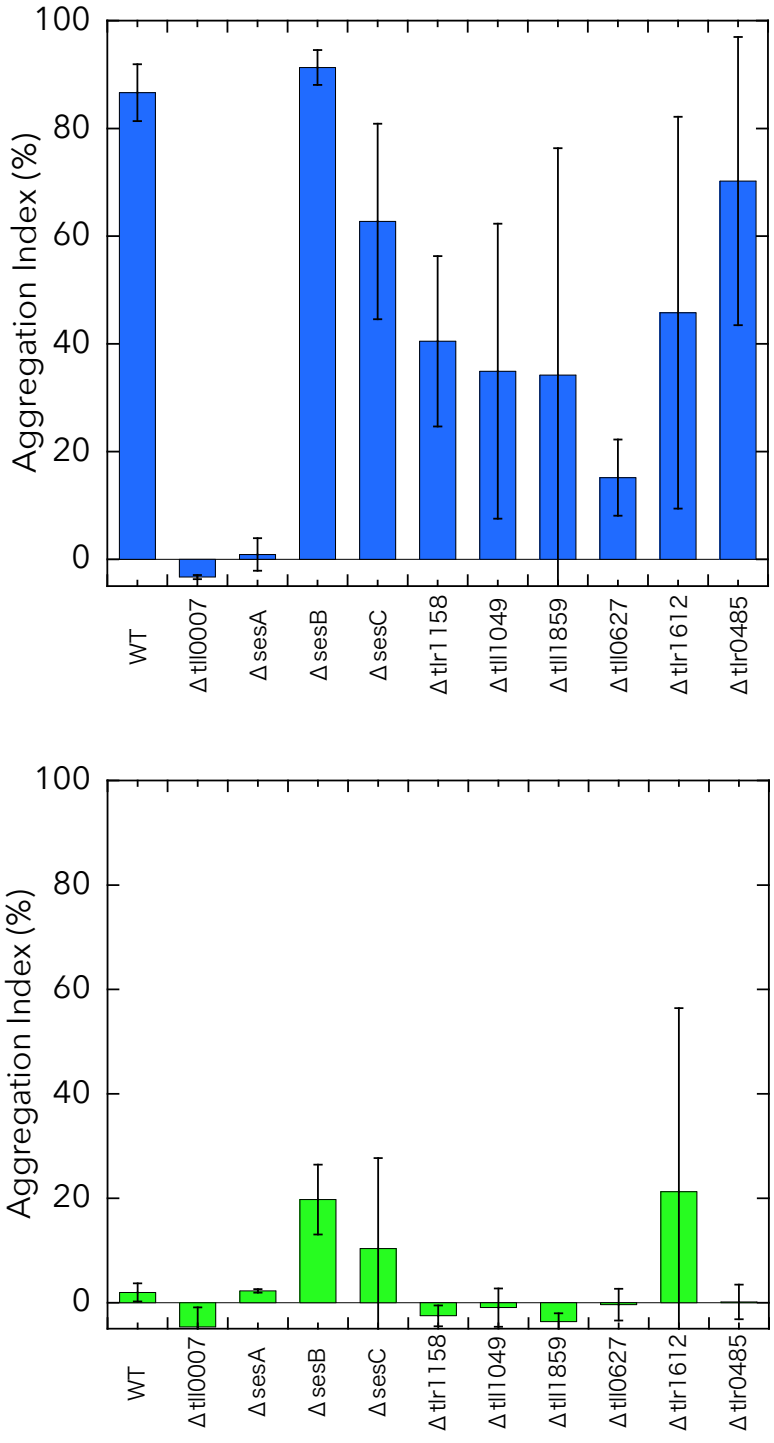

Fig. 3_6. Systematic assessment of cell aggregation of single DGC/PDE-encoding gene disruption mutants.
Aggregation index values for wild type (WT) and its single gene-disrupted mutants were shown. Cells were cultured at 31 °C for 48 h under blue light (***A***) or teal-green light (***B***). Error bar represents the SD of the average of at least three biological replicates. The data of WT, Δ*sesA*, Δ*sesB*, and Δ*sesC* are extracted from Chapter 2.

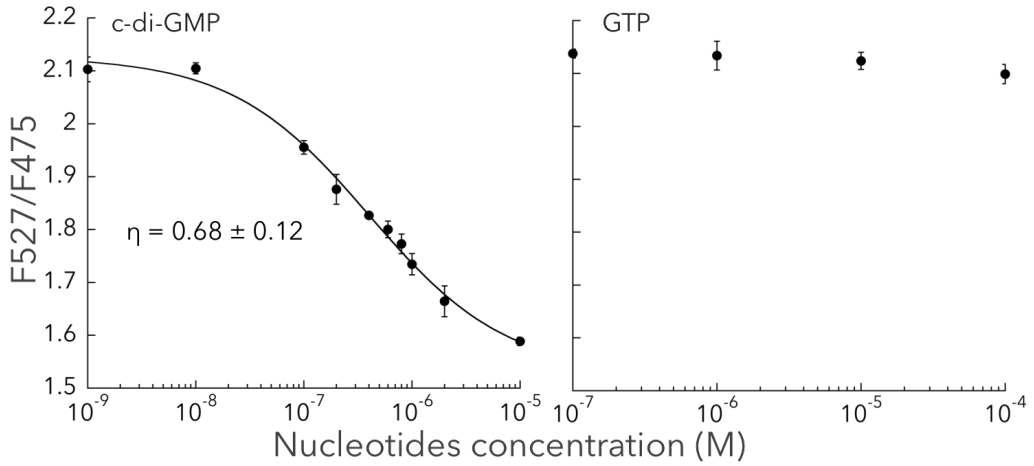

Fig. 3_7. FRET-based biosensor assay for assessment of c-di-GMP binding by the *E. coli* YcgR protein.

The nucleotide concentration-responsive curve of the FRET efficiency (YFP emission/ CFP emission) for c-di-GMP (left) and GTP (right). Error bar represents the SD of the average of three independent experiments. The Hill coefficient (η) was estimated by curve fitting.

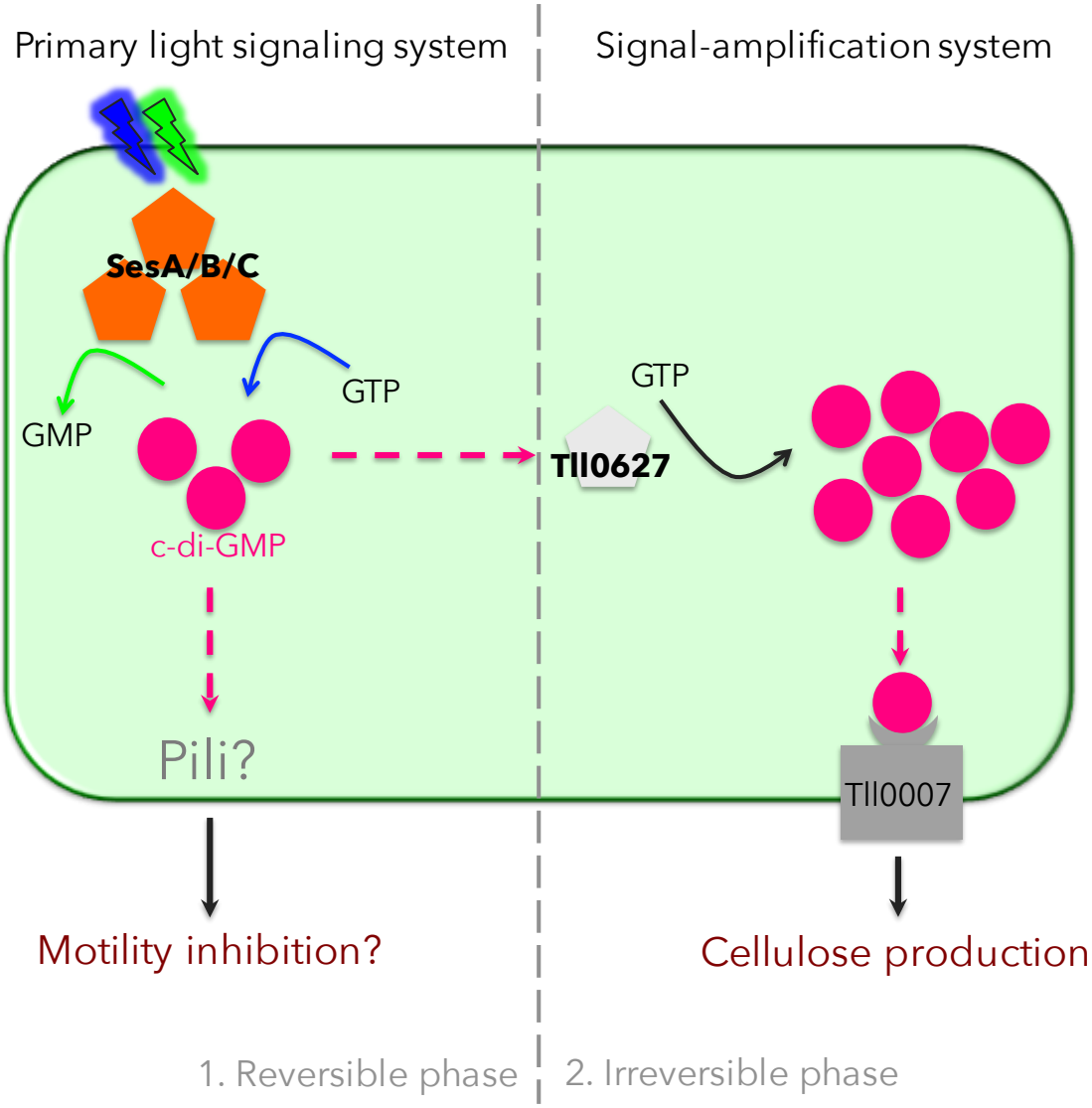

Fig. 3_8. A model for signal amplification by two-step c-di-GMP signaling for regulating cell aggregation in *Thermosynechococcus vulcanus*.
In the primary light signaling system, SesA, SesB, and SesC may regulate a certain c-di-GMP pool at μM levels of c-di-GMP concentration, given that the DGC activity of the main trigger SesA is subject to product feedback inhibition. By narrowing the range of light-regulated c-di-GMP levels, SesA/B/C can adjust the c-di-GMP levels quickly and energy-efficiently in responding to fluctuating light conditions. The quick c-di-GMP pool at μM levels may regulate motility. Cell aggregation can be suspended or cancelled in the "first" phase.

When c-di-GMP activation by light exceeds the threshold, another DGC (probably Tll0627) may be activated, and it amplifies the c-di-GMP signal. The slow c-di-GMP pool at high levels activates Tll0007 and cellulose matrix formation is started as a later step of cell aggregation. Once entering this "second" phase, cell aggregation cannot be cancelled.

Table 3_1. Primers used in this study.

Purpose	Name	Sequence
CyPet (A206K)	CyPet-1F	caatctaaattatctaaagatccaaacgaaaag
	CyPet-2R	agataatttagattgagtggataagtaatggtt
YPet (A206K)	YPet-1F	caatctaaattatTcaaagatccaaacgaaaag
	YPet-2R	gAataatttagattgaTAggataagtaatggtt
FRET-biosensor	pET28TEV-1R	CATATGGCTCTGAAAATACAG
	PET28_R1	GGATCCGAATTCGAGCTC
	CyPet-3FTEV	TTTCAGAGCCATATGtctaaaggtgaagaa
	CyPet-4R	tttgtacaattcatccatac
	YPet-3F	tctaaaggtgaagaatta
	YPet-4R28a	CTCGAATTCGGAtccttatttgtacaattcatTcatac
	ycgR-1FCYP	gatgaattgtacaaaactagtATGAGTCATTACCATGAGC
	ycgR-2RYPe	ttcttcacctttagaggtaccGTCGCGCACTTTGTCCGC
	Tll0007-15FCYP	ttgtacaaaactagtCCGAGTCGGCGCCAAAG
	Tll0007-16RYPe	acctttagaggtaccACCATAAAGCAGTTGTACC
Tll0007 (R605A)	tll0007-32F	AAGCGATgcCTTTCCCGTTTGCACTGTG
	tll0007-33R	GGAAAGgcATCGCTTTGGCGCCGACT
SesA (R676A)	tlr0924-28F	ATTTGCAGgcGGCAGGGGATTTGGCCAC
	tlr0924-29R	CTGCCgcCTGCAAATGGCTTTCCAAAA
Δ*tlr1158*	tlr1158-1F1R	aacgacggccagtgaAGATCAGAGGCAGGGTCAC
	tlr1158-2Rup	gcgagcaggggaattGCCCTAACCAGAATCGATTG
	tlr1158-3Fcom	ccgcttcgcaatattGCTAAAAAAAGTGCAGGAAC
	tlr1158-4R2F	gaaacagctatgaccGCGGCGACTCAATCATATC
Δ*tll1049*	tll1049-1F1R	aacgacggccagtgaTGGGAGAACTTTGGGTACAG
	tll1049-2Rup	gcgagcaggggaattACCTAGCCGCCAATAGCCC
	tll1049-3Fcom	ccgcttcgcaatattTGGCCATTTTGCTTTATCAC
	tll1049-4R2F	gaaacagctatgaccGCTTATTGCTCTTGGGAGGA
Δ*tll1859*	tll1859-1F1R	aacgacggccagtgaGCTCATAGGTGGTGAAACGA
	tll1859-2Rup	gcgagcaggggaattAAAATATCCTAGCTTAAGTGC
	tll1859-3Fcom	ccgcttcgcaatattGGAGCAGGATGACTCACCT
	tll1859-4R2F	gaaacagctatgaccTTGTCTTTCTAGGGGGTGTG
Δ*tll0627*	tll0627-1F1R	aacgacggccagtgaTTCAGAATGCTGTCCTTGGC
	tll0627-2Rup	gcgagcaggggaattATCAATGGCCTCGGCAAGGA
	tll0627-3Fcom	ccgcttcgcaatattGAAGTCTGATCTGCCGAAGA
	tll0627-4R2F	gaaacagctatgaccGTTTCCGCCAAAATAGAC
Δ*tlr1612*	tlr1612-1F1R	aacgacggccagtgaTCTTTGGCTCCCAGGCGAT
	tlr1612-2Rup	gcgagcaggggaattGGAAAGCCGCTTGTAAAGCT
	tlr1612-3Fcom	ccgcttcgcaatattaGGATGGTTCCTCACCACGCT
	tlr1612-4R2F	gaaacagctatgaccTCCCAATCCTCAAGATTG

General Discussion

In this thesis, I used a thermophilic cyanobacterium *Thermosynechococcus* as a model organism to study the molecular mechanisms of CBCR signaling system that utilizes c-di-GMP. Firstly, I studied the optical properties of *Thermosynechococcus elongatus* SesB, focusing mainly on the functions of conserved cysteine residues by chemical modification analyses (Chapter 1). Then, I demonstrated that CBCRs SesA, SesB, and SesC cooperatively regulate cell aggregation of *Thermosynechococcus vulcanus* by c-di-GMP signaling (Chapter 2). Finally, I proposed that the two-step c-di-GMP signaling system might work for orchestrating cell aggregation (Chapter 3). This study will pave the way for elucidation of how CBCR signaling utilizing c-di-GMP works for light-color acclimation responses in cyanobacteria. This study may also provide clues as to what principles underlies the diversity of CBCR and c-di-GMP signaling proteins from a molecular and physiological perspective.

Prevalence of Light-Regulated c-di-GMP Signaling

There seems to be no homolog of full-length SesA, SesB and SesC in cyanobacteria other than *Thermosynechococcus*. Further, there are no cyanobacteria that have such many photoreceptors with c-di-GMP synthesis/degradation domains. This suggests that the most sophisticated light-responsive c-di-GMP signaling system has been developed for *Thermosynechococcus*. However, CBCR-GAF and c-di-GMP related domains are ubiquitously found in cyanobacteria, except for marine cyanobacteria with reduced genomes such as *Prochlorococcus* and marine *Synechococcus*, which live in relatively constant and energy-limited conditions reflecting that they may be poor at environmental responses (Biller *et al.*, 2015, Agostoni & Montgomery, 2014). Further, there are blue light-responsive

CBCRs with GGDEF domain like SesA in many cyanobacteria (Savakis *et al.*, 2012). c-di-GMP usually induces multicellular, sessile lifestyles and inhibits planktonic ones and motility in almost all of bacteria (Römling *et al.*, 2013, Hengge, 2009), and cyanobacteria seem to be no exception. These facts suggest that blue light-induced sessile lifestyles via c-di-GMP signaling may be prevalent in cyanobacteria. Indeed, blue light induced motility inhibition, biofilm formation, and cellular deposition via elevated c-di-GMP are reported in *Synechocystis* sp. PCC 6803 (Savakis *et al.*, 2012, Agostoni *et al.*, 2016). However, in *Fremyella diplosiphon*, blue light decreases the intracellular concentration of c-di-GMP (Agostoni *et al.*, 2013), implying that the light-regulation of c-di-GMP in cyanobacteria is more diverse than anticipated. It is of note that there are no known c-di-GMP receptors in these cyanobacteria, suggesting that a new type of c-di-GMP receptor(s) should be awaiting identification in cyanobacteria. c-di-GMP is widespread among bacteria, but its signaling mechanisms are remarkably diverse even among closely related strains or varieties within a single species (Römling *et al.*, 2013, Hengge, 2009). In cyanobacteria, c-di-GMP signaling may have been evolved to perform appropriate regulation of characteristic oxygenic photosynthesis and it is an attractive target of future research. One possible hint may be that a GGDEF domain-containing PsfR was identified as a factor that stimulates *psbAI* (D1 protein of the photosystem II reaction center) expression (Thomas *et al.*, 2004), although its GGDEF domain is highly degenerate.

LOV-type and BLUF-type photoreceptors that have DGC/PDE activities are also prevalent even in bacteria other than cyanobacteria (Kanazawa *et al.*, 2010, Barends *et al.*, 2009, Gomelsky & Hoff, 2011). These photoreceptors utilize flavin species as chromophore and perceive blue light signal (Herrou & Crosson, 2011, Losi & Gärtner, 2012). Although these photoreceptors may work as a “light” sensor instead of as a “blue” sensor in

these organisms, the blue-light regulation of c-di-GMP signaling appears to be a universal strategy in the bacterial kingdom.

Intramolecular Signaling in Cyanobacteriochromes

The molecular mechanism of how CBCRs regulate their output domains' activities remains elusive. Recently in phytochromes, the PHY domain, which always locates next to the GAF domain, is proposed to be crucial for intramolecular signaling (Takala *et al.*, 2014, Anders *et al.*, 2013), but the knowledge is not applicable to CBCRs because CBCRs lack PHY domains. CBCRs have modular nature; the photosensory CBCR-GAF domain(s), the output domain(s), and some regulatory domain(s) are connected modularly. CBCR-GAF domain works as a light-input domain to regulate the activity of the output domain even though it does not sit next to each other (like in SesB and SesC). Thus, the regulation seems to be performed in a distant manner and indirect modification of the output domain. One promising candidate of regulation mechanisms is the modification of the orientation of the output domain. CBCR-GAF domain forms a dimer using the six-helix bundle formed by the distal helices (Narikawa *et al.*, 2013, Rockwell *et al.*, 2013). The subtle change of the dimer interaction can change the relative orientation of each polypeptide's output domain. In fact, the dimer orientation and interface is crucial for regulation of other GGDEF, EAL, or histidine kinase proteins (Casino *et al.*, 2009, Barends *et al.*, 2009, Chan *et al.*, 2004, Wassmann *et al.*, 2007). This hypothesis is attractive and promising, but experimental verification is necessary. In terms of the intramolecular signaling mechanisms, all of SesA, SesB, and SesC are interesting targets because SesA shows the very strict light regulation; SesB shows two independent activation by teal light and GTP; and SesC shows opposite regulation of two output domains by its single CBCR-GAF domain. The further characterization of SesA/B/C proteins by protein crystallography may reveal

a common principle in the molecular mechanisms of the intramolecular signaling. Further, there are some CBCRs that lack putative output domains, suggesting that they might transduce signals to separate output protein(s) via intermolecular interaction (Rockwell *et al.*, 2015a, Bussell & Kehoe, 2013). CBCRs' regulation may be more diverse than had been anticipated.

Nucleotide-Based Second Messengers in Cyanobacteria

Besides c-di-GMP, other nucleotide-based second messengers seem to work in cyanobacteria (Agostoni & Montgomery, 2014). cAMP has been most intensively studied as a second messenger in cyanobacteria (Ohmori & Okamoto, 2004). cAMP is mainly implicated in motility induction in *Arthrospira platensis* and *Synechocystis* sp. PCC 6803 (Ohmori *et al.*, 1993, Terauchi & Ohmori, 1999). cAMP is widespread in cyanobacteria except for *Prochlorococcus* and marine *Synechococcus,* like c-di-GMP (Agostoni & Montgomery, 2014). It is of note that a previous study in my laboratory showed that *Thermosynechococcus* Tlr0485 is a cAMP-activated PDE to degrade c-di-GMP (Kamiya, 2015). There seems to be an interconnection in the signaling network between cAMP and c-di-GMP in cyanobacteria.

Guanosine pentaphosphate and guanosine tetraphosphate (collectively referred to as (p)ppGpp) are involved in the stringent response, during which alterations in metabolism and gene expression occur to support survival under unfavorable conditions such as limitation in the availability of amino acids or nitrogen sources (Hauryliuk *et al.*, 2015). All cyanobacterial genomes contain a gene encoding a (p)ppGpp homeostasis enzyme, suggesting the prevalence of (p)ppGpp in cyanobacteria (Agostoni & Montgomery, 2014). The enzyme is known to be necessary for heterocyst (specialized cell types for nitrogen-fixation) development in *Anabaena* sp. strain PCC 7120 under nitrogen deprivation (Zhang *et al.*, 2013).

c-di-AMP is also a second messenger involved in cell wall peptidoglycan

metabolism, potassium homeostasis, and DNA repair mainly in Gram-positive bacteria (Commichau *et al.*, 2015, Corrigan & Grundling, 2013). To date, all cyanobacteria have a gene encoding a diadenylate cyclase domain protein in the genomes (Agostoni & Montgomery, 2014). Cyanobacteria are classified as Gram-negative bacteria, but their cell envelope has Gram-positive features, including thick peptidoglycan layer and cross-linking degree (Pereira *et al.*, 2015). c-di-AMP may be important for the cell envelope architecture in cyanobacteria. Further, some reports suggested that cGMP is also working in *Synechocystis* sp. PCC 6803 (Linder, 2010, Rauch *et al.*, 2008). Taken together, cyanobacteria may be the most "intelligent" bacteria (Galperin, 2005), using all of (p)ppGpp, cAMP, cGMP, c-di-GMP, and c-di-AMP (Gomelsky, 2011).

Acknowledgements

I thank Prof. Masahiko Ikeuchi for teaching me everything and giving me fruitful time in his laboratory. I thank Dr. Rei Narikawa for his wonderful advice and great discussions. I thank Dr. Yu Hirose for teaching me anything about basic research skills and attitude. I thank Prof. Clark J. Lagarias and Dr. Nathan C. Rockwell for very helpful discussions and suggestions, especially for Chapter 1. I thank Drs. Yu Kanesaki and Hirofumi Yoshikawa for providing the nucleic acid sequences of *T. vulcanus*. I thank Dr. Ni-Ni-Win for creating Δ*sesA* single gene disruption mutant of *T. vulcanus*. I thank Ms. Yukiko Okuda for construction the DNAs for creating gene disruption mutants of *tlr1158*, *tll1049*, *tll1859*, *tll0627*, and *tlr1612*. I thank my colleagues, friends, and family for all of their support.

References

Agostoni, M., B.J. Koestler, C.M. Waters, B.L. Williams & B.L. Montgomery, (2013) Occurrence of cyclic di-GMP-modulating output domains in cyanobacteria: an illuminating perspective. *mBio* **4**.

Agostoni, M. & B.L. Montgomery, (2014) Survival strategies in the aquatic and terrestrial world: the impact of second messengers on cyanobacterial processes. *Life* **4**: 745-769.

Agostoni, M., C.M. Waters & B.L. Montgomery, (2016) Regulation of biofilm formation and cellular buoyancy through modulating intracellular cyclic di-GMP levels in engineered cyanobacteria. *Biotechnol. Bioeng.* **113**: 311–319.

Amikam, D. & M.Y. Galperin, (2006) PilZ domain is part of the bacterial c-di-GMP binding protein. *Bioinformatics* **22**: 3–6.

Anders, K., G. Daminelli-Widany, M.A. Mroginski, D. von Stetten & L.O. Essen, (2013) Structure of the cyanobacterial phytochrome 2 photosensor implies a tryptophan switch for phytochrome signaling. *J. Biol. Chem.* **288**: 35714-35725.

Anders, K. & L.O. Essen, (2015) The family of phytochrome-like photoreceptors: diverse, complex and multi-colored, but very useful. *Curr. Opin. Struct. Biol.* **35**: 7-16.

Anders, K., D. von Stetten, J. Mailliet, S. Kiontke, V.A. Sineshchekov, P. Hildebrandt, J. Hughes & L.O. Essen, (2011) Spectroscopic and photochemical characterization of the red-light sensitive photosensory module of Cph2 from *Synechocystis* PCC 6803. *Photochem. Photobiol.* **87**: 160-173.

Aravind, L. & C.P. Ponting, (1997) The GAF domain: an evolutionary link between diverse phototransducing proteins. *Trends Biochem. Sci.* **22**: 458–459.

Auldridge, M.E. & K.T. Forest, (2011) Bacterial phytochromes: more than meets the light. *Crit. Rev. Biochem. Mol. Biol.* **46**: 67-88.

Barends, T.R., E. Hartmann, J.J. Griese, T. Beitlich, N.V. Kirienko, D.A. Ryjenkov, J. Reinstein, R.L. Shoeman, M. Gomelsky & I. Schlichting, (2009) Structure and mechanism of a bacterial light-regulated cyclic nucleotide phosphodiesterase. *Nature* **459**: 1015–1018.

Benach, J., S.S. Swaminathan, R. Tamayo, S.K. Handelman, E. Folta-Stogniew, J.E. Ramos, F. Forouhar, H. Neely, J. Seetharaman, A. Camilli & J.F. Hunt, (2007) The structural basis of cyclic diguanylate signal transduction by PilZ domains. *EMBO J.* **26**: 5153–5166.

Berkelman, T.R. & J.C. Lagarias, (1986) Visualization of bilin-linked peptides and proteins in polyacrylamide gels. *Anal. Biochem.* **156**: 194–201.

Biller, S.J., P.M. Berube, D. Lindell & S.W. Chisholm, (2015) *Prochlorococcus*: the structure and function of collective diversity. *Nat. Rev. Microbiol.* **13**: 13-27.

Blot, N., X.J. Wu, J.C. Thomas, J. Zhang, L. Garczarek, S. Bohm, J.M. Tu, M. Zhou, M. Ploscher, L. Eichacker, F. Partensky, H. Scheer & K.H. Zhao, (2009) Phycourobilin in trichromatic phycocyanin from oceanic cyanobacteria is formed post-translationally by a phycoerythrobilin lyase-isomerase. *J. Biol. Chem.* **284**: 9290–9298.

Boehm, A., S. Steiner, F. Zaehringer, A. Casanova, F. Hamburger, D. Ritz, W. Keck, M. Ackermann, T. Schirmer & U. Jenal, (2009) Second messenger signalling governs *Escherichia coli* biofilm induction upon ribosomal stress. *Mol. Microbiol.* **72**: 1500-1516.

Braslavsky, S.E., W. Gärtner & K. Schaffner, (1997) Phytochrome photoconversion. *Plant,*

Cell Environ. **20**: 700–706.

Bryant, D.A. & N.-U. Frigaard, (2006) Prokaryotic photosynthesis and phototrophy illuminated. *Trends Microbiol.* **14**: 488-496.

Burgie, E.S., A.N. Bussell, J.M. Walker, K. Dubiel & R.D. Vierstra, (2014) Crystal structure of the photosensing module from a red/far-red light-absorbing plant phytochrome. *Proc. Natl. Acad. Sci. USA* **111**: 10179-10184.

Burgie, E.S. & R.D. Vierstra, (2014) Phytochromes: an atomic perspective on photoactivation and signaling. *Plant Cell* **26**: 4568-4583.

Burgie, E.S., J.M. Walker, G.N. Phillips, Jr. & R.D. Vierstra, (2013) A photo-labile thioether linkage to phycoviolobilin provides the foundation for the blue/green photocycles in DXCF-cyanobacteriochromes. *Structure* **21**: 88-97.

Bussell, A.N. & D.M. Kehoe, (2013) Control of a four-color sensing photoreceptor by a two-color sensing photoreceptor reveals complex light regulation in cyanobacteria. *Proc. Natl. Acad. Sci. USA* **110**: 12834-12839.

Caly, D.L., D. Bellini, M.A. Walsh, J.M. Dow & R.P. Ryan, (2015) Targeting cyclic di-GMP signalling: a strategy to control biofilm formation? *Curr. Pharm. Des.* **21**: 12-24.

Campbell, E.L., K.D. Hagen, R. Chen, D.D. Risser, D.P. Ferreira & J.C. Meeks, (2015) Genetic analysis reveals the identity of the photoreceptor for phototaxis in hormogonium filaments of *Nostoc punctiforme*. *J. Bacteriol.* **197**: 782-791.

Cao, Z., E. Livoti, A. Losi & W. Gartner, (2010) A blue light-inducible phosphodiesterase activity in the cyanobacterium *Synechococcus elongatus*. *Photochem. Photobiol.* **86**: 606–611.

Casino, P., V. Rubio & A. Marina, (2009) Structural insight into partner specificity and phosphoryl transfer in two-component signal transduction. *Cell* **139**: 325–336.

Chan, C., R. Paul, D. Samoray, N.C. Amiot, B. Giese, U. Jenal & T. Schirmer, (2004) Structural basis of activity and allosteric control of diguanylate cyclase. *Proc. Natl. Acad. Sci. USA* **101**: 17084–17089.

Chen, L., H. Kinoshita & K. Inomata, (2009) Synthesis of doubly locked 5*Zs*15*Za*-biliverdin derivatives and their unique spectral behavior. *Chem. Lett.* **38**: 602–603.

Chen, M., (2014) Chlorophyll modifications and their spectral extension in oxygenic photosynthesis. *Annu. Rev. Biochem.* **83**: 317-340.

Chen, M., Y. Li, D. Birch & R.D. Willows, (2012) A cyanobacterium that contains chlorophyll *f*-a red-absorbing photopigment. *FEBS Lett.* **586**: 3249-3254.

Chou, S.-H. & M.Y. Galperin, (2016) Diversity of c-di-GMP-binding proteins and mechanisms. *J. Bacteriol.* **198**: 32-46.

Christen, B., M. Christen, R. Paul, F. Schmid, M. Folcher, P. Jenoe, M. Meuwly & U. Jenal, (2006) Allosteric control of cyclic di-GMP signaling. *J. Biol. Chem.* **281**: 32015–32024.

Christen, M., B. Christen, M.G. Allan, M. Folcher, P. Jeno, S. Grzesiek & U. Jenal, (2007) DgrA is a member of a new family of cyclic diguanosine monophosphate receptors and controls flagellar motor function in *Caulobacter crescentus*. *Proc. Natl. Acad. Sci. USA* **104**: 4112–4117.

Christen, M., B. Christen, M. Folcher, A. Schauerte & U. Jenal, (2005) Identification and characterization of a cyclic di-GMP-specific phosphodiesterase and its allosteric control by GTP. *J. Biol. Chem.* **280**: 30829–30837.

Christen, M., H.D. Kulasekara, B. Christen, B.R. Kulasekara, L.R. Hoffman & S.I. Miller,

(2010) Asymmetrical distribution of the second messenger c-di-GMP upon bacterial cell division. *Science* **328**: 1295–1297.

Commichau, F.M., A. Dickmanns, J. Gundlach, R. Ficner & J. Stulke, (2015) A jack of all trades: the multiple roles of the unique essential second messenger cyclic di-AMP. *Mol. Microbiol.* **97**: 189-204.

Corrigan, R.M. & A. Grundling, (2013) Cyclic di-AMP: another second messenger enters the fray. *Nat. Rev. Microbiol.* **11**: 513-524.

Dasgupta, J., R.R. Frontiera, K.C. Taylor, J.C. Lagarias & R.A. Mathies, (2009) Ultrafast excited-state isomerization in phytochrome revealed by femtosecond stimulated Raman spectroscopy. *Proc. Natl. Acad. Sci. USA* **106**: 1784–1789.

De, N., M.V. Navarro, R.V. Raghavan & H. Sondermann, (2009) Determinants for the activation and autoinhibition of the diguanylate cyclase response regulator WspR. *J. Mol. Biol.* **393**: 619–633.

De, N., M. Pirruccello, P.V. Krasteva, N. Bae, R.V. Raghavan & H. Sondermann, (2008) Phosphorylation-independent regulation of the diguanylate cyclase WspR. *PLoS Biol.* **6**: e67.

Deepthi, A., C.W. Liew, Z.X. Liang, K. Swaminathan & J. Lescar, (2014) Structure of a diguanylate cyclase from Thermotoga maritima: insights into activation, feedback inhibition and thermostability. *PloS one* **9**: e110912.

Duerig, A., S. Abel, M. Folcher, M. Nicollier, T. Schwede, N. Amiot, B. Giese & U. Jenal, (2009) Second messenger-mediated spatiotemporal control of protein degradation regulates bacterial cell cycle progression. *Genes Dev.* **23**: 93–104.

Enomoto, G., R. Nomura, T. Shimada, W. Ni Ni, R. Narikawa & M. Ikeuchi, (2014) Cyanobacteriochrome SesA is a diguanylate cyclase that induces cell aggregation in *Thermosynechococcus*. *J. Biol. Chem.* **289**: 24801-24809.

Essen, L.O., J. Mailliet & J. Hughes, (2008) The structure of a complete phytochrome sensory module in the Pr ground state. *Proc. Natl. Acad. Sci. USA* **105**: 14709–14714.

Ferreira, R.B., L.C. Antunes, E.P. Greenberg & L.L. McCarter, (2008) *Vibrio parahaemolyticus* ScrC modulates cyclic dimeric GMP regulation of gene expression relevant to growth on surfaces. *J. Bacteriol.* **190**: 851–860.

Flemming, H.C. & J. Wingender, (2010) The biofilm matrix. *Nat. Rev. Microbiol.* **8**: 623–633.

Galperin, M.Y., (2005) A census of membrane-bound and intracellular signal transduction proteins in bacteria: bacterial IQ, extroverts and introverts. *BMC Microbiol.* **5**: 35.

Galperin, M.Y., A.N. Nikolskaya & E.V. Koonin, (2001) Novel domains of the prokaryotic two-component signal transduction systems. *FEMS Microbiol. Lett.* **203**: 11–21.

Gan, F. & D.A. Bryant, (2015) Adaptive and acclimative responses of cyanobacteria to far-red light. *Environ. Microbiol.* **17**: 3450-3465.

Gan, F., S. Zhang, N.C. Rockwell, S.S. Martin, J.C. Lagarias & D.A. Bryant, (2014) Extensive remodeling of a cyanobacterial photosynthetic apparatus in far-red light. *Science* **345**: 1312-1317.

Gasser, C., S. Taiber, C.M. Yeh, C.H. Wittig, P. Hegemann, S. Ryu, F. Wunder & A. Möglich, (2014) Engineering of a red-light-activated human cAMP/cGMP-specific phosphodiesterase. *Proc. Natl. Acad. Sci. USA* **111**: 8803-8808.

Gomelsky, M., (2011) cAMP, c-di-GMP, c-di-AMP and now cGMP: bacteria use them all! *Mol. Microbiol.* **79**: 562–565.

Gomelsky, M. & W.D. Hoff, (2011) Light helps bacteria make important lifestyle decisions. *Trends Microbiol.* **19**: 441–448.

Guzzo, C.R., R.K. Salinas, M.O. Andrade & C.S. Farah, (2009) PILZ protein structure and interactions with PILB and the FIMX EAL domain: implications for control of type IV pilus biogenesis. *J. Mol. Biol.* **393**: 848–866.

Ha, D.-G., apos & G.A. Toole, (2015) c-di-GMP and its effects on biofilm formation and dispersion: a *Pseudomonas aeruginosa* review. *Microbiology Spectrum* **3**.

Habazettl, J., M.G. Allan, U. Jenal & S. Grzesiek, (2011) Solution structure of the PilZ domain protein PA4608 complex with cyclic di-GMP identifies charge clustering as molecular readout. *J. Biol. Chem.* **286**: 14304–14314.

Hansen, R.E. & J.R. Winther, (2009) An introduction to methods for analyzing thiols and disulfides: Reactions, reagents, and practical considerations. *Anal. Biochem.* **394**: 147–158.

Hauryliuk, V., G.C. Atkinson, K.S. Murakami, T. Tenson & K. Gerdes, (2015) Recent functional insights into the role of (p)ppGpp in bacterial physiology. *Nat. Rev. Microbiol.* **13**: 298-309.

Hengge, R., (2009) Principles of c-di-GMP signalling in bacteria. *Nat. Rev. Microbiol.* **7**: 263–273.

Herrou, J. & S. Crosson, (2011) Function, structure and mechanism of bacterial photosensory LOV proteins. *Nat. Rev. Microbiol.* **9**: 713–723.

Hickman, J.W. & C.S. Harwood, (2008) Identification of FleQ from *Pseudomonas aeruginosa* as ac-di-GMP-responsive transcription factor. *Mol. Microbiol.* **69**: 376-389.

Hirose, Y., N.C. Rockwell, K. Nishiyama, R. Narikawa, Y. Ukaji, K. Inomata, J.C. Lagarias & M. Ikeuchi, (2013) Green/red cyanobacteriochromes regulate complementary chromatic acclimation via a protochromic photocycle. *Proc. Natl. Acad. Sci. USA* **110**: 4974–4979.

Hughes, J., (2013) Phytochrome cytoplasmic signaling. *Annu. Rev. Plant Biol.* **64**: 377-402.

Ikeuchi, M. & T. Ishizuka, (2008) Cyanobacteriochromes: a new superfamily of tetrapyrrole-binding photoreceptors in cyanobacteria. *Photochem. Photobiol. Sci* **7**: 1159–1167.

Ishizuka, T., A. Kamiya, H. Suzuki, R. Narikawa, T. Noguchi, T. Kohchi, K. Inomata & M. Ikeuchi, (2011) The cyanobacteriochrome, TePixJ, isomerizes its own chromophore by converting phycocyanobilin to phycoviolobilin. *Biochemistry* **50**: 953–961.

Ishizuka, T., R. Narikawa, T. Kohchi, M. Katayama & M. Ikeuchi, (2007) Cyanobacteriochrome TePixJ of *Thermosynechococcus elongatus* harbors phycoviolobilin as a chromophore. *Plant Cell Physiol.* **48**: 1385–1390.

Ishizuka, T., T. Shimada, K. Okajima, S. Yoshihara, Y. Ochiai, M. Katayama & M. Ikeuchi, (2006) Characterization of cyanobacteriochrome TePixJ from a thermophilic cyanobacterium *Thermosynechococcus elongatus* strain BP-1. *Plant Cell Physiol.* **47**: 1251–1261.

Iwai, M., H. Katoh, M. Katayama & M. Ikeuchi, (2004) Improved genetic transformation of the thermophilic cyanobacterium, *Thermosynechococcus elongatus* BP-1. *Plant Cell Physiol.* **45**: 171–175.

Jenal, U., (2004) Cyclic di-guanosine-monophosphate comes of age: a novel secondary messenger involved in modulating cell surface structures in bacteria? *Curr. Opin.*

Microbiol. **7**: 185-191.

Jones, M.A., W. Hu, S. Litthauer, J.C. Lagarias & S.L. Harmer, (2015) A constitutively active allele of phytochrome B maintains circadian robustness in the absence of light. *Plant Physiol.* **169**: 814-825.

Kader, A., R. Simm, U. Gerstel, M. Morr & U. Römling, (2006) Hierarchical involvement of various GGDEF domain proteins in rdar morphotype development of *Salmonella enterica* serovar Typhimurium. *Mol. Microbiol.* **60**: 602-616.

Kalia, D., G. Merey, S. Nakayama, Y. Zheng, J. Zhou, Y. Luo, M. Guo, B.T. Roembke & H.O. Sintim, (2013) Nucleotide, c-di-GMP, c-di-AMP, cGMP, cAMP, (p)ppGpp signaling in bacteria and implications in pathogenesis. *Chem. Soc. Rev.* **42**: 305-341.

Kamiya, A., (2015) 好熱性シアノバクテリアにおけるサイクリックヌクレオチドシグナリング間のクロストーク因子の解析 Master's thesis

Kanazawa, T., S. Ren, M. Maekawa, K. Hasegawa, F. Arisaka, M. Hyodo, Y. Hayakawa, H. Ohta & S. Masuda, (2010) Biochemical and physiological characterization of a BLUF protein-EAL protein complex involved in blue light-dependent degradation of cyclic diguanylate in the purple bacterium *Rhodopseudomonas palustris*. *Biochemistry* **49**: 10647–10655.

Karniol, B., J.R. Wagner, J.M. Walker & R.D. Vierstra, (2005) Phylogenetic analysis of the phytochrome superfamily reveals distinct microbial subfamilies of photoreceptors. *Biochem. J.* **392**: 103–116.

Kawai, H., T. Kanegae, S. Christensen, T. Kiyosue, Y. Sato, T. Imaizumi, A. Kadota & M. Wada, (2003) Responses of ferns to red light are mediated by an unconventional photoreceptor. *Nature* **421**: 287-290.

Kawano, Y., T. Saotome, Y. Ochiai, M. Katayama, R. Narikawa & M. Ikeuchi, (2011) Cellulose accumulation and a cellulose synthase gene are responsible for cell aggregation in the cyanobacterium *Thermosynechococcus vulcanus* RKN. *Plant Cell Physiol.* **52**: 957–966.

Kehoe, D.M. & A.R. Grossman, (1996) Similarity of a chromatic adaptation sensor to phytochrome and ethylene receptors. *Science* **273**: 1409–1412.

Kehoe, D.M. & A. Gutu, (2006) Responding to color: the regulation of complementary chromatic adaptation. *Annu. Rev. Plant Biol.* **57**: 127–150.

Ko, J., K.-S. Ryu, H. Kim, J.-S. Shin, J.-O. Lee, C. Cheong & B.-S. Choi, (2010) Structure of PP4397 reveals the molecular basis for different c-di-GMP binding modes by Pilz domain proteins. *J. Mol. Biol.* **398**: 97–110.

Krasteva, P.V., J.C. Fong, N.J. Shikuma, S. Beyhan, M.V. Navarro, F.H. Yildiz & H. Sondermann, (2010) *Vibrio cholerae* VpsT regulates matrix production and motility by directly sensing cyclic di-GMP. *Science* **327**: 866–868.

Küfer, W. & H. Scheer, (1982) Rubins and rubinoid addition products from phycocyanin. *Z. Naturforsch.* **37**: 179-192.

Larkin, M.A., G. Blackshields, N.P. Brown, R. Chenna, P.A. McGettigan, H. McWilliam, F. Valentin, I.M. Wallace, A. Wilm, R. Lopez, J.D. Thompson, T.J. Gibson & D.G. Higgins, (2007) Clustal W and Clustal X version 2.0. *Bioinformatics* **23**: 2947–2948.

Lee, E.R., J.L. Baker, Z. Weinberg, N. Sudarsan & R.R. Breaker, (2010) An allosteric self-splicing ribozyme triggered by a bacterial second messenger. *Science* **329**: 845–848.

Lee, V.T., J.M. Matewish, J.L. Kessler, M. Hyodo, Y. Hayakawa & S. Lory, (2007) A

cyclic-di-GMP receptor required for bacterial exopolysaccharide production. *Mol. Microbiol.* **65**: 1474–1484.

Letunic, I., T. Doerks & P. Bork, (2012) SMART 7: recent updates to the protein domain annotation resource. *Nucleic Acids Res.* **40**: D302–305.

Li, F.W., M. Melkonian, C.J. Rothfels, J.C. Villarreal, D.W. Stevenson, S.W. Graham, G.K. Wong, K.M. Pryer & S. Mathews, (2015) Phytochrome diversity in green plants and the origin of canonical plant phytochromes. *Nature communications* **6**: 7852.

Lim, S., N.C. Rockwell, S.S. Martin, J.L. Dallas, J.C. Lagarias & J.B. Ames, (2014) Photoconversion changes bilin chromophore conjugation and protein secondary structure in the violet/orange cyanobacteriochrome NpF2163g3. *Photochem. Photobiol. Sci* **13**: 951-962.

Linder, J.U., (2010) cGMP production in bacteria. *Mol. Cell. Biochem.* **334**: 215–219.

Liu, N., Y. Xu, S. Hossain, N. Huang, D. Coursolle, J.A. Gralnick & E.M. Boon, (2012) Nitric oxide regulation of cyclic di-GMP synthesis and hydrolysis in *Shewanella woodyi*. *Biochemistry* **51**: 2087-2099.

Losi, A. & W. Gärtner, (2012) The evolution of flavin-binding photoreceptors: an ancient chromophore serving trendy blue-light sensors. *Annu. Rev. Plant Biol.* **63**: 49–72.

Mandalari, C., A. Losi & W. Gartner, (2013) Distance-tree analysis, distribution and co-presence of bilin- and flavin-binding prokaryotic photoreceptors for visible light. *Photochem. Photobiol. Sci* **12**: 1144-1157.

Massie, J.P., E.L. Reynolds, B.J. Koestler, J.P. Cong, M. Agostoni & C.M. Waters, (2012) Quantification of high-specificity cyclic diguanylate signaling. *Proc. Natl. Acad. Sci. USA* **109**: 12746–12751.

Mattick, J.S., (2002) Type IV pili and twitching motility. *Annu. Rev. Microbiol.* **56**: 289–314.

McDonough, K.A. & A. Rodriguez, (2012) The myriad roles of cyclic AMP in microbial pathogens: from signal to sword. *Nat. Rev. Microbiol.* **10**: 27-38.

Midorikawa, T., K. Matsumoto, R. Narikawa & M. Ikeuchi, (2009) An Rrf2-type transcriptional regulator is required for expression of *psaAB* genes in the cyanobacterium *Synechocystis* sp. PCC 6803. *Plant Physiol.* **151**: 882–892.

Miroux, B. & J.E. Walker, (1996) Over-production of proteins in *Escherichia coli*: mutant hosts that allow synthesis of some membrane proteins and globular proteins at high levels. *J. Mol. Biol.* **260**: 289–298.

Möglich, A. & K. Moffat, (2010) Engineered photoreceptors as novel optogenetic tools. *Photochem. Photobiol. Sci* **9**: 1286–1300.

Möglich, A., X. Yang, R.A. Ayers & K. Moffat, (2010) Structure and function of plant photoreceptors. *Annu. Rev. Plant Biol.* **61**: 21–47.

Morgan, J.L., J.T. McNamara & J. Zimmer, (2014) Mechanism of activation of bacterial cellulose synthase by cyclic di-GMP. *Nat. Struct. Mol. Biol.* **21**: 489-496.

Mukougawa, K., H. Kanamoto, T. Kobayashi, A. Yokota & T. Kohchi, (2006) Metabolic engineering to produce phytochromes with phytochromobilin, phycocyanobilin, or phycoerythrobilin chromophore in *Escherichia coli*. *FEBS Lett.* **580**: 1333–1338.

Nakamura, Y., T. Kaneko, S. Sato, M. Ikeuchi, H. Katoh, S. Sasamoto, A. Watanabe, M. Iriguchi, K. Kawashima, T. Kimura, Y. Kishida, C. Kiyokawa, M. Kohara, M. Matsumoto, A. Matsuno, N. Nakazaki, S. Shimpo, M. Sugimoto, C. Takeuchi, M. Yamada & S. Tabata, (2002) Complete genome structure of the thermophilic cyanobacterium

Thermosynechococcus elongatus BP-1. *DNA Res.* **9**: 123–130.

Narikawa, R., G. Enomoto, W. Ni Ni, K. Fushimi & M. Ikeuchi, (2014) A new type of dual-Cys cyanobacteriochrome GAF domain found in cyanobacterium *Acaryochloris marina*, which has an unusual red/blue reversible photoconversion cycle. *Biochemistry* **53**: 5051-5059.

Narikawa, R., K. Fushimi, W. Ni Ni & M. Ikeuchi, (2015a) Red-shifted red/green-type cyanobacteriochrome AM1_1870g3 from the chlorophyll *d*-bearing cyanobacterium *Acaryochloris marina*. *Biochem. Biophys. Res. Commun.* **461**: 390-395.

Narikawa, R., T. Ishizuka, N. Muraki, T. Shiba, G. Kurisu & M. Ikeuchi, (2013) Structures of cyanobacteriochromes from phototaxis regulators AnPixJ and TePixJ reveal general and specific photoconversion mechanism. *Proc. Natl. Acad. Sci. USA* **110**: 918–923.

Narikawa, R., T. Kohchi & M. Ikeuchi, (2008) Characterization of the photoactive GAF domain of the CikA homolog (SyCikA, Slr1969) of the cyanobacterium *Synechocystis* sp. PCC 6803. *Photochem. Photobiol. Sci* **7**: 1253–1259.

Narikawa, R., T. Nakajima, Y. Aono, K. Fushimi, G. Enomoto, W. Ni Ni, S. Itoh, M. Sato & M. Ikeuchi, (2015b) A biliverdin-binding cyanobacteriochrome from the chlorophyll *d*-bearing cyanobacterium *Acaryochloris marina*. *Scientific reports* **5**: 7950.

Narikawa, R., F. Suzuki, S. Yoshihara, S. Higashi, M. Watanabe & M. Ikeuchi, (2011) Novel photosensory two-component system (PixA-NixB-NixC) involved in the regulation of positive and negative phototaxis of cyanobacterium *Synechocystis* sp. PCC 6803. *Plant Cell Physiol.* **52**: 2214–2224.

Navarro, M.V.A.S., N. De, N. Bae, Q. Wang & H. Sondermann, (2009) Structural analysis of the GGDEF-EAL domain-containing c-di-GMP receptor FimX. *Structure* **17**: 1104–1116.

Neunuebel, M.R. & J.W. Golden, (2008) The *Anabaena* sp. strain PCC 7120 gene all2874 encodes a diguanylate cyclase and is required for normal heterocyst development under high-light growth conditions. *J. Bacteriol.* **190**: 6829–6836.

Newell, P.D., R.D. Monds & G.A. O'Toole, (2009) LapD is a bis-(3′,5′)-cyclic dimeric GMP-binding protein that regulates surface attachment by *Pseudomonas fluorescens* Pf0–1. *Proc. Natl. Acad. Sci. USA* **106**: 3461-3466.

Ng, W.O., A.R. Grossman & D. Bhaya, (2003) Multiple light inputs control phototaxis in *Synechocystis* sp. strain PCC6803. *J. Bacteriol.* **185**: 1599-1607.

Nishiyama, Y., S.I. Allakhverdiev & N. Murata, (2011) Protein synthesis is the primary target of reactive oxygen species in the photoinhibition of photosystem II. *Physiol. Plant.* **142**: 35–46.

Ohmori, K., M. Hirose & M. Ohmori, (1993) An increase in the intracellular concentration of cAMP triggers formation of an algal mat by the cyanobacterium *Spirulina platensis*. *Plant and Cell Physiology* **34**: 169-171.

Ohmori, M. & S. Okamoto, (2004) Photoresponsive cAMP signal transduction in cyanobacteria. *Photochem. Photobiol. Sci* **3**: 503-511.

Okajima, K., S. Yoshihara, Y. Fukushima, X. Geng, M. Katayama, S. Higashi, M. Watanabe, S. Sato, S. Tabata, Y. Shibata, S. Itoh & M. Ikeuchi, (2005) Biochemical and functional characterization of BLUF-type flavin-binding proteins of two species of cyanobacteria. *J. Biochem.* **137**: 741–750.

Oliveira, M.C., R.D. Teixeira, M.O. Andrade, G.M. Pinheiro, C.H. Ramos & C.S. Farah, (2015) Cooperative substrate binding by a diguanylate cyclase. *J. Mol. Biol.* **427**: 415-432.

Paul, R., S. Weiser, N.C. Amiot, C. Chan, T. Schirmer, B. Giese & U. Jenal, (2004) Cell cycle-dependent dynamic localization of a bacterial response regulator with a novel di-guanylate cyclase output domain. *Genes Dev.* **18**: 715–727.

Pereira, S.B., R. Mota, C.P. Vieira, J. Vieira & P. Tamagnini, (2015) Phylum-wide analysis of genes/proteins related to the last steps of assembly and export of extracellular polymeric substances (EPS) in cyanobacteria. *Scientific reports* **5**: 14835.

Pesavento, C., G. Becker, N. Sommerfeldt, A. Possling, N. Tschowri, A. Mehlis & R. Hengge, (2008) Inverse regulatory coordination of motility and curli-mediated adhesion in *Escherichia coli*. *Genes Dev.* **22**: 2434-2446.

Ponting, C.P. & L. Aravind, (1997) PAS: a multifunctional domain family comes to light. *Curr. Biol.* **7**: R674–677.

Pultz, I.S., M. Christen, H.D. Kulasekara, A. Kennard, B. Kulasekara & S.I. Miller, (2012) The response threshold of *Salmonella* PilZ domain proteins is determined by their binding affinities for c-di-GMP. *Mol. Microbiol.* **86**: 1424–1440.

Raghunathan, G., N. Soundrarajan, S. Sokalingam, H. Yun & S.G. Lee, (2012) Deletional protein engineering based on stable fold. *PloS one* **7**: e51510.

Rao, F., S. Pasunooti, Y. Ng, W. Zhuo, L. Lim, A.W. Liu & Z.X. Liang, (2009) Enzymatic synthesis of c-di-GMP using a thermophilic diguanylate cyclase. *Anal. Biochem.* **389**: 138–142.

Rauch, A., M. Leipelt, M. Russwurm & C. Steegborn, (2008) Crystal structure of the guanylyl cyclase Cya2. *Proc. Natl. Acad. Sci. USA* **105**: 15720–15725.

Rockwell, N.C., D. Duanmu, S.S. Martin, C. Bachy, D.C. Price, D. Bhattacharya, A.Z. Worden & J.C. Lagarias, (2014a) Eukaryotic algal phytochromes span the visible spectrum. *Proc. Natl. Acad. Sci. USA* **111**: 3871-3876.

Rockwell, N.C. & J.C. Lagarias, (2010) A brief history of phytochromes. *Chemphyschem* **11**: 1172–1180.

Rockwell, N.C., S.S. Martin, K. Feoktistova & J.C. Lagarias, (2011) Diverse two-cysteine photocycles in phytochromes and cyanobacteriochromes. *Proc. Natl. Acad. Sci. USA* **108**: 11854–11859.

Rockwell, N.C., S.S. Martin, A.G. Gulevich & J.C. Lagarias, (2012a) Phycoviolobilin formation and spectral tuning in the DXCF cyanobacteriochrome subfamily. *Biochemistry* **51**: 1449–1463.

Rockwell, N.C., S.S. Martin, A.G. Gulevich & J.C. Lagarias, (2014b) Conserved phenylalanine residues are required for blue-shifting of cyanobacteriochrome photoproducts. *Biochemistry* **53**: 3118-3130.

Rockwell, N.C., S.S. Martin & J.C. Lagarias, (2012b) Mechanistic insight into the photosensory versatility of DXCF cyanobacteriochromes. *Biochemistry* **51**: 3576–3585.

Rockwell, N.C., S.S. Martin & J.C. Lagarias, (2012c) Red/green cyanobacteriochromes: sensors of color and power. *Biochemistry* **51**: 9667–9677.

Rockwell, N.C., S.S. Martin & J.C. Lagarias, (2015a) Identification of DXCF cyanobacteriochrome lineages with predictable photocycles. *Photochem. Photobiol. Sci* **14**: 929-941.

Rockwell, N.C., S.S. Martin, S. Lim, J.C. Lagarias & J.B. Ames, (2015b) Characterization of red/green cyanobacteriochrome NpR6012g4 by solution nuclear magnetic resonance spectroscopy: a protonated bilin ring system in both photostates. *Biochemistry* **54**:

2581-2600.

Rockwell, N.C., S.L. Njuguna, L. Roberts, E. Castillo, V.L. Parson, S. Dwojak, J.C. Lagarias & S.C. Spiller, (2008) A second conserved GAF domain cysteine is required for the blue/green photoreversibility of cyanobacteriochrome Tlr0924 from *Thermosynechococcus elongatus*. *Biochemistry* **47**: 7304–7316.

Rockwell, N.C., R. Ohlendorf & A. Möglich, (2013) Cyanobacteriochromes in full color and three dimensions. *Proc. Natl. Acad. Sci. USA* **110**: 806–807.

Rockwell, N.C., Y.S. Su & J.C. Lagarias, (2006) Phytochrome structure and signaling mechanisms. *Annu. Rev. Plant Biol.* **57**: 837–858.

Römling, U. & M.Y. Galperin, (2015) Bacterial cellulose biosynthesis: diversity of operons, subunits, products, and functions. *Trends Microbiol.* **23**: 545-557.

Römling, U., M.Y. Galperin & M. Gomelsky, (2013) Cyclic di-GMP: the first 25 years of a universal bacterial second messenger. *Microbiol. Mol. Biol. Rev.* **77**: 1–52.

Ross, P., H. Weinhouse, Y. Aloni, D. Michaeli, P. Weinberger-Ohana, R. Mayer, S. Braun, E. de Vroom, G.A. van der Marel, J.H. van Boom & M. Benziman, (1987) Regulation of cellulose synthesis in *Acetobacter xylinum* by cyclic diguanylic acid. *Nature* **325**: 279–281.

Ryan, R.P., Y. Fouhy, J.F. Lucey, L.C. Crossman, S. Spiro, Y.W. He, L.H. Zhang, S. Heeb, M. Camara, P. Williams & J.M. Dow, (2006) Cell-cell signaling in *Xanthomonas campestris* involves an HD-GYP domain protein that functions in cyclic di-GMP turnover. *Proc. Natl. Acad. Sci. USA* **103**: 6712–6717.

Ryan, R.P., T. Tolker-Nielsen & J.M. Dow, (2012) When the PilZ don't work: effectors for cyclic di-GMP action in bacteria. *Trends Microbiol.* **20**: 235–242.

Ryjenkov, D.A., R. Simm, U. Römling & M. Gomelsky, (2006) The PilZ domain is a receptor for the second messenger c-di-GMP: the PilZ domain protein YcgR controls motility in enterobacteria. *J. Biol. Chem*. **281**: 30310–30314.

Ryjenkov, D.A., M. Tarutina, O.V. Moskvin & M. Gomelsky, (2005) Cyclic diguanylate is a ubiquitous signaling molecule in bacteria: insights into biochemistry of the GGDEF protein domain. *J. Bacteriol.* **187**: 1792–1798.

Ryu, M.H., I.H. Kang, M.D. Nelson, T.M. Jensen, A.I. Lyuksyutova, J. Siltberg-Liberles, D.M. Raizen & M. Gomelsky, (2014) Engineering adenylate cyclases regulated by near-infrared window light. *Proc. Natl. Acad. Sci. USA* **111**: 10167-10172.

Savakis, P., S. De Causmaecker, V. Angerer, U. Ruppert, K. Anders, L.O. Essen & A. Wilde, (2012) Light-induced alteration of c-di-GMP level controls motility of *Synechocystis* sp. PCC 6803. *Mol. Microbiol.* **85**: 239–251.

Schirmer, T. & U. Jenal, (2009) Structural and mechanistic determinants of c-di-GMP signalling. *Nat. Rev. Microbiol.* **7**: 724–735.

Schmidt, A.J., D.A. Ryjenkov & M. Gomelsky, (2005) The ubiquitous protein domain EAL is a cyclic diguanylate-specific phosphodiesterase: enzymatically active and inactive EAL domains. *J. Bacteriol.* **187**: 4774–4781.

Shen, J.R., (2015) The structure of photosystem II and the mechanism of water oxidation in photosynthesis. *Annu. Rev. Plant Biol.* **66**: 23-48.

Simm, R., M. Morr, A. Kader, M. Nimtz & U. Römling, (2004) GGDEF and EAL domains inversely regulate cyclic di-GMP levels and transition from sessility to motility. *Mol. Microbiol.* **53**: 1123–1134.

Song, C., G. Psakis, C. Lang, J. Mailliet, W. Gärtner, J. Hughes & J. Matysik, (2011a) Two

ground state isoforms and a chromophore D-ring photoflip triggering extensive intramolecular changes in a canonical phytochrome. *Proc. Natl. Acad. Sci. USA* **108**: 3842–3847.

Song, J.Y., H.S. Cho, J.I. Cho, J.S. Jeon, J.C. Lagarias & Y.I. Park, (2011b) Near-UV cyanobacteriochrome signaling system elicits negative phototaxis in the cyanobacterium *Synechocystis* sp. PCC 6803. *Proc. Natl. Acad. Sci. USA* **108**: 10780–10785.

Stanier, R.Y., R. Kunisawa, M. Mandel & G. Cohen-Bazire, (1971) Purification and properties of unicellular blue-green algae (order *Chroococcales*). *Bacteriol Rev* **35**: 171–205.

Sudarsan, N., E.R. Lee, Z. Weinberg, R.H. Moy, J.N. Kim, K.H. Link & R.R. Breaker, (2008) Riboswitches in eubacteria sense the second messenger cyclic di-GMP. *Science* **321**: 411–413.

Sundriyal, A., C. Massa, D. Samoray, F. Zehender, T. Sharpe, U. Jenal & T. Schirmer, (2014) Inherent regulation of EAL domain-catalyzed hydrolysis of second messenger cyclic di-GMP. *J. Biol. Chem.* **289**: 6978-6990.

Takala, H., A. Bjorling, O. Berntsson, H. Lehtivuori, S. Niebling, M. Hoernke, I. Kosheleva, R. Henning, A. Menzel, J.A. Ihalainen & S. Westenhoff, (2014) Signal amplification and transduction in phytochrome photosensors. *Nature* **509**: 245-248.

Tal, R., H.C. Wong, R. Calhoon, D. Gelfand, A.L. Fear, G. Volman, R. Mayer, P. Ross, D. Amikam, H. Weinhouse, A. Cohen, S. Sapir, P. Ohana & M. Benziman, (1998) Three cdg operons control cellular turnover of cyclic di-GMP in *Acetobacter xylinum*: genetic organization and occurrence of conserved domains in isoenzymes. *J. Bacteriol.* **180**: 4416–4425.

Tamura, J., (2012) 好熱性シアノバクテリアにおける c-di-GMP が調節する生理的機能 Master's thesis

Tao, F., Y.W. He, D.H. Wu, S. Swarup & L.H. Zhang, (2010) The cyclic nucleotide monophosphate domain of *Xanthomonas campestris* global regulator Clp defines a new class of cyclic di-GMP effectors. *J. Bacteriol.* **192**: 1020-1029.

Terauchi, K. & M. Ohmori, (1999) An adenylate cyclase, Cya1, regulates cell motility in the cyanobacterium *Synechocystis* sp. PCC 6803. *Plant Cell Physiol.* **40**: 248-251.

Terry, M.J., M.D. Maines & J.C. Lagarias, (1993) Inactivation of phytochrome- and phycobiliprotein-chromophore precursors by rat liver biliverdin reductase. *J. Biol. Chem.* **268**: 26099–26106.

Thomas, C., C.R. Andersson, S.R. Canales & S.S. Golden, (2004) PsfR, a factor that stimulates *psbAI* expression in the cyanobacterium *Synechococcus elongatus* PCC 7942. *Microbiology* **150**: 1031–1040.

Tu, J.M., M. Zhou, R. Haessner, M. Ploscher, L. Eichacker, H. Scheer & K.H. Zhao, (2009) Toward a mechanism for biliprotein lyases: revisiting nucleophilic addition to phycocyanobilin. *J. Am. Chem. Soc.* **131**: 5399–5401.

Tuckerman, J.R., G. Gonzalez & M.A. Gilles-Gonzalez, (2011) Cyclic di-GMP activation of polynucleotide phosphorylase signal-dependent RNA processing. *J. Mol. Biol.* **407**: 633-639.

Ulijasz, A.T., G. Cornilescu, D. von Stetten, C. Cornilescu, F. Velazquez Escobar, J. Zhang, R.J. Stankey, M. Rivera, P. Hildebrandt & R.D. Vierstra, (2009) Cyanochromes are blue/green light photoreversible photoreceptors defined by a stable double cysteine

linkage to a phycoviolobilin-type chromophore. *J. Biol. Chem.* **284**: 29757–29772.

Velazquez Escobar, F., T. Utesch, R. Narikawa, M. Ikeuchi, M.A. Mroginski, W. G√§rtner & P. Hildebrandt, (2013) Photoconversion mechanism of the second GAF domain of cyanobacteriochrome AnPixJ and the cofactor structure of its green-absorbing state. *Biochemistry* **52**: 4871-4880.

Wagner, J.R., J.S. Brunzelle, K.T. Forest & R.D. Vierstra, (2005) A light-sensing knot revealed by the structure of the chromophore-binding domain of phytochrome. *Nature* **438**: 325–331.

Wassmann, P., C. Chan, R. Paul, A. Beck, H. Heerklotz, U. Jenal & T. Schirmer, (2007) Structure of BeF3- -modified response regulator PleD: implications for diguanylate cyclase activation, catalysis, and feedback inhibition. *Structure* **15**: 915–927.

Whiteley, C.G. & D.J. Lee, (2015) Bacterial diguanylate cyclases: structure, function and mechanism in exopolysaccharide biofilm development. *Biotechnol. Adv.* **33**: 124-141.

Whitney, J.C., G.B. Whitfield, L.S. Marmont, P. Yip, A.M. Neculai, Y.D. Lobsanov, H. Robinson, D.E. Ohman & P.L. Howell, (2015) Dimeric c-di-GMP is required for post-translational regulation of alginate production in *Pseudomonas aeruginosa*. *J. Biol. Chem.* **290**: 12451-12462.

Wilde, A. & C.W. Mullineaux, (2015) Motility in cyanobacteria: polysaccharide tracks and Type IV pilus motors. *Mol. Microbiol.*

Yeh, K.C., S.H. Wu, J.T. Murphy & J.C. Lagarias, (1997) A cyanobacterial phytochrome two-component light sensory system. *Science* **277**: 1505–1508.

Yoshihara, S. & M. Ikeuchi, (2004) Phototactic motility in the unicellular cyanobacterium *Synechocystis* sp. PCC 6803. *Photochem. Photobiol. Sci* **3**: 512–518.

Yoshihara, S., M. Katayama, X. Geng & M. Ikeuchi, (2004) Cyanobacterial phytochrome-like PixJ1 holoprotein shows novel reversible photoconversion between blue- and green-absorbing forms. *Plant Cell Physiol.* **45**: 1729–1737.

Yu, D., W.C. Gustafson, C. Han, C. Lafaye, M. Noirclerc-Savoye, W.P. Ge, D.A. Thayer, H. Huang, T.B. Kornberg, A. Royant, L.Y. Jan, Y.N. Jan, W.A. Weiss & X. Shu, (2014) An improved monomeric infrared fluorescent protein for neuronal and tumour brain imaging. *Nature communications* **5**: 3626.

Zacharias, D.A., J.D. Violin, A.C. Newton & R.Y. Tsien, (2002) Partitioning of lipid-modified monomeric GFPs into membrane microdomains of live cells. *Science* **296**: 913-916.

Zahringer, F., E. Lacanna, U. Jenal, T. Schirmer & A. Boehm, (2013) Structure and signaling mechanism of a zinc-sensory diguanylate cyclase. *Structure* **21**: 1149-1157.

Zhang, S.-R., G.-M. Lin, W.-L. Chen, L. Wang & C.-C. Zhang, (2013) ppGpp metabolism is involved in heterocyst development in the cyanobacterium *Anabaena* sp. strain PCC 7120. *J. Bacteriol.* **195**: 4536-4544.